Event-Triggered Control for Synchronization

SERGEJ GOLFINGER

KTH Electrical Engineering

Degree project in
Automatic Control
Master's thesis
Stockholm, Sweden, 2012

XR-EE-RT 2012:002

September 2011 to February 2012

Event-Triggered Control for Synchronization
— Diploma Thesis —

SERGEJ GOLFINGER [1]

Automatic Control Laboratory
School of Electrical Engineering, KTH Royal Institute of Technology, Sweden
and
Institute for Systems Theory and Automatic Control
Universität Stuttgart, Germany

Supervisor
Dr. D. V. Dimarogonas
KTH Stockholm

Examiner
Dr. D. V. Dimarogonas
KTH Stockholm

Stockholm, February 17, 2012

[1] sergejgo@kth.se

Abstract

The first main part of this thesis presents a novel distributed event-based control strategy for the synchronization of a network consisting of N identical dynamical linear systems. The problem statement can be interpreted as a generalization of a classical event-based consensus problem. Each system updates its control signals according to some triggering conditions based on local information only. Starting with the event-based synchronization with state feedback two different approaches are derived. The trigger functions of the first approach depend on the transfered system states, while the trigger conditions of the second approach depend on the control inputs. The advantages (or otherwise) of both approaches and implementations are discussed. Furthermore, we extend the problem setup to the synchronization with a dynamic output feedback coupling and transfer the both event-based methods to this problem. The novel proposed approaches yields to the general results for the event-based synchronization for linear systems. In the second smaller part we present a new method for the distributed event-based synchronization of Kuramoto oscillators. We assume a uniform Kuramoto model of N all-to-all connected oscillators with different natural frequencies. Throughout the report, simulation results validate and illustrate the proposed theoretical results.

Acknowledgments

First and foremost, I want to thank my supervisor Dr. Dimos V. Dimarogonas for giving me the opportunity to work on my thesis project. I am sincerely grateful to him for providing excellent guidance, always supporting me and for all of the interesting discussions. Furthermore, I want to thank Prof. Dr. Karl Henrik Johansson with the Department for Automatic Control at KTH, Stockholm for accepting me as exchange student and for the friendly and productive atmosphere.
Second, I want to express my gratitude for the support and help to my supervisor Dipl.-Ing. Georg Seyboth of the Institute for Systems Theory and Automatic Control at the University of Stuttgart. I also thank Prof. Dr.-Ing. Frank Allgöwer for giving me the possibility to write my thesis abroad.
Most of all, I would like to thank my parents for every time supporting and advising me. Without them I would not be able to achieve this stage of life and study. Last but no least, great thanks goes to my friends and all people I met during my stay in Stockholm. They made my visit to an unforgettable pleasure.

Sergej Golfinger
February 17, 2012

Contents

1 Introduction

The main goal of this work is the interconnection between synchronization and event-based control. In this thesis project we consider two different kinds of synchronization: Synchronization of linear identical systems and synchronization of Kuramoto oscillators. This chapter gives a brief introduction to cooperative control of multi-agent systems and the consensus problem, followed by event-based control and the two fields of synchronization. We conclude the chapter with our contributions and the outline of this report.

1.1 Multi-agent Systems and Consensus Problem

The recent years have witnessed a thriving research of the control community in cooperative control and motion coordination. There is a growing interest in the use of autonomous vehicles to execute cooperative tasks, as for instance unmanned air vehicles and autonomous underwater vehicles. By cooperating and sharing information with each other, a team of vehicles (referred as agents) can perform complex and dangerous tasks, which cannot be accomplished by a single agent. Beyond that, many applications of multi-agent cooperative control have been investigated, such as multi-agent robotics, distributed estimation, formation control, flocking and many more [1, 2, 3, 4, 5, 6, 7, 8].
The challenges in the control design are the communication and connectivity constraints (local information and limited sensing capabilities). In general, a multi-agent system consists of a group of agents and is associated with a network structure (graph), which encodes how information is shared between the agents. In distributed control strategies, agents in such networks cooperate with each other in order to achieve a desired global objective, but without access to global information of the overall system. Therefore, the activity of each agent is based on its own and the neighbors' information, while accomplishing the collective behavior of the group. One of the main tasks in a multi-agent system is the consensus problem. In a network of agents, consensus is the collective objective of reaching agreement of the agents states to a common value by regarding some variables of interest. The consensus protocol specifies the rule of information exchange between the neighboring agents. Reviews and survey articles can be found in [9, 10, 11].
Consensus and agreement problems have been recently researched for distributed control of multi-agents systems [12, 13, 14, 15, 16]. There are several applications such as flocking, swarming, robotic coordination, distributed computation, just to name a few. In the literature of consensus, the main focus is on the communication constraints and less on the individual dynamics. In most papers with consensus problems the agents are modeled as single integrator dynamics and the communication topology is modeled by graphs. The exchange information

of the agents obeyed a communication graph, which is not necessarily complete, symmetric or time-invariant. Normally, the agreement variables have no dynamics.

1.2 Synchronization

In the recent years, several coordination and synchronization problems have been popular issues in the control community. In comparison to the consensus literature the emphasis is on the individual dynamics. In the synchronization literature the assumption is often a complete (all-to-all) communication graph but the variables of the system can be oscillatory or even chaotic. Similar to the consensus problem, the objective of the interconnection is to reach synchronization to a common solution of the individual dynamics [17, 18, 19, 20, 21]. Many applications in physics, biology, and engineering world yield coordination problems, which can be rewritten to consensus or synchronization problems. In the recent literature [17, 22, 23, 24, 25, 26], the main task has been to design control laws in order to synchronize relevant system variables by taking account of individual dynamics and communication constraints. In [17], the synchronization of a group of identical linear systems described by the state-space model (A, B, C) with general interconnection topologies has been investigated. The proposed dynamic output controller ensures under some assumptions that the solutions exponentially synchronize to a solution of the decoupled open loop system. The approaches can be interpreted as a generalization of the conventional consensus problem. The first main part of this report is based on the proposed methods in [17].
Another field of our interest is the synchronization of coupled oscillators, namely the Kuramoto model introduced by Kuramoto [27]. There are many examples for the application of Kuramoto oscillators in biology [28, 29], in physics [30, 31, 32, 33] and in dynamical systems communities [34, 35, 36]. We refer the reader to the excellent reviews [37, 38]. The nonlinear synchronization of Kuramoto oscillators is closely related to the problem of consensus among multi-agent systems [12, 39, 40, 41]. In [42, 43, 30] the connection between power network synchronization, Kuramoto oscillators, and consensus problems has been recognized. [44] showed that the transient stability analysis of a power network model can be reduced to the synchronization analysis of non-uniform Kuramoto model. Moreover, the available results for Kuramoto oscillators have been used to analyze synchronization in power networks [45]. As one can see, the three fields synchronization, consensus protocol and Kuramoto oscillators are closely related.

1.3 Event-based Control

In many applications, the implementation of the controller is realized on a digital platform. Specifically, each subsystem is equipped with a small embedded digital micro-processor, which coordinates the communication with neighboring agents and controller updates in a discrete-time manner. In a conventional time-scheduled implementation the control task is executed periodically, i.e. the signals are sampled equidistant. Between the updates the signal are held constant via *zero order hold*. The feature of this time-scheduled control is the simple design and analysis.
However, synchronization problems arise often in multi-agent systems. The traditional sampled-data control is often not suitable for distributed systems because of resource constraints. Due to reducing the energy consumption and traffic it is favorable to decrease the controller actu-

ations and the communication between the agents. Event-based control is an alternative for time-scheduled control. In the event-based control strategy the signals are updated only when significant events occurs, for example, when a measured signal exceeds a certain threshold or limit. In data acquisition the idea is referred as send-on-delta concept [46]. There are many conceptual advantages in event-based control [47, 48], such as a more scalable and efficient trade-off between control performance and communication cost. In [49, 50] stochastic event-driven strategies have been studying. The deterministic event-triggered strategy for control applications is introduced in [51]. Based on this event-triggered method, an event-based implementation of the consensus protocol for multi-agent systems is developed in [52, 53, 54], which render the control signals piecewise constant while a continuous communication between agents is required. In [55] a new event-based control strategy is developed which scheduled also the measurement broadcasts in an event-based fashion.
Remark, the closed-loop system of a continuous-time plant and an event-based controller is a hybrid system. For hybrid systems we have not only to ensure stability but also we need to show that Zeno-behavior is excluded [56, 57, 58, 59]. Zeno behavior means that there are infinitely many events in finite time, i.e. there is an accumulation point of events. Compared to time-scheduled control the analysis of event-based control is more challenging, but provides the possibility to reduce the transmissions over the network.

1.4 Contributions

There are two contributions in the present work. The first main contribution of this thesis is the development of novel approaches for the decentralized event-based control for synchronization of linear systems. Our approaches extend the usually used single-integrator system in multi-agent systems to general linear dynamical systems. The starting point is the latest work for synchronization of linear identical systems [17] and the above discussed event-based cooperative control of multi-agent systems [55]. We start with the event-based synchronization with linear feedback and extend this to the event-based synchronization with an output feedback controller. Two different event-based approaches/implementations are presented throughout the event-based synchronization of linear identical systems.
As a second contribution, we present a new event-based method for the synchronization of uniform Kuramoto oscillators. Based on the work of [40] we derive a distributed event-triggered control which synchronize the all-to-all connected oscillators. This approach shall serve as a first basic step for the event-based synchronization of power networks.

1.5 Outline

The remainder of this report is organized as follows. Chapter 2 introduces the preliminaries and basics about the algebraic graph theory and consensus problem, which are needed for the comprehension of this thesis. Furthermore, the problem statement of this work is presented. In Chapter 3 we investigate new approaches for the event-based synchronization of linear system where state coupling among systems is allowed. Two different kinds of setups are presented and discussed. In Chapter 4 we extend the event-based approaches first to synchronization with dynamic feedback controller and finally to synchronization with dynamic output controller. Chapter 5 presents a new method for the synchronization of coupled oscillators which are described by the uniform Kuramoto model. The report concludes with conclusions and future work in Chapter 6. Throughout the work, the theoretical results are confirmed and validated by numerical simulations.

2 Basics and Problem Statement

This chapter provides the problem formulation and the basics which are relevant for the comprehension of this thesis. In the first section the notation and preliminaries are introduced. For the analysis of our problems we use the algebraic theory of communication graphs. Therefore, a brief review of graph theory is summarized in Section 2.2 with particular emphasis on the matrix objects, such as the adjacency and Laplacian matrices. Synchronization problems are closely related to consensus problems on graphs. Section 2.3 introduces the consensus protocol. In the last section the problem statements for event-based synchronization of identical dynamical systems and Kuramoto oscillators are presented.

2.1 Notation and Preliminaries

Throughout this work we use the following notation. For N given vectors $x_1, x_2, \ldots, x_N$ we denote with x the stack vector $x = [x_1^T, x_2^T, \ldots, x_N^T]^T$. We indicate with I_N the $N \times N$ diagonal identity matrix and with $\mathbf{1}$ the column vector $[1, \ldots, 1]^T \in \mathbb{R}^N$. The Euclidean norm for vectors or the induced norm for matrices is denoted as $\| \cdot \|$. We symbolize the Kronecker product of two given matrices $A \in \mathbb{R}^{m\times n}$ and $B \in \mathbb{R}^{p\times q}$ with $A \otimes B \in \mathbb{R}^{mp\times nq}$, which satisfies the properties

$$(A \otimes B)^T = A^T \otimes B^T, \tag{2.1a}$$

$$(A \otimes I_p)(C \otimes I_p) = (AC) \otimes I_p. \tag{2.1b}$$

For notational convenience, we write $\tilde{A}_N = I_N \otimes A$ and $\bar{A}_N = A \otimes I_N$.

2.2 Graph Theory

This section reviews the for us important facts from algebraic graph theory [60, 61]. A network can be modelled as a graph, where vertices correspond to individual agents, and edges correspond to the existence of an inter-agent communication link. The graph theory provides us with useful tools for analyzing, designing and controlling such multi-agent systems. A *graph* $G = (\mathcal{V}, \mathcal{E})$ with N vertices and m edges consists of a *set of vertices* (or nodes) $\mathcal{V} = \{v_1, \ldots v_N\}$ and a *set of edges* $\mathcal{E} = \{(i,j) \subseteq \mathcal{V} \times \mathcal{V}\}$. When an edge exists between vertices v_i and v_j, then we call them *adjacent*. In this case, edge (i,j) is called *incident* with vertices v_i and v_j. The *neighborhood* $\mathcal{N}_i \subseteq \mathcal{V}$ of the vertex v_i is defined as the set $\{v_j \in \mathcal{V} | (v_i, v_j) \in \mathcal{E}\}$, i.e. the set of all vertices that are adjacent to v_i. A *path*, which starts with vertice v_i and ends with vertice v_j, is given by a sequence of distinct vertices such that consecutive vertices are

adjacent. For the case that the vertices of the path are distinct expect for its end vertices, we call the path a *cycle*. Vertices v_i and v_j are called *connected* if there exists a path from v_i to v_j. Moreover, we call the graph G connected, if there is a path between any two vertices in $\mathcal{V}$. For undirected graphs the degree of a vertex d_i is given by the cardinality of the neighborhood set $\mathcal{N}_i$, which is equal to the total number of vertices that are adjacent to vertex v_i.
We can also representate a graph in terms of matrices. For an undirected graph G with N nodes the *degree matrix* D is the diagonal, positive semi-definite $N \times N$-matrix of d_i's. The *adjacency matrix* is the $N \times N$ matrix $A = A(G)$ whose entries a_{ij} are given by

$$a_{ij} = \begin{cases} 1, & \text{if } (v_i, v_j) \in \mathcal{E} \\ 0, & \text{otherwise.} \end{cases}$$

By definition $A(G)$ is a real symmetric matrix and the trace of $A(G)$ is zero. The $N \times m$ *incidence matrix* $B(G)$ is $b_{ij} = 1$ if the edge j is incoming to vertex i, $b_{ij} = -1$ if edge j is outcoming from the vertex i, and 0 otherwise. The *Laplacian matrix* L associated with an undirected graph G is a squared matrix defined as

$$L = D - A. \tag{2.2}$$

The entries l_{kj} of the Laplacian matrix can be also calculated with

$$l_{kj} = \begin{cases} \sum_{i=1}^{N} a_{ki} & j = k \\ -a_{kj} & j \neq k. \end{cases} \tag{2.3}$$

By construction, the row-sum of each row of L is equal to zero, that is $L\mathbf{1} = 0$. Alternatively, for the case for an arbitrary orientated graph with the associated edge set E, the Laplacian matrix can also be calculated through

$$L = BB^T, \tag{2.4}$$

where B is the corresponding incidence matrix. Considering this definition, it is obvious that the Laplacian matrix L is symmetric and positive semi-definite. Remark, the two definitions in (2.4) and (2.2) are equivalent, since the graph is undirected. The matrix

$$L_W = BWB^T \tag{2.5}$$

is a weighted Laplacian with the $m \times m$ weighting matrix $W = \mathrm{diag}(w_i)$.
The Laplacian matrix L is known to be symmetric and positive semidefinite, thus the ordered and real eigenvalues are given by

$$\lambda_1(G) < \lambda_2(G) < \ldots < \lambda_N(G),$$

with $\lambda_1(G) = 0$. For a better understanding of this graph theory we consider the following example.

Example 1. Figure 2.1 shows an example with $N = 4$ agents for an undirected graph. Specifically, the graph $G = (\mathcal{V}, \mathcal{E})$ in that figure is described with

$$\mathcal{V} = \{1, 2, 3, 4\} \text{ and } \mathcal{E} = \{(1, 2), (2, 1), (1, 3), (3, 1), (2, 3), (3, 2), (3, 4), (4, 3)\}.$$

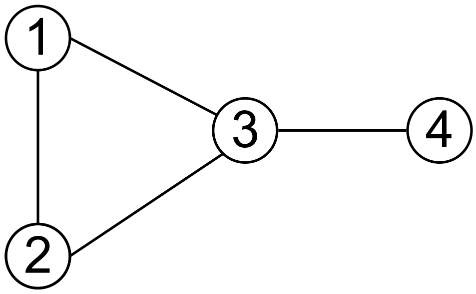

Figure 2.1: Example for an undirected graph G over $N = 4$ vertices.

The corresponding adjacency matrix and the degree matrix are given by

$$A = \begin{bmatrix} 0 & 1 & 1 & 0 \\ 1 & 0 & 1 & 0 \\ 1 & 1 & 0 & 1 \\ 0 & 0 & 1 & 0 \end{bmatrix}, \quad D = \begin{bmatrix} 2 & 0 & 0 & 0 \\ 0 & 2 & 0 & 0 \\ 0 & 0 & 3 & 0 \\ 0 & 0 & 0 & 1 \end{bmatrix}.$$

The Laplacian can be calculated with

$$L = D - A = \begin{bmatrix} 2 & -1 & -1 & 0 \\ -1 & 2 & -1 & 0 \\ -1 & -1 & 3 & -1 \\ 0 & 0 & -1 & 1 \end{bmatrix}. \tag{2.6}$$

As one can see, the Laplacian matrix is symmetric and the sum of the rows is equal to zero. This communication topology will be used in further examples.

2.3 Consensus Protocol

Agreement is one of the fundamental problems in multi-agent systems. In many multi-agents systems, groups of agents need to agree on a joint state value. Example for multi-agents agreement problems are flocking, attitude alignment, swarming and distributed computation. A classical *agreement* or *consensus* protocol which solves the average consensus problem for N agents exchanging information about their state vector $x_i, i = 1, \ldots, N$ is

$$\dot{x}_i = \sum_{j=1}^{N} a_{ij}(x_j - x_i), \quad i = 1, \ldots, N. \tag{2.7}$$

With the Laplacian matrix equation (2.7) can be equivalently written in stack vector notation

$$\dot{x} = -\bar{L}_n x. \tag{2.8}$$

The solutions of (2.8) asymptotically converge to the average of all agents states.

Theorem 2.1. *[17] Let x_i, $k = 1, \ldots, N$, belong to a finite-dimensional Euclidean space W. Let G be a uniformly connected digraph and L the corresponding Laplacian matrix bounded and piecewise continuous in time. Then the equilibrium sets of consensus states of (2.8) are uniformly exponentially stable. Furthermore the solutions of (2.8) asymptotically converge to a consensus value $1_N \otimes \beta$ for some $\beta \in W$.*

A general proof can be found in [12] and [13]. The synchronization problems of identical dynamical systems and Kuramoto oscillators are closely related to consensus problems on graphs.

2.4 Problem Statement

The goal of this thesis is to derive approaches for an event-based control for synchronization. In a conventional time-scheduled implementation the control task is executed periodically with a constant sampling period. An event-driven control seems more favorable, since embedded micro-processor are resource-limited. In this implementation the control task is executed according to some ruling (after the occurrence of an event). The problem is now to find decentralized event-triggered strategies and to design an event-triggering mechanism. Based on local informations we need a rule which decides when to update the control law of each agent i. In order to derive an event-based synchronization strategy we define *trigger functions* $f_i(\cdot)$, which depend only on local information of agent i. An event is triggered whenever $f_i(\cdot) > 0$ holds. For each agent i we get a separate sequence of events $t_0^i, t_1^i, \ldots$. The broadcasting times t_k^i are determined recursively by the event trigger function as

$$t_{k+1}^i = \inf\{t : t > t_k^i, f_i(t) > 0\}.$$

The event-triggered approach leads to piecewise constant controller updates.

2.4.1 Identical Dynamical Systems

In the first main part of this work we want to apply an event-based strategy to synchronization problems of dynamic systems. We consider N identical systems described by the model

$$\dot{x}_i = f(t, x_i, u_i) \tag{2.9a}$$

$$y_i = h(x_i) \tag{2.9b}$$

for $i = 1, 2, \ldots, N$, where $x_i \in \mathbb{R}^n$ is the state of the system, $u_i \in \mathbb{R}^m$ is the control and $y_i \in \mathbb{R}^p$ is the output. We refer a control law *dynamic* if it depends on an internal (controller) state, otherwise we call it *static*. The communication topology of the systems 2.9 is described by the communication graph G. We assume there is only a coupling between the output differences $y_i - y_j$ and the controller state differences $\eta_i - \eta_j$. Synchronization of systems is reached whenever the control action of each system vanishes asymptotically and the solutions of the closed-loop systems converge asymptotically to a common solution of the individual systems. We consider the following event-based synchronization problem of identical systems:
Given N identical systems described by the model (2.9) and a communication graph G. Derive piecewise constant control inputs and event times $t_0^i, t_1^i, \ldots,$ for each agent i such that the solutions of (2.9) asymptotically synchronize to a solution of the open-loop system $\dot{x}_0 = f(t, x_0, 0)$.

2.4.2 Kuramoto Oscillators

In the second part of this thesis we consider the event-based synchronization of Kuramoto oscillators. The Kuramoto model consists of N oscillators which are described by

$$\dot{\theta}_i = \omega_i + \frac{K}{N}\sum_{j=1}^{N}\sin(\theta_j - \theta_i), \quad i = 1, 2, \ldots, N \tag{2.10}$$

where θ_i is the phase of oscillator i, ω_i is its natural frequency and $K > 0$ is the coupling gain. In this section we consider a finite (N) number of Kuramoto oscillator with an *all - to - all* topology, i.e. that all nodes are connected to all other nodes. Furthermore, we let the natural frequencies ω_i be from the set of reals and we do not claim any particular probability distribution on them. The oscillators are said to be synchronized if

$$\dot{\theta}_i - \dot{\theta}_j \to 0 \text{ as } t \to \infty \; \forall i, j = 1, \ldots, N$$

holds, i.e. the phase difference $\theta_i - \theta_j \;\; \forall i, j = 1, \ldots, N$ become asymptotically constant.
Once again, we need to derive a decentralized event-based strategy for the synchronization of Kuramoto oscillators. We require that each oscillator has only access to local information, i.e. $\theta_i, \dot{\theta}_i$ of agent i. Between two consecutive events the value of the frequency $\dot{\theta}_i$ is held constant, i.e.

$$\hat{\dot{\theta}}_i(t) = \dot{\theta}_i(t_k^i), \quad t \in [t_k^i, t_{k+1}^i[. \tag{2.11}$$

Now we can state the problem formulation:
Given N oscillators described by the model (5.1) and a graph G. Derive frequencies of the form (2.11) and event times $t_0^i, t_1^i, \ldots,$ for each agent i such that the phase difference $\theta_i - \theta_j \;\; \forall i, j = 1, \ldots, N$ become asymptotically constant.

3 Event-Based Synchronization of Linear Systems with State Feedback

This chapter provides new approaches for the event-based synchronization of linear system where state coupling among systems is allowed. The presented approaches are the base for the extension to an event-based synchronization with dynamic controller in Chapter 4. In [17] the synchronization of a multi-agent system of identical linear state-space models is investigated. On this basis, we use the main results and propose new event-based strategies. This chapter is divided in two different decentralized strategies for event-based synchronization. The first event-based control strategy in Section 3.1 requires a change of variables in order to monitor the transformed system states. The trigger mechanism of the second method in Section 3.2 utilize control signals. In the last section we discuss the proposed methods.

Before we can start, we review the main results from [17] for synchronization of linear systems with state feedback. We assume N identical linear systems which are described by the linear model

$$\dot{x}_i = Ax_i + Bu_i, \quad i = 1, \ldots, N \tag{3.1}$$

with system matrix $A \in \mathbb{R}^{n\times n}$, input matrix $B \in \mathbb{R}^{n\times m}$, state vector $x_i \in \mathbb{R}^n$ and control vector $u_i \in \mathbb{R}^m$. The systems (3.1) can be stacked to

$$\dot{x} = \tilde{A}_N x + \tilde{B}_N u.$$

Assume that B is a $n \times n$ nonsingular matrix. With the control law

$$u_i = B^{-1} \sum_{j=1}^{N} a_{ij}(x_j - x_i), \quad i = 1, \ldots, N \tag{3.2}$$

and systems (3.1) we get the closed-loop system

$$\dot{x}_i = Ax_i + \sum_{j=1}^{N} a_{ij}(x_j - x_i), \quad i = 1, \ldots, N, \tag{3.3}$$

which is equivalent to

$$\dot{x} = \tilde{A}_N x - \bar{L}_n x = (\tilde{A}_N - \bar{L}_n)x. \tag{3.4}$$

The following theorem can be interpreted as a generalization of Theorem 2.1 (with $A = 0$ and $B = I$).

Theorem 3.1. *[17] Consider the closed loop system (3.4). Assume that all the eigenvalues of A belong to the imaginary axis, the communication graph G is connected and the corresponding Laplacian matrix L piecewise continuous and bounded. Then all solutions of (3.4) synchronize to a solution of the system $\dot{x}_0 = Ax_0$.*

Proof. With the change of variable $z_i = \mathrm{e}^{-At}x_i$, $i = 1, \ldots, N$ we can rewrite the closed-loop system (3.4) to

$$\dot{z}_i = -A\mathrm{e}^{-At}x_i + \mathrm{e}^{-At}Ax_i + \mathrm{e}^{-At}\sum_{j=1}^{N} a_{ij}(x_j - x_i) = \sum_{j=1}^{N} a_{ij}(z_j - z_i)$$

or in compact form

$$\dot{z} = -\bar{L}_n z.$$

We know from Theorem 2.1 that the solutions exponentially converge to a common value. In the original coordinates means that all solutions exponentially synchronize to a solution of the open loop system. The complete proof can be found in [17].

Remark 3.1. The results of Theorem 3.1 remain unchanged if A possesses also eigenvalues which belong to the left-half complex plane. Modes of eigenvalues with negative real part synchronize exponentially to zero, even without coupling. For the case that A has eigenvalues with positive real part Theorem 3.1 is only true if the graph connectivity is sufficiently strong to dominate the unstable modes of the system.

3.1 Trigger Functions Depending on System States

In this section we present a new approach for event-based control for synchronization of linear systems with state feedback. We consider N identical linear systems (3.1) where B is a $n \times n$ nonsingular matrix and assume that A possesses no eigenvalues with positive real part. Furthermore, we consider only fixed undirected connected communication graph G and assume there are no communication time-delays.

In [55] a new event-based control strategy for the average consensus problem for multi-agent systems is presented. The system states converge to average consensus asymptotically and the trigger functions are depending on the system states. We try to transfer the derived event trigger approaches and synthesis of [55] to our problem. In our case the system states can be of an oscillating motion and do not asymptotically converge to a common value. But in the proof of Theorem 3.1 it has been shown that synchronization is reached when the transfered system states $z(t)$ with the change of variables $z_i = \mathrm{e}^{-At}x_i$ exponentially converge to a common value.

In order to derive an event-based synchronization strategy we define trigger functions $f_i(\cdot)$, which depend only on local information of agent i. We propose the following decentralized trigger mechanism. Agent i has only access on $z_i(t)$ and the latest triggered value $\hat{z}_i(t)$. An event is triggered whenever the trigger condition

$$f_i\left(z_i(t), \hat{z}_i(t)\right) > 0 \tag{3.5}$$

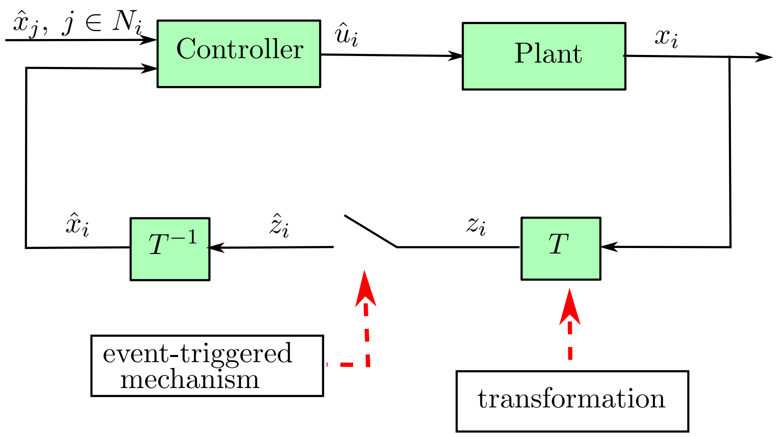

Figure 3.1: Event-triggered control schematic for trigger functions (3.5)

holds. We denote the event times for each agent i by $t_0^i, t_1^i, \ldots$. The transfered system state of agent i

$$\hat{z}_i(t) = z_i(t_k^i), \quad t \in [t_k^i, t_{k+1}^i[$$

is held constant between $t \in [t_k^i, t_{k+1}^i[$ and thus the system states

$$\hat{x}_i(t) = x_i(t_k^i), \quad t \in [t_k^i, t_{k+1}^i[$$

remain also constant. Considering (3.2), the control inputs become piecewise constant.
The event-triggered implementation with trigger function (3.5) for one agent is shown in Figure 3.1. In order to use the trigger mechanism the system states x_i need to be transformed in z-variables. If the trigger function is fulfilled, the actual measurement value is transformed back in x-variables and broadcasted over the network. The controller is updated only when agent i sends a new measurement update or its neighbors $j \in N$ transmit a new measurement value. According to (3.2), the control output $\hat{u}_i$ is updated piecewise constant. We call in Figure 3.1 the implementation Setup A.
The problem is now to find suitable trigger functions such that all solutions of (3.1) synchronize to a solution of the open loop system $\dot{x}_0 = Ax_0$ with as few events as possible and similar performance compared to the time-scheduled implementation. Moreover, we have to ensure that the system does not reach an undesired accumulation point, i.e. we have to prove that Zeno behavior is excluded.
In order to construct a suitable trigger function $f_i(\cdot)$ we define for each agent i the measurement error

$$\epsilon_i(t) = \hat{z}_i(t) - z_i(t). \tag{3.6}$$

and denote the stack vector $\epsilon = [\epsilon_1, \epsilon_2, \ldots \epsilon_N]^T$. The transfered nominal closed loop system in z-coordinates is given by

$$\dot{z}(t) = -\bar{L}_n z(t). \tag{3.7}$$

In presence of an event trigger mechanism the system (3.7) changes to

$$\dot{z}(t) = -\bar{L}_n \hat{z}(t) = -\bar{L}_n (z(t) + \epsilon(t)). \tag{3.8}$$

This notation is inspired by [51] and plays a big part in the analysis of the event-triggered strategy. The average value can be defined as

$$a(t) = \frac{1}{N} \sum_{i=1}^{N} z_i(t). \tag{3.9}$$

For the time derivative of the average value (3.9) we get

$$\dot{a}(t) = \frac{1}{N} \sum_{i=1}^{N} \dot{z}_i(t) = \frac{1}{N} \mathbf{1}^T \dot{z}_i(t) = -\frac{1}{N} \mathbf{1}^T \bar{L}_n (z(t) + \epsilon(t)) = 0,$$

since $\mathbf{1}^T \bar{L}_n = 0$. It is obvious that the average value $a(t) = a(0) = a$ is a constant value and can be calculated according to

$$a = a(0) = \frac{1}{N} \sum_{i=1}^{N} z_i(0) = \frac{1}{N} \sum_{i=1}^{N} \mathrm{e}^{-A0} x_i(0) = \frac{1}{N} \sum_{i=1}^{N} x_i(0).$$

Following [16], we introduce the disagreement vector $\delta(t)$ and split the transfered variables to

$$z(t) = \mathbf{1} a + \delta(t). \tag{3.10}$$

By construction, we know that the disagreement vector has zero average, i.e. $\mathbf{1}^T \delta(t) = 0$. The time derivative of the disagreement vector yields with (3.8) and (3.10) to

$$\dot{\delta}(t) = \dot{z}(t) = -\bar{L}_n (z(t) + \epsilon(t)) = -\bar{L}_n ((\mathbf{1} a + \delta(t)) + \epsilon(t))$$

and therefore

$$\dot{\delta}(t) = -\bar{L}_n (\delta(t)) + \epsilon(t)) = -\bar{L}_n \delta(t) - \bar{L}_n \epsilon(t). \tag{3.11}$$

Moreover, the condition $\bar{L}_n z(t) = \bar{L}_n \delta(t)$ holds. Before the results of our approaches are presented, we consider the following Lemma.

Lemma 3.2. *[55] Suppose L is the Laplacian of an undirected connected graph G. Then, for all $t \geq 0$ and all vectors $v \in \mathbb{R}^N$ with zero average, i.e. $\mathbf{1}^T v = 0$, it holds*

$$\|e^{-Lt} v\| \leq e^{-\lambda_2(G) t} \|v\|.$$

The proof can be found in [55]. Lemma 3.2 help us to proof the main convergence results of this work.

3.1.1 Static Trigger Functions

Motivated by [55], we propose in our first approach static trigger functions of the form

$$f_i(\epsilon_i(t)) = \|\epsilon_i(t)\| - c_0. \tag{3.12}$$

The origin idea of this condition is to trigger when the states cross a certain threshold [48, 46]. In our case, an event is triggered whenever the norm of the measurement error (3.6) becomes larger than c_0, i.e. as soon as the difference between the latest broadcasted control value and the current control value crosses a certain threshold c_0.

Theorem 3.3. *Consider N linear system (3.1) with feedback control (3.2) and trigger functions of the form (3.12). Assume for A that all eigenvalues $Re[\lambda_k(A)] \leq 0, k = 1, \ldots, n$, and B is a $n \times n$ nonsingular matrix. Let the communication graph G be undirected and connected, then for all initial conditions $x(0) \in \mathbb{R}^n$ and $t > 0$, it holds*

$$\|\delta(t)\| \leq \frac{\|\bar{L}_n\|}{\lambda_2(G)}\sqrt{N}c_0 + e^{-\lambda_2(G)t}\left(\|\delta(0)\| - \frac{\|\bar{L}_n\|}{\lambda_2(G)}\sqrt{N}c_0\right).$$

Furthermore, the closed-loop system does not exhibit Zeno behavior.

Proof. We rewrite the closed loop system (3.4) in z-coordinates and obtain (3.7). This can be treated now as a usual consensus problem and the argumentation is the same as in [55]. In order to get a clue of the proof technique we resume the main parts.
In presence of the error (3.6) the disagreement dynamics are given by

$$\dot{\delta}(t) = -\bar{L}_n(\delta(t) + \epsilon(t)) = -\bar{L}_n\delta(t) - \bar{L}_n\epsilon(t)$$

The analytical solution of the disagreement dynamics (3.11) can be calculated with

$$\delta(t) = \mathrm{e}^{-\bar{L}_n t}\delta(0) - \int_0^t \mathrm{e}^{-\bar{L}_n(t-\tau)}\bar{L}_n\epsilon(\tau)d\tau. \tag{3.13}$$

We bound the disagreement vector (3.13) as

$$\begin{aligned}\|\delta(t)\| &\leq \|\mathrm{e}^{-\bar{L}_n t}\delta(0)\| + \|\int_0^t \mathrm{e}^{-\bar{L}_n(t-\tau)}\bar{L}_n\epsilon(\tau)d\tau\| \\ &\leq \|\mathrm{e}^{-\bar{L}_n t}\delta(0)\| + \int_0^t \|\mathrm{e}^{-\bar{L}_n(t-\tau)}\bar{L}_n\epsilon(\tau)\|d\tau.\end{aligned}$$

Remark that $\bar{L}_n\mathbf{1} = 0$ and therefore the vector $\bar{L}_n\epsilon(\tau)$ has zero average. We can exploit this circumstance and apply Lemma 3.2

$$\|\delta(t)\| \leq \mathrm{e}^{-\lambda_2(G)t}\|\delta(0)\| + \int_0^t \mathrm{e}^{-\lambda_2(G)(t-\tau)}\|\bar{L}_n\|\|\epsilon(\tau)\|d\tau. \tag{3.14}$$

The trigger condition (3.12) enforces $\|\epsilon_i(\tau)\| \leq c_0$, so that $\|\epsilon(\tau)\| \leq \sqrt{N}c_0$ and

$$\|\delta(t)\| \leq \mathrm{e}^{-\lambda_2(G)t}\|\delta(0)\| + \int_0^t \mathrm{e}^{-\lambda_2(G)(t-\tau)}\|\bar{L}_n\|\sqrt{N}c_0 d\tau \tag{3.15}$$

holds. The integration of (3.15) leads to

$$\begin{aligned}\|\delta(t)\| &\leq \mathrm{e}^{-\lambda_2(G)t}\|\delta(0)\| + \frac{\|\bar{L}_n\|}{\lambda_2(G)}\sqrt{N}c_0\left(1-\mathrm{e}^{-\lambda_2(G)t}\right)\\ &= \frac{\|\bar{L}_n\|}{\lambda_2(G)}\sqrt{N}c_0 + \mathrm{e}^{-\lambda_2(G)t}\left(\|\delta(0)\| - \frac{\|\bar{L}_n\|}{\lambda_2(G)}\sqrt{N}c_0\right). \end{aligned} \tag{3.16}$$

It remains to show that Zeno behavior is excluded. We assume that the latest event trigger of agent i occurs at $t = t^* > 0$. Then it holds $\|\epsilon(t^*)\| = 0$ and $f_i(0) = -c_0 < 0$. Hence, agent i can not trigger again at the same time instance. Between two consecutive trigger events it holds that $\dot{\epsilon}_i(t) = -\dot{z}_i(t)$. With (3.8) and condition $\|\bar{L}_n z(t)\| = \|\bar{L}_n\delta(t)\|$ we get

$$\begin{aligned}\|\dot{\epsilon}_i(t)\| \leq \|\dot{\epsilon}(t)\| &\leq \|\bar{L}_n z(t) + \bar{L}_n\epsilon(t)\|\\ &\leq \|\bar{L}_n z(t)\| + \|\bar{L}_n\|\|\epsilon(t)\|\\ &\leq \|\bar{L}_n z(t)\| + \|\bar{L}_n\|\sqrt{N}c_0\\ &= \|\bar{L}_n \delta(t)\| + \|\bar{L}_n\|\sqrt{N}c_0\\ &\leq \|\bar{L}_n\|\|\delta(t)\| + \|\bar{L}_n\|\sqrt{N}c_0.\end{aligned}$$

An upper bound for (3.16) is

$$\|\delta(t)\| \leq \|\delta(0)\| + \frac{\|\bar{L}_n\|}{\lambda_2(G)}\sqrt{N}c_0 \quad \forall t \geq t^*.$$

Then for any t between t^* and the next event time for agent i

$$\begin{aligned}\|\epsilon_i(t)\| \leq \|\epsilon(t)\| &\leq \int_{t^*}^{t} \|\dot{\epsilon}(\tau)\| d\tau\\ &\leq \int_{t^*}^{t} \|\bar{L}_n\|\left(\|\delta(t)\| + \sqrt{N}c_0\right) d\tau\\ &\leq \int_{t^*}^{t} \|\bar{L}_n\|\left(\|\delta(0)\| + \frac{\|\bar{L}_n\|}{\lambda_2(G)}\sqrt{N}c_0 + \sqrt{N}c_0\right) d\tau\\ &= \|\bar{L}_n\|\left(\|\delta(0)\| + \frac{\|\bar{L}_n\|}{\lambda_2(G)}\sqrt{N}c_0 + \sqrt{N}c_0\right)(t-t^*).\end{aligned}$$

The next event is triggered as soon as $\epsilon(t)$ reaches the value of c_0, i.e.

$$\|\bar{L}_n\|\left(\|\delta(0)\| + \frac{\|\bar{L}_n\|}{\lambda_2(G)}\sqrt{N}c_0 + \sqrt{N}c_0\right)(t-t^*) = c_0.$$

Thus, a lower positive bound on the inter-event times is given by

$$\tau = \frac{c_0}{\|\bar{L}_n\|\left(\|\delta(0)\| + \frac{\|\bar{L}_n\|}{\lambda_2(G)}\sqrt{N}c_0 + \sqrt{N}c_0\right)}. \tag{3.17}$$

□

Theorem 3.3 proves that all z_i's with trigger functions (3.12) exponentially converges to a region around the average point a if the errors are bounded by $\|\epsilon_i(t)\| \leq c_0$. Moreover, it states an explicit bound of this region depending on c_0. Since the transformed variables $z(t)$ converge to a common value, we conclude the system is synchronized.

Example 2. We demonstrate in this example the event-based synchronization with some simulation results. We consider a group of N harmonic oscillators

$$\begin{aligned} \dot{x}_{1i} &= x_{2i} + u_{1i} \\ \dot{x}_{2i} &= -x_{1i} + u_{2i} \end{aligned} \tag{3.18}$$

which corresponds to system (3.1) with

$$A = \begin{bmatrix} 0 & 1 \\ -1 & 0 \end{bmatrix}, \quad B = \begin{bmatrix} 1 & 0 \\ 0 & 1 \end{bmatrix}. \tag{3.19}$$

We use the same communication topology as shown in Figure 2.1 and the same Laplacian (2.6) of Example 1. The initial conditions are chosen to $x(0) = \begin{bmatrix} 2 & 2 & 3 & 3 & -1 & -1 & -2 & -2 \end{bmatrix}^T$. For the simulations we use trigger functions (3.12) with $c_0 = 0.03$. Figure 3.2 shows the synchronization of each system to a solution of the open loop system. Like expected the transformed system states $z(t)$ converge to a region around the average value a (see Figure 3.3). Figure 3.4 shows the norm of measurement errors and the events for each agent. The density of the events is very high for small t. We need to check that the inter-event times have a lower positive bound τ. According to (3.17) the lower positive bound for this example is $\tau = 6.269 \cdot 10^{-4}$s. In Figure 3.5 one can see that all inter-event times are above the lower positive bound τ (red line) and therefore there is no Zeno-behavior.

The numerical simulations show also the smaller c_0 the more dense of the events for small times t. However, for larger c_0 we get a bigger bound region around the common value a, which could yield to unsynchronized states. The choice of c_0 is a compromise between the high density of events at the beginning and a big region of convergence. The static trigger functions (3.12) seems to be unsuitable for the event-based synchronization. In the next subsection, we alleviate this problem by another choice of trigger functions.

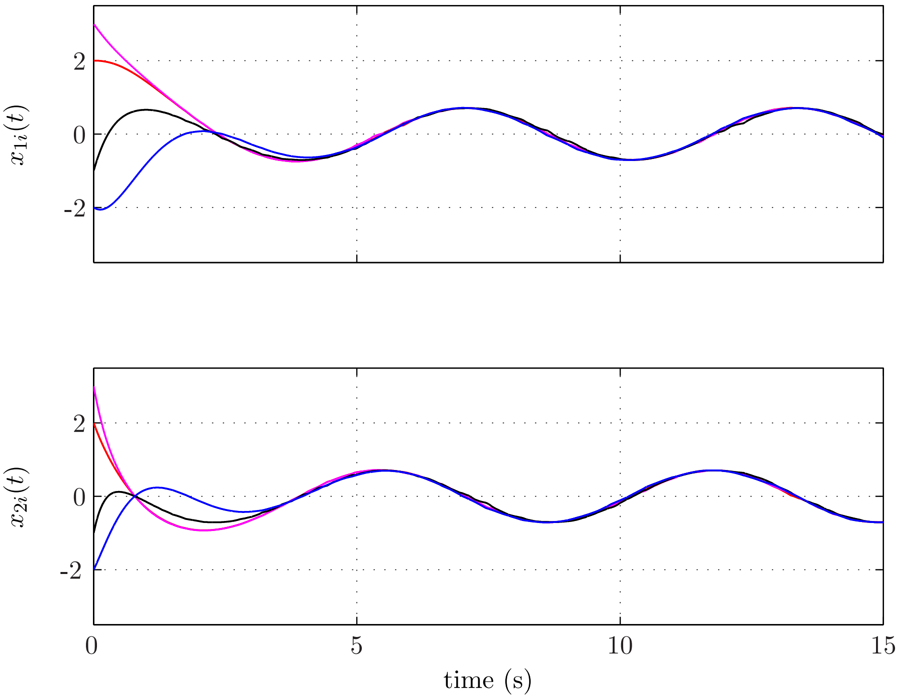

Figure 3.2: Synchronization with trigger function (3.12): System states $x_i(t)$

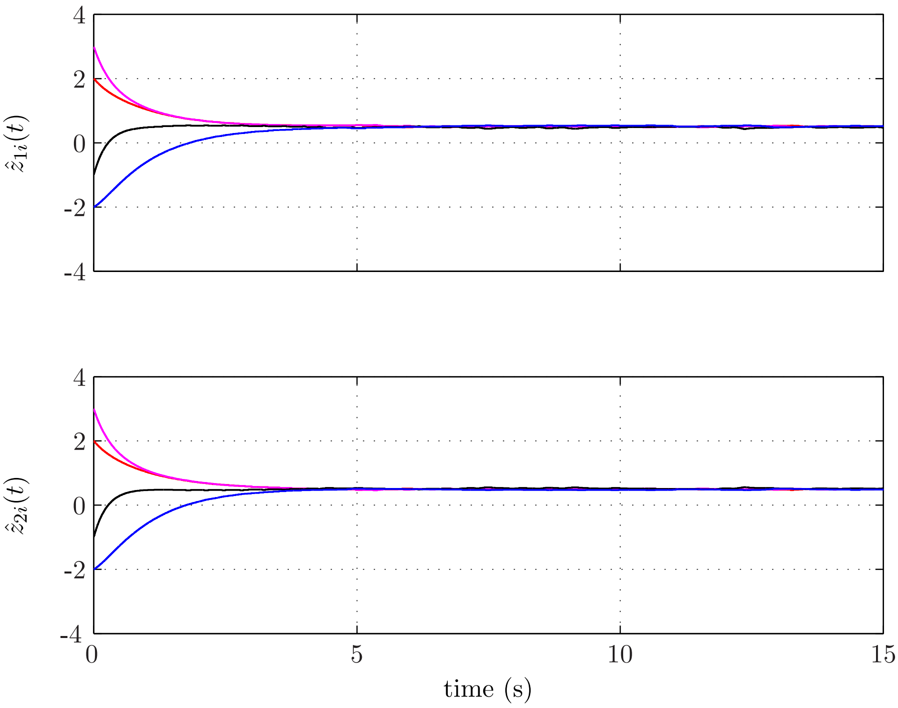

Figure 3.3: Synchronization with trigger function (3.12): Transformed system states $\hat{z}_i(t)$

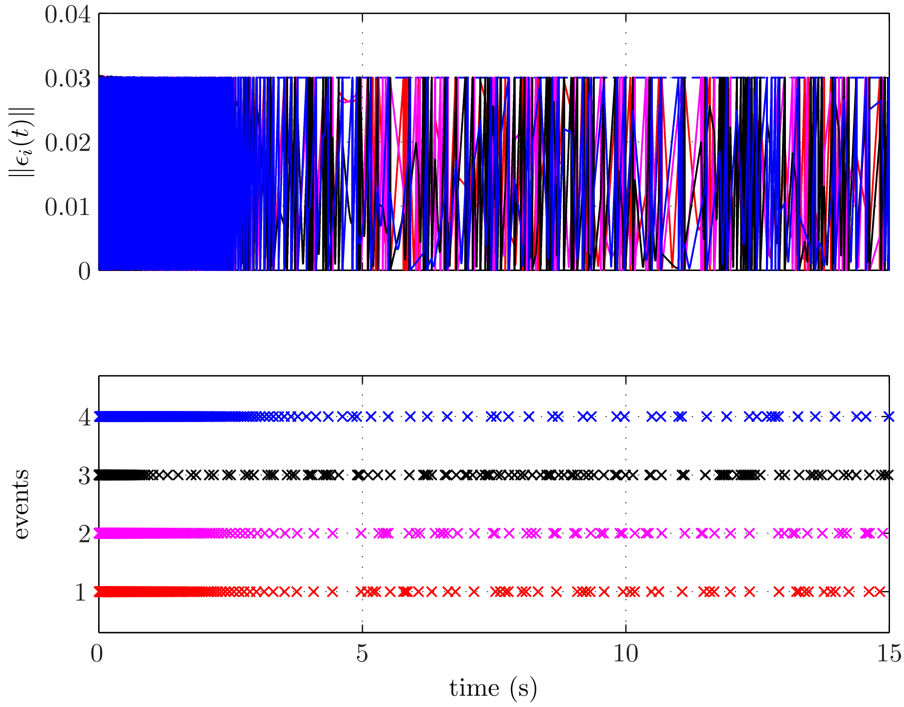

Figure 3.4: Synchronization with trigger function (3.12): Measurement errors $\|\epsilon_i(t)\|$

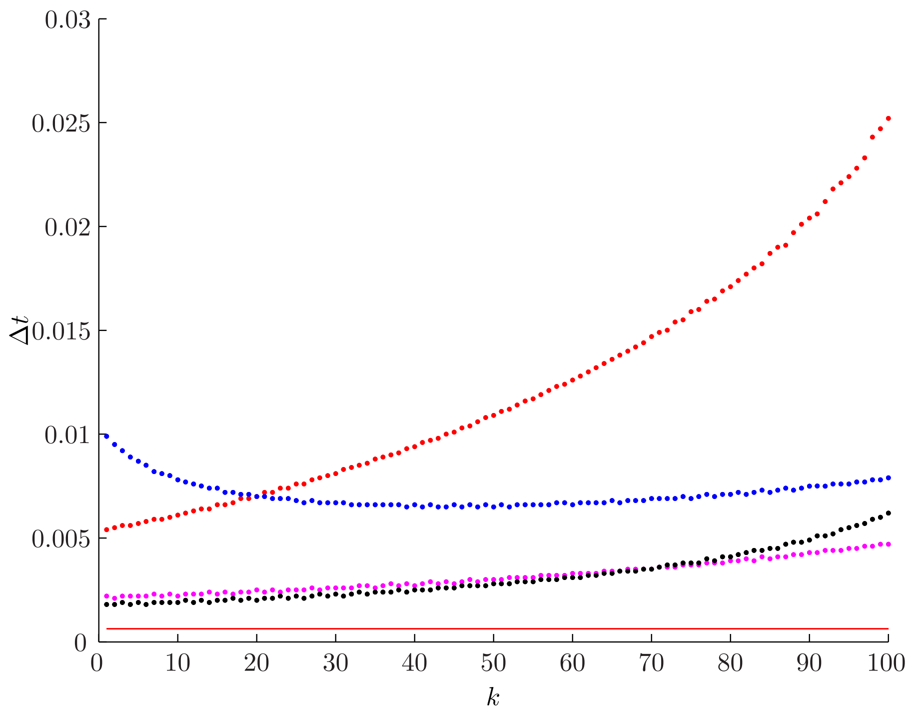

Figure 3.5: Interevents times with trigger function (3.12) ($\tau = 6.269 \cdot 10^{-4}$s)

3.1.2 Dynamic Trigger Functions

Analog to [55] we propose exponentially decreasing threshold trigger functions with a constant offset. The time-dependent trigger functions are described by

$$f_i(\epsilon_i(t)) = \|\epsilon_i(t)\| - (c_1 + c_2 \mathrm{e}^{-\alpha t}), \tag{3.20}$$

where $c_1 \geq 0$, $c_2 > 0$ and $\alpha > 0$. The advantage of trigger condition (3.20) is that we have now three parameters to tune.

Theorem 3.4. *Consider N linear system (3.1) with feedback control (3.2) and trigger functions of the form (3.20). Assume for A that all eigenvalues $Re[\lambda_k(A)] \leq 0, k = 1, \ldots, n$, and B is a $n \times n$ nonsingular matrix. Let the communication graph G be undirected and connected, then for all initial conditions $x(0) \in \mathbb{R}^n$ and $t > 0$, it holds*

$$\begin{aligned}\|\delta(t)\| \leq & \|\bar{L}_n\|\sqrt{N}\frac{c_1}{\lambda_2(G)} + e^{-\alpha t}\|\bar{L}_n\|\sqrt{N}\frac{c_2}{\lambda_2(G)-\alpha} \\ & + e^{-\lambda_2(G)t}\left(\|\delta(0)\| - \|\bar{L}_n\|\sqrt{N}\left(\frac{c_1}{\lambda_2(G)} + \frac{c_2}{\lambda_2(G)-\alpha}\right)\right).\end{aligned}$$

Furthermore, the closed-loop system does not exhibit Zeno behavior.

Proof. Again the proof is almost the same as in [55]. For the comprehension we outline the main steps of the proof. Same proceeding as before, we start with (3.14)

$$\|\delta(t)\| \leq \mathrm{e}^{-\lambda_2(G)t}\|\delta(0)\| + \int_0^t \mathrm{e}^{-\lambda_2(G)(t-\tau)}\|\bar{L}_n\|\|\epsilon(\tau)\|d\tau$$

The trigger function (3.20) enforces

$$\|\epsilon(\tau)\| \leq \sqrt{N}(c_1 + c_2\mathrm{e}^{-\alpha\tau}).$$

This yields to

$$\|\delta(t)\| \leq \mathrm{e}^{-\lambda_2(G)t}\|\delta(0)\| + \int_0^t \mathrm{e}^{-\lambda_2(G)(t-\tau)}\|\bar{L}_n\|\sqrt{N}(c_1 + c_2\mathrm{e}^{-\alpha\tau})d\tau$$

after integration and reordering we get

$$\begin{aligned}\|\delta(t)\| \leq & \|\bar{L}_n\|\sqrt{N}\frac{c_1}{\lambda_2(G)} + \mathrm{e}^{-\alpha t}\|\bar{L}_n\|\sqrt{N}\frac{c_2}{\lambda_2(G)-\alpha} \\ & + \mathrm{e}^{-\lambda_2(G)t}\left(\|\delta(0)\| - \|\bar{L}_n\|\sqrt{N}\left(\frac{c_1}{\lambda_2(G)} + \frac{c_2}{\lambda_2(G)-\alpha}\right)\right).\end{aligned} \tag{3.21}$$

We have also to show that there exists a positive lower bound for the inter-event times. An upper bound for (3.21) is

$$\|\delta(t)\| \leq \|\bar{L}_n\|\sqrt{N}\frac{c_1}{\lambda_2(G)} + \mathrm{e}^{-\alpha t}\|\bar{L}_n\|\sqrt{N}\frac{c_2}{\lambda_2(G)-\alpha} + \mathrm{e}^{-\lambda_2(G)t}\|\delta(0)\| \tag{3.22}$$

Proceeding as before, it holds that

$$\|\dot{\epsilon}_i(t)\| \leq \|\bar{L}_n\|\|\delta(t)\| + \|\bar{L}_n\|\|\epsilon(t)\| = \|\bar{L}_n\|\|\delta(t)\| + \|\bar{L}_n\|(c_1 + c_2\mathrm{e}^{-\alpha t}). \tag{3.23}$$

For convenience, we denote

$$k_1 = \|\bar{L}_n\|\|\delta(0)\|$$
$$k_2 = \|\bar{L}_n\|\sqrt{N}c_2\left(1 + \frac{\bar{L}_n\|}{\lambda_2(G) - \alpha}\right)$$
$$k_3 = \|\bar{L}_n\|\sqrt{N}c_1\left(1 + \frac{\bar{L}_n\|}{\lambda_2(G)}\right)$$

and inserting (3.22) in (3.23) we derive

$$\|\dot{\epsilon}_i(t)\| \leq k_1 \mathrm{e}^{-\lambda_2(G)t} + k_2 \mathrm{e}^{-\alpha t} + k_3. \tag{3.24}$$

It is easy to see that $\|\dot{\epsilon}_i(t)\| \leq k_1 + k_2 + k_3$ for all $t \geq 0$. The error of agent i can be bounded by

$$\|\epsilon_i(t)\| \leq \|\epsilon(t)\| \leq \int_{t^*}^{t} \|\dot{\epsilon}(\tau)\| d\tau \leq \int_{t^*}^{t} (k_1 + k_2 + k_3) d\tau = (k_1 + k_2 + k_3)(t - t^*).$$

A new trigger event will not be executed before $\|\epsilon_i(t)\| = c_1 \leq c_1 + c_2 \mathrm{e}^{-\alpha t}$ is fullfilled. Hence, a lower bound τ on the inter-execution time is given by

$$\tau = \frac{c_1}{k_1 + k_2 + k_3}.$$

Now we consider the case $c_1 = 0$ and thus $k_3 = 0$. In that situation the disagreement vector is bounded by

$$\|\delta(t)\| \leq \mathrm{e}^{-\lambda_2(G)t}\|\delta(0)\| + \|\bar{L}_n\|\sqrt{N}\frac{c_2}{\lambda_2(G) - \alpha}\left(\mathrm{e}^{-\alpha t} - \mathrm{e}^{-\lambda_2(G)t}\right).$$

The overall system converges asymptotically to the average consensus. In order to exclude Zeno behavior we bound (3.24) with $k_3 = 0$ as

$$\|\epsilon_i(t)\| \leq \|\epsilon(t)\| \leq k_1 \mathrm{e}^{-\lambda_2(G)t} + k_2 \mathrm{e}^{-\alpha t} \leq k_1 \mathrm{e}^{-\lambda_2(G)t^*} + k_2 \mathrm{e}^{-\alpha t^*}$$

for $t^* \leq t$ and hence

$$\|\epsilon_i(t)\| \leq \int_{t^*}^{t} k_1 \mathrm{e}^{-\lambda_2(G)t^*} + k_2 \mathrm{e}^{-\alpha t^*} d\tau = \left(k_1 \mathrm{e}^{-\lambda_2(G)t^*} + k_2 \mathrm{e}^{-\alpha t^*}\right)(t - t*)$$

With $c_1 = 0$ and according to (3.20) an event is not triggered before

$$\|\epsilon_i(t)\| = c_2 \mathrm{e}^{-\alpha t}.$$

Consequently, a lower bound on the inter-event intervals is given by

$$\left(k_1 \mathrm{e}^{-\lambda_2(G)t^*} + k_2 \mathrm{e}^{-\alpha t^*}\right)\tau = c_2 \mathrm{e}^{-\alpha t},$$

which is the same as

$$\left(\frac{k_1}{c_2}\mathrm{e}^{(\alpha - \lambda_2(G))t^*} + \frac{k_2}{c_2}\right)\tau = \mathrm{e}^{-\alpha\tau}. \tag{3.25}$$

The left and right hand side of (3.25) are always positive. For $\alpha < \lambda_2(G)$ the term in the brackets is upper bounded by $\frac{k_1+k_2}{c_2}$ and lower bounded by $\frac{k_1}{c_2}$. Thus, we conclude that the lower bound on inter-event intervals τ is positive for all $t^* \geq 0$. $\square$

For the case $c_1 = 0$, it is sufficient that $\alpha < \lambda_2(G)$ in order to exclude Zeno-behavior. In applications a constant offset is favorable due to measurement noise. Small amplitudes of noise can cause trigger action since for large time the trigger condition exponentially decrease to zero. Theorem 3.3 can be interpreted as a special case of Theorem 3.4 (with $c_1 = 0$ and $\alpha = 0$). With the parameter c_0 one can tune the size of the region around the common value a. Since the parameter c_1 is dominating c_0 for small times, we can adjust with c_1 the density of events at the beginning. Thus, a larger c_1 leads to a smaller density of events for small times t. With the parameter α we can specify the speed of convergence of the exponential function of (3.20). With trigger function (3.20) we get more flexibility to design the desired event-based synchronization.

Example 3. We use exactly the same example system as in Example 1 but now with trigger function 3.20). The settings for the constants are $c_1 = 0.015$, $c_2 = 0.9$ and $\alpha = 0.4$. Figure 3.6 and 3.7 show that the systems are synchronized. The density of the events at the beginning is distinctly less compared to the case with the static trigger function (3.12), see Figure 3.8. This results of the circumstance that the threshold is much bigger for small t. Unlike as expected the events are more dense for larger times. This can be coherent with the permanent change of variables and the dynamics of the system. Nevertheless, much less events are generated compared to the previous subsection.

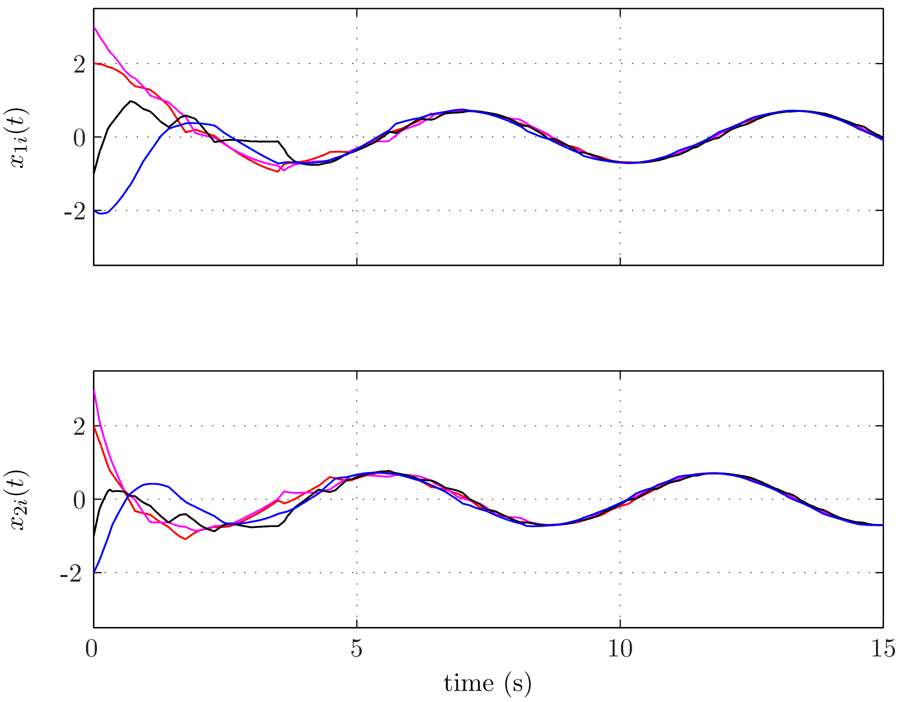

Figure 3.6: Synchronization with trigger function (3.20): System states $x_i(t)$

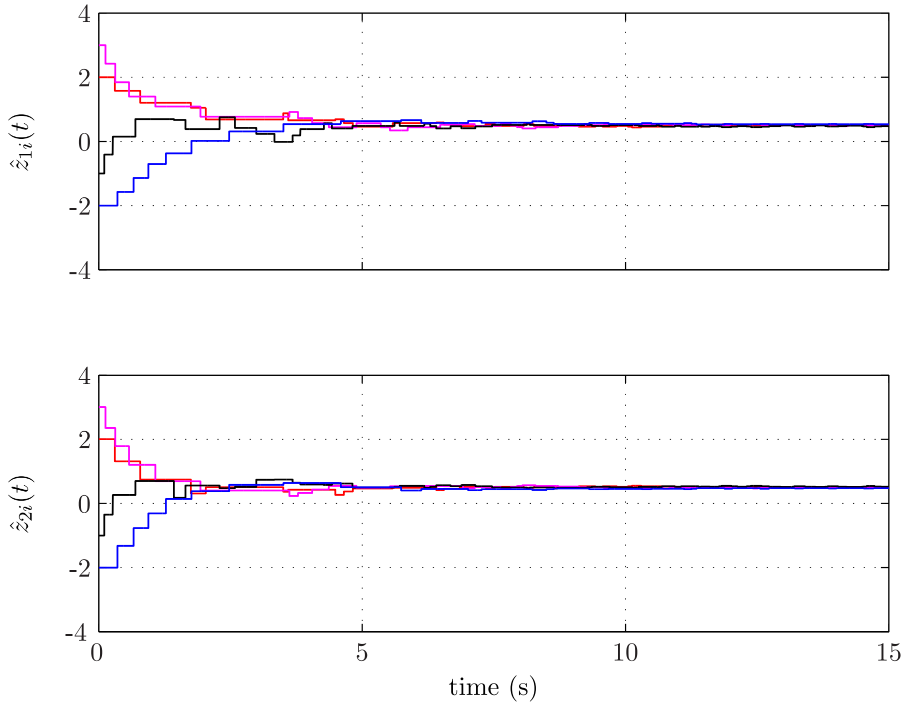

Figure 3.7: Synchronization with trigger function (3.20): Transformed system states $\hat{z}_i(t)$

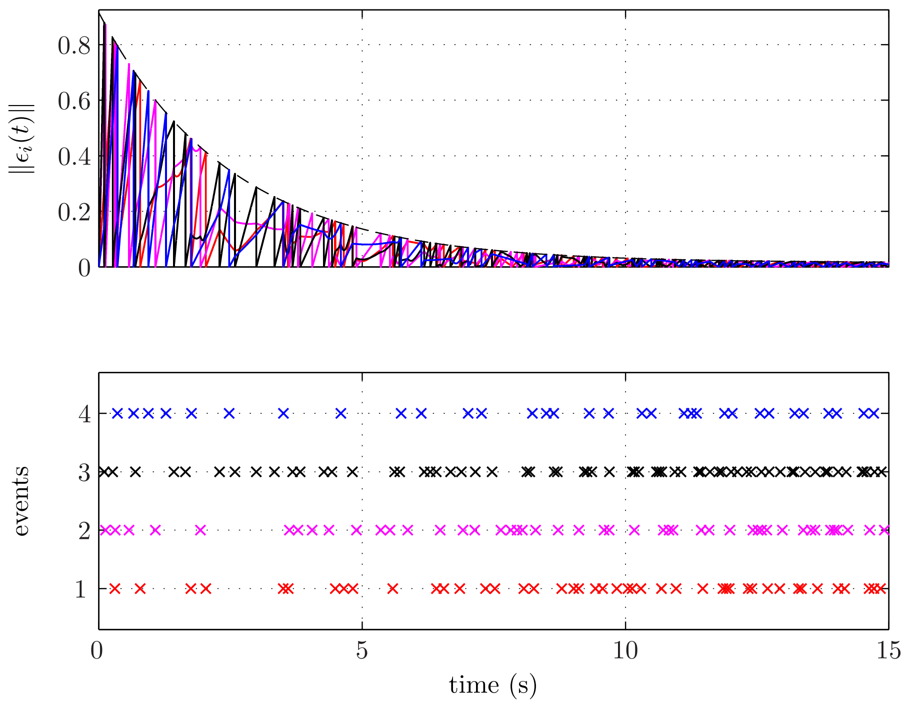

Figure 3.8: Synchronization with trigger function (3.20): Control measurement errors $\|\epsilon_i(t)\|$

3.2 Trigger Functions Depending on Control Input

In the previous section we have considered trigger functions which are depending on the transformed system variables $z_i = \mathrm{e}^{-At}x_i$. This section shows that linear identical system can be synchronized in an event-based fashion by trigger functions depending on the controller signals. The idea is the following. Synchronization of systems is reached whenever the control action of each system vanishes asymptotically and the solutions of the closed-loop systems converge asymptotically to a common solution of the individual systems. For our purpose we use the fact that the control outputs $u_i(t)$ converge asymptotically to zero.
Figure 3.9 illustrates the event-triggered implementation with trigger function (3.9). The trigger mechanism is placed after the controller. If the trigger condition is fulfilled, the actual control measurement value is is held constant till the next trigger event. The plant receives only piecewise constant control inputs $\hat{u}_i(t)$. In comparison to the configuration of the previous section we require continuous communication between the agents. We call this implementation Setup B.

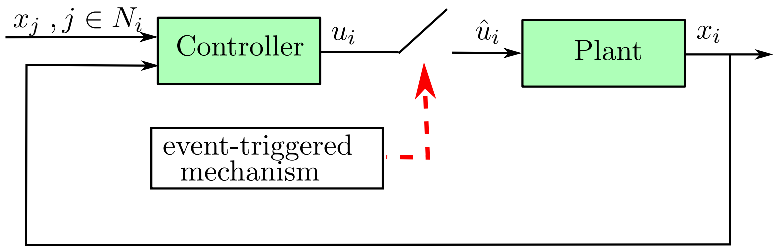

Figure 3.9: Event-triggered control schematic for trigger functions depending on control input

3.2.1 Time Depended Trigger Function

Especially the change of variables is unfavorable since this leads to more computation on the resource-limited micro-processor. Furthermore, we need an exact model of the system (system matrix A) in order to get the desired trigger mechanism. Small differences between the real system and the model can result in a not correctly working event-based trigger mechanism. Therefore, we present in this section a new approach which avoids the change of variables.
Analog to the previous section the control law of agent i (3.2) is updated whenever the trigger function

$$f_i\left(u_i(t), \hat{u}_i(t)\right) > 0. \tag{3.26}$$

Agent i has only access on $u_i(t)$ and latest triggered value $\hat{u}_i(t)$. Again, the broadcasting times t_k^i are determined recursively by the event trigger function as

$$t_{k+1}^i = \inf\{t : t > t_k^i, f_i(t) > 0\}.$$

The control input of agent i

$$\hat{u}_i(t) = u_i(t_k^i), \quad t \in [t_k^i, t_{k+1}^i[\tag{3.27}$$

is a piecewise constant function. In order to find suitable trigger function $f_i(\cdot)$ we define for each agent i the control measurement error

$$e_i(t) = \hat{u}_i(t) - u_i(t). \tag{3.28}$$

and the denote the stack vector $e = [e_1, e_2, \dots e_N]^T$. Besides, we consider only exponentially decreasing trigger functions of the form

$$f_i(e_i(t)) = \|e_i(t)\| - c\mathrm{e}^{-\alpha t}, \tag{3.29}$$

which are similar to (3.20) but without an additional constant offset.

Theorem 3.5. *Consider N linear system (3.1) with feedback control (3.2) and trigger functions of the form (3.29). Assume A is diagonalizable, all eigenvalues of A belong to the imaginary axis and B is a $n \times n$ nonsingular matrix. Let the communication graph G be undirected and connected, then for all initial conditions $x(0) \in \mathbb{R}^n$ and $t > 0$, it holds*

$$\|\delta(t)\| \leq e^{-\lambda_2(G)t}\|\delta(0)\| + k_V\sqrt{N}c\frac{\|\tilde{B}_N\|}{\alpha}\left(1 - e^{-\alpha t}\right),$$

with a positive constant $k_V = \|V\|\|V^{-1}\|$, where V is the matrix of the eigenvectors of $\tilde{A}_N$. Furthermore, the closed-loop system does not exhibit Zeno behavior.

Proof. For the closed-loop system with event-triggering we get

$$\begin{aligned}
\dot{x}_i &= Ax_i + B\hat{u}_i \\
&= Ax_i + B(u_i + e_i) \\
&= Ax_i + \sum_{j=1}^{N} a_{ij}(x_j - x_i) + Be_i.
\end{aligned}$$

Analog to the proofs of Theorem 3.3/3.4 we transform the coordinates $z_i = \mathrm{e}^{-At}x_i$. The time derivative of z_i yields to

$$\begin{aligned}
\dot{z}_i &= -\mathrm{e}^{-At}Ax_i + \mathrm{e}^{-At}\dot{x}_i \\
&= -\mathrm{e}^{-At}Ax_i + \mathrm{e}^{-At}(Ax_i + \sum_{j=1}^{N} a_{ij}(x_j - x_i) + Be_i) \\
&= \mathrm{e}^{-At}\sum_{j=1}^{N} a_{ij}(x_j - x_i) + \mathrm{e}^{-At}Be_i \\
&= \sum_{j=1}^{N} a_{ij}(z_j - z_i) + \mathrm{e}^{-At}Be_i
\end{aligned}$$

or in compact form

$$\dot{z}(t) = -\bar{L}_n z(t) + \mathrm{e}^{-\tilde{A}_N t}\tilde{B}_N e(t), \tag{3.30}$$

where $\mathrm{e}^{-\tilde{A}_N t} = I_N \otimes \mathrm{e}^{-At}$. We rewrite (3.30) in form of the disagreement vector to

$$\dot{\delta}(t) = -\bar{L}_n \delta(t) + \mathrm{e}^{-\tilde{A}_N t} \tilde{B}_N e(t). \tag{3.31}$$

The analytical solution of (3.31) is

$$\delta(t) = \mathrm{e}^{-\bar{L}_n t} \delta(0) + \int_0^t \mathrm{e}^{-\bar{L}_n (t-\tau)} \mathrm{e}^{-\tilde{A}_N \tau} \tilde{B}_N e(\tau) d\tau.$$

Since $\delta(t)$ has zero average, we bound the analytical solution with Lemma 3.2 as

$$\|\delta(t)\| \leq \mathrm{e}^{-\lambda_2(G)t} \|\delta(0)\| + \int_0^t \|\mathrm{e}^{-\bar{L}_n (t-\tau)}\| \|\mathrm{e}^{-\tilde{A}_N \tau}\| \|\tilde{B}_N\| \|e(\tau)\| d\tau. \tag{3.32}$$

Since the communication graph G is undirected connected, it holds $L = L^T \succeq 0$ and L is diagonalizable. Hence, the Laplacian matrix $\bar{L}_n$ can be decomposed according to

$$\bar{L}_n = W D_L W^{-1} \rightarrow \mathrm{e}^{-\bar{L}_n t} = W \mathrm{e}^{-D_L t} W^{-1},$$

where $D_L = \operatorname{diag}(0, \lambda_2, \ldots, \lambda_N)$ is the diagonal matrix of the eigenvalues of L_n and W is the matrix with the corresponding eigenvectors as its columns. The eigenvalues of L are denoted by $0 = \lambda_1 < \lambda_2 < \ldots < \lambda_n$. Since L is symmetric, we can always compute the eigenvectors as a orthonormal basis and it holds $\|W\| = \|W^{-1}\| = 1$. For the exponential diagonal matrix we have $\mathrm{e}^{-D_L t} = \operatorname{diag}\left(1, \mathrm{e}^{-\lambda_2 t}, \ldots, \mathrm{e}^{-\lambda_N t}\right)$ and $\lambda_{max}(\mathrm{e}^{-D_L t}) = 1$ for all $t \geq 0$. Hence we get for its Euclidean norm

$$\|\mathrm{e}^{-D_L t}\| = \sqrt{\lambda_{max}\left((\mathrm{e}^{-D_L t})^T \mathrm{e}^{-D_L t}\right)} = 1$$

and it follows

$$\begin{aligned} \mathrm{e}^{-\bar{L}_n t} &\leq \|\mathrm{e}^{-\bar{L}_n t}\| \\ &\leq \|W \mathrm{e}^{-D_L t} W^{-1}\| \\ &\leq \|W\| \|\mathrm{e}^{-D_L t}\| \|W^{-1}\| = 1. \end{aligned}$$

By assumption, the system matrix A is diagonalizable, i.e. all eigenvalues of A are distinct. Thus, we can always compute a set of eigenvectors which is linearly independent and can be used as a basis. Similar to the case of the Laplacian we write

$$\tilde{A}_N = V \Lambda V^{-1} \rightarrow \mathrm{e}^{-\tilde{A}_N t} = V \mathrm{e}^{-\Lambda t} V^{-1},$$

where Λ is a diagonal matrix with the eigenvalues occurring on the main diagonal and the columns of V are the eigenvectors of $\tilde{A}_N$. The system matrix has by assumption only eigenvalues which belong to the imaginary axis. Hence, the eigenvalues are of the form $\lambda_i = j\beta_i$, where j is the imaginary unit. We have

$$\mathrm{e}^{-\Lambda t} = I_N \otimes \operatorname{diag}(\mathrm{e}^{-\lambda_1 t}, \ldots \mathrm{e}^{-\lambda_n t}) = I_N \otimes \operatorname{diag}(\mathrm{e}^{-j\beta_1 t}, \ldots \mathrm{e}^{-j\beta_n t}).$$

With the identity $\mathrm{e}^{-j\beta_i t} = \cos(-\beta_i t) + j \sin(-\beta_i t)$ it is easy to see that the values are moving on the unit circle of the complex plane. Thus, $\|\mathrm{e}^{-\Lambda t}\| \leq 1$ and it holds

$$\begin{aligned} \mathrm{e}^{-\tilde{A}_N t} &= \|\mathrm{e}^{-\tilde{A}_N t}\| \\ &\leq \|V\| \|\mathrm{e}^{-\Lambda t}\| \|V^{-1}\| \\ &\leq \|V\| \|\|V^{-1}\| \|\mathrm{e}^{-\Lambda t}\| = \|V\| \|\|V^{-1}\|. \end{aligned}$$

Remark 3.2. If A has *repeated* eigenvalues (eigenvalues with multiplicity 2 or higher) it may not have a diagonal form representation. This bound holds only for a diagonalizable stable matrix and do not include the case of a general diagonal Jordan form representation [62, 63].

We proceed with (3.32) and the trigger function (3.29) enforces $\|e(\tau)\| \leq \sqrt{N} c \mathrm{e}^{-\alpha\tau}$. With the above stated bounds and defining $k_V = \|V\|\|V^{-1}\|$ we have

$$\begin{aligned}
\|\delta(t)\| &\leq \mathrm{e}^{-\lambda_2(G)t}\|\delta(0)\| + \int_0^t \|\mathrm{e}^{-\bar{L}_n(t-\tau)}\|\|\mathrm{e}^{-\tilde{A}_N\tau}\|\|\tilde{B}_N\|\sqrt{N} c\mathrm{e}^{-\alpha\tau} d\tau \\
&\leq \mathrm{e}^{-\lambda_2(G)t}\|\delta(0)\| + \int_0^t \|V\|\|V^{-1}\|\|\tilde{B}_N\|\sqrt{N} c\mathrm{e}^{-\alpha\tau} d\tau \\
&= \mathrm{e}^{-\lambda_2(G)t}\|\delta(0)\| + k_V\|\tilde{B}_N\|\sqrt{N} c \int_0^t \mathrm{e}^{-\alpha\tau} d\tau.
\end{aligned}$$

The integration yields finally to

$$\|\delta(t)\| \leq \mathrm{e}^{-\lambda_2(G)t}\|\delta(0)\| + k_V\sqrt{N} c \frac{\|\tilde{B}_N\|}{\alpha}\left(1 - \mathrm{e}^{-\alpha t}\right).$$

We have here also to ensure that there exists a positive lower bound on the inter-event times. The time derivative of control law (3.2) is given by

$$\begin{aligned}
\dot{u}_i &= B^{-1}\sum_{j=1}^N a_{ij}(\dot{x}_j - \dot{x}_i) \\
&= B^{-1}\sum_{j=1}^N a_{ij}(A(x_j - x_i) + B(\hat{u}_j - \hat{u}_i)) \\
&= B^{-1}A\sum_{j=1}^N a_{ij}(x_j - x_i) + \sum_{j=1}^N a_{ij}(\hat{u}_j - \hat{u}_i). \qquad (3.33)
\end{aligned}$$

We know that

$$Bu_i = \sum_{j=1}^N a_{ij}(x_j - x_i) \qquad (3.34)$$

holds and with (3.33) and (3.34) we derive

$$\begin{aligned}
\dot{u}_i &= B^{-1}ABu_i + \sum_{j=1}^N a_{ij}(\hat{u}_j - \hat{u}_i) \\
&= A^* u_i + \sum_{j=1}^N a_{ij}(\hat{u}_j - \hat{u}_i), \qquad (3.35)
\end{aligned}$$

where $A^* = B^{-1}AB$. Equation (3.35) can with the control measurement error (3.28) be rewritten to

$$\dot{u}_i = A^* u_i + \sum_{j=1}^N a_{ij}(e_j - e_i + u_j - u_i)$$

or in compact form

$$\begin{aligned}\dot{u}(t) &= \tilde{A}_N^* u(t) - \bar{L}_n u(t) - \bar{L}_n e(t)\\ &= (\tilde{A}_N^* - \bar{L}_n)u(t) - \bar{L}_n e(t).\end{aligned} \tag{3.36}$$

Remark 3.3. The transformation of the form $A^* = B^{-1}AB$ is a similarity transformation. The similarity transformation is a linear change of coordinates. A and A^* are similar matrices, i.e. they represent the same linear transformation after a change of basis. For our proof it is important that the eigenvalues of A^* are the same as for A.

The analytical solution of (3.36) is

$$u(t) = \mathrm{e}^{(\tilde{A}_N^* - \bar{L}_n)t} u(0) - \int_0^t \mathrm{e}^{(\tilde{A}_N^* - \bar{L}_n)(t-\tau)} \bar{L}_n e(\tau) d\tau.$$

We decompose $\mathrm{e}^{\tilde{A}_N^* t} = V^* \mathrm{e}^{\Lambda t} V^{*-1}$ and it holds

$$\mathrm{e}^{\tilde{A}_N^* t} \leq \|V^*\| \|\mathrm{e}^{\Lambda t}\| \|V^{*-1}\| \leq \|V^*\| \|V^{*-1}\| = k_{V^*}. \tag{3.37}$$

Thereby, the columns of V^* are the eigenvectors of A_N^*. Since $\|\mathrm{e}^{-\bar{L}_n t}\| \leq 1$, $\|\mathrm{e}^{\tilde{A}_N^* t}\| \leq k_{V^*}$ and $\|e(\tau)\| \leq \sqrt{N} c \mathrm{e}^{-\alpha\tau}$, we bound the analytical solution as follows

$$\begin{aligned}\|u(t)\| &\leq \|\mathrm{e}^{(\tilde{A}_N^* - \bar{L}_n)t} u(0)\| + \|\int_0^t \mathrm{e}^{(\tilde{A}_N^* - \bar{L}_n)(t-\tau)} \bar{L}_n e(\tau) d\tau\|\\ &\leq \|\mathrm{e}^{(\tilde{A}_N^* - \bar{L}_n)t}\| \|u(0)\| + \int_0^t \|\mathrm{e}^{(\tilde{A}_N^* - \bar{L}_n)(t-\tau))}\| \|\bar{L}_n\| \|e(\tau)\| d\tau\\ &\leq k_{V^*} \|u(0)\| + \int_0^t k_{V^*} \|\bar{L}_n\| \|e(\tau)\| d\tau\\ &\leq k_{V^*} \|u(0)\| + \int_0^t k_{V^*} \|\bar{L}_n\| \sqrt{N} c \mathrm{e}^{-\alpha\tau} d\tau\\ &= k_{V^*} \left(\|u(0)\| + \frac{\|\bar{L}_n\|}{\alpha} \sqrt{N} c (1 - \mathrm{e}^{-\alpha t}) \right).\end{aligned} \tag{3.38}$$

We assume that the latest event trigger of agent i occurs at $t = t^* > 0$. Then it holds $\|e(t^*)\| = 0$ and agent i can not trigger again at the same time instance. Between two consecutive trigger events it holds that $\dot{e}_i(t) = -\dot{u}_i(t)$. With (3.36) we get

$$\begin{aligned}\|\dot{e}_i(t)\| \leq \|\dot{e}(t)\| &\leq \|\tilde{A}_N^* - \bar{L}_n\| \|u(t)\| + \|\bar{L}_n\| \|e(t)\|\\ &\leq \|\tilde{A}_N^* - \bar{L}_n\| \|u(t)\| + \|\bar{L}_n\| \sqrt{N} c \mathrm{e}^{-\alpha t}.\end{aligned} \tag{3.39}$$

An upper bound for (3.38) is

$$\|u(t)\| \leq k_{V^*} \left(\|u(0)\| + \sqrt{N} c \frac{\|\bar{L}_n\|}{\alpha} \right) \tag{3.40}$$

and with

$$\begin{aligned}k_1 &= k_{V^*} \|\tilde{A}_N^* - \bar{L}_n\| \left(\|u(0)\| + \sqrt{N} c \frac{\|\bar{L}_n\|}{\alpha} \right)\\ k_2 &= \|\bar{L}_n\| \sqrt{N} c\end{aligned}$$

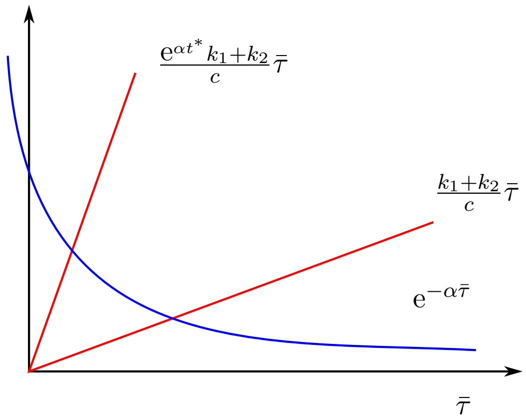

Figure 3.10: Graphical solution of (3.41)

we derive

$$\|\dot{e}_i(t)\| \leq k_1 + k_2\mathrm{e}^{-\alpha t} \leq k_1 + k_2\mathrm{e}^{-\alpha t^*}$$

for all $t > t^*$. Therefore, an upper bound on the control measurement error is

$$\|e_i(t)\| \leq \left(k_1 + k_2\mathrm{e}^{-\alpha t^*}\right)(t - t^*).$$

The next event is triggered as soon as

$$\|e_i(t)\| = c\mathrm{e}^{-\alpha t}.$$

Thus, a lower positive bound on the inter-event times $\tau = t - t^*$ is given by

$$\left(\mathrm{e}^{\alpha t^*}\frac{k_1}{c} + \frac{k_2}{c}\right)\tau = \mathrm{e}^{-\alpha\tau} \tag{3.41}$$

The right hand side and left hand side of (3.41) are strictly positive since $\alpha > 0$. The left hand side is upper bounded by $\mathrm{e}^{\alpha t^*}\frac{k_1+k_2}{c}$ and lower bounded by $\frac{k_1+k_2}{c}$. From Figure 3.10 it is clear that there exists a positive value of τ for all $t^* \geq 0$. $\square$

Unfortunately, we have to make stronger restrictions on the system matrix A. Considering (3.32), there remains the term $\mathrm{e}^{-\tilde{A}_N\tau}$ caused by the change of variables. If we allow that $\mathrm{Re}[\lambda_k(A)] \leq 0$, then we cannot bound (3.32) since $\|\mathrm{e}^{-\tilde{A}_N\tau}\| \overset{\tau\to\infty}{\to} \infty$. For those reasons we have to assume that A is diagonalizable and all eigenvalues belong to the imaginary axis.

Example 3.1. As in the previous examples we use the same example system but now with trigger function (3.29) and Setup B of the event-trigger mechanism like in Figure 3.9. The parameters are set to $c = 1.5$ and $\alpha = 0.4$. Figure 3.11 depicts the event-based synchronization of our four identical linear systems. As expected, in Figure 3.12 one can see that the transformed variables $z(t)$ converge to a common value. Figure 3.14 shows that the control action of each system converge piecewise constantly to zero. Furthermore, we have distinctly less events compared to the previous Examples 2 and 3, see Figure 3.13.

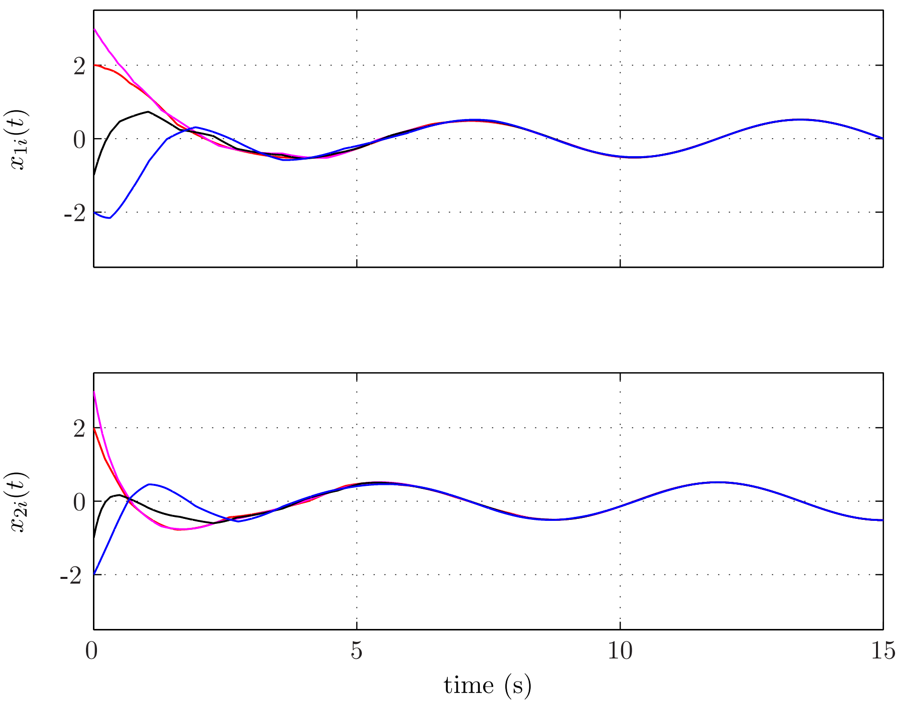

Figure 3.11: Synchronization with trigger function (3.29): System states $x_i(t)$

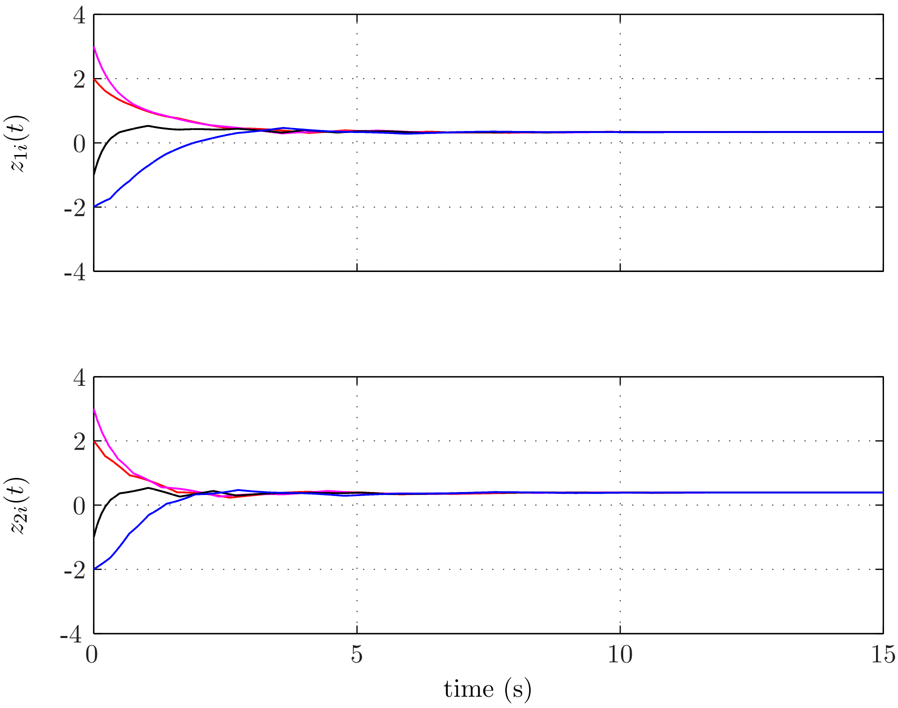

Figure 3.12: Synchronization with trigger function (3.29): Transformed system states $z_i(t)$

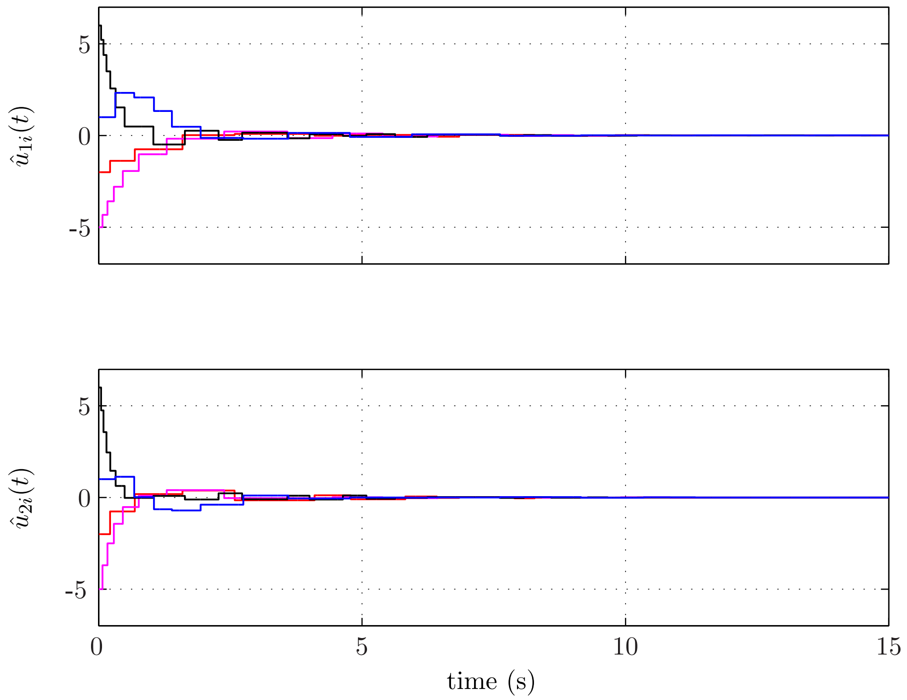

Figure 3.13: Synchronization with trigger function (3.29): Control inputs $\hat{u}_i(t)$

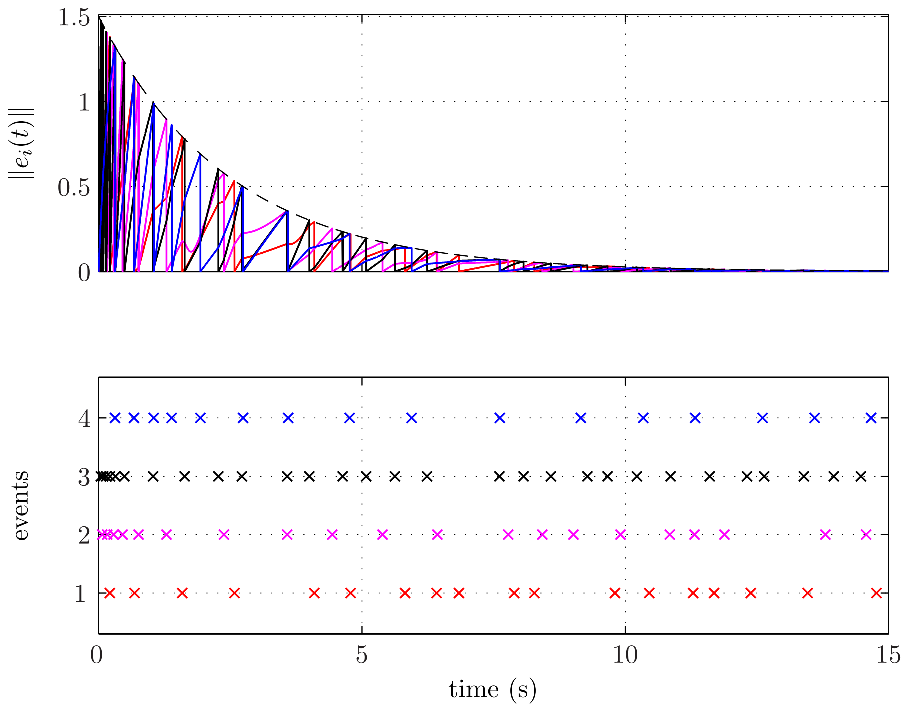

Figure 3.14: Synchronization with trigger function (3.29): Control measurement errors $\|e_i(t)\|$

3.2.2 Customized Time Depended Trigger Functions

The simulations of Example 3.1 show us that the event-based synchronization with Theorem 3.5 works very well. But compared to the theorems in Section 3.1 we have in Theorem 3.5 more assumptions on system matrix A. In this subsection we avoid the strict assumptions on A by taking a change of variables into account.
First, we define customized control measurement error

$$\varepsilon_i(t) = \mathrm{e}^{-At} B \left(\hat{u}_i(t) - u_i(t)\right) \tag{3.42}$$

and propose the time depended trigger functions

$$f_i(\varepsilon_i(t)) = ||\varepsilon_i(t)|| - c\mathrm{e}^{-\alpha t}. \tag{3.43}$$

Now we can state the following theorem.

Theorem 3.6. *Consider N linear system (3.1) with feedback control (3.2) and trigger functions of the form (3.43). Assume A is diagonalizable, all eigenvalues $Re[\lambda_k(A)] \leq 0, k = 1, \dots, n$ and B is a $n \times n$ nonsingular matrix. Let the communication graph G be undirected and connected, then for all initial conditions $x(0) \in \mathbb{R}^n$ and $t > 0$, it holds*

$$\|\delta(t)\| \leq e^{-\lambda_2 t}\|\delta(0)\| + \frac{\sqrt{N}c}{\alpha}\left(1 - e^{-\alpha t}\right).$$

Furthermore, the closed-loop system does not exhibit Zeno behavior.

Proof. We get for the latest triggered control input

$$\hat{u}_i(t) = B^{-1}\mathrm{e}^{At}\varepsilon_i(t) + u_i(t). \tag{3.44}$$

For the closed-loop system with event-trigger we obtain with (3.44) and the control law (3.2)

$$\begin{aligned}
\dot{x}_i &= Ax_i + B\hat{u}_i \\
&= Ax_i + B(B^{-1}\mathrm{e}^{At}\varepsilon_i + u_i) \\
&= Ax_i + \sum_{j=1}^{N} a_{ij}(x_j - x_i) + \mathrm{e}^{At}\varepsilon_i.
\end{aligned}$$

We change the variables $z_i = \mathrm{e}^{-At}x_i$, and get

$$\begin{aligned}
\dot{z}_i &= -\mathrm{e}^{-At}Ax_i + \mathrm{e}^{-At}\dot{x}_i \\
&= -\mathrm{e}^{-At}Ax_i + \mathrm{e}^{-At}(Ax_i + \sum_{j=1}^{N} a_{ij}(x_j - x_i) + \mathrm{e}^{At}\varepsilon_i) \\
&= \mathrm{e}^{-At}\sum_{j=1}^{N} a_{ij}(x_j - x_i) + \varepsilon_i \\
&= \sum_{j=1}^{N} a_{ij}(z_j - z_i) + \varepsilon_i
\end{aligned}$$

and in compact form

$$\dot{z} = -\bar{L}_n z + \varepsilon. \tag{3.45}$$

The disagreement dynamics are given by

$$\dot{\delta}(t) = -\bar{L}_n \delta(t) + \varepsilon(t). \tag{3.46}$$

The analytical solution of (3.46) is

$$\delta(t) = \mathrm{e}^{-\bar{L}_n t}\delta(0) + \int_0^t \mathrm{e}^{-\bar{L}_n(t-\tau)}\varepsilon(\tau)d\tau$$

and can be bounded as

$$\|\delta(t)\| \leq \mathrm{e}^{-\lambda_2 t}\|\delta(0)\| + \int_0^t \|\mathrm{e}^{-\bar{L}_n(t-\tau)}\|\|\varepsilon(\tau)\|d\tau.$$

It holds again that $\|\mathrm{e}^{-\bar{L}_n t}\| \leq 1$ and $\|\varepsilon(\tau)\| \leq \sqrt{N}c\mathrm{e}^{-\alpha\tau}$, hence

$$\begin{aligned}\|\delta(t)\| &\leq \mathrm{e}^{-\lambda_2 t}\|\delta(0)\| + \int_0^t \sqrt{N}c\mathrm{e}^{-\alpha\tau}d\tau \\ &= \mathrm{e}^{-\lambda_2 t}\|\delta(0)\| + \frac{\sqrt{N}c}{\alpha}\left(1 - \mathrm{e}^{-\alpha t}\right).\end{aligned}$$

Next we have to exclude Zeno-behavior. Same procedure as before, we start with (3.35) and get with $\hat{u}_i = B^{-1}\mathrm{e}^{At}\varepsilon_i + u_i$

$$\begin{aligned}\dot{u}_i &= A^* u_i + \sum_{j=1}^N a_{ij}(\hat{u}_j - \hat{u}_i) \\ &= A^* u_i + \sum_{j=1}^N a_{ij}(u_j - u_i) + B^{-1}\mathrm{e}^{At}\sum_{j=1}^N a_{ij}(\varepsilon_j - \varepsilon_i)\end{aligned}$$

or in compact form

$$\dot{u}(t) = (\tilde{A}_N^* - \bar{L}_n)u(t) - \tilde{B}_N^{-1}\mathrm{e}^{\tilde{A}_N t}\bar{L}_n\varepsilon(t). \tag{3.47}$$

The analytical solution of (3.47) is given by

$$\dot{u}(t) = \mathrm{e}^{(\tilde{A}_N^* - \bar{L}_n)t}u(0) - \int_0^t \mathrm{e}^{(\tilde{A}_N^* - \bar{L}_n)(t-\tau)}\tilde{B}_N^{-1}\mathrm{e}^{\tilde{A}_N t}\bar{L}_n\varepsilon(\tau)d\tau.$$

The matrix $\tilde{A}_N^*$ is diagonalizable by assumptions. Thus, we can decompose according to

$$\tilde{A}_N^* = V^* D_A V^{*-1} \Rightarrow \mathrm{e}^{\tilde{A}_N^* t} = V^*\mathrm{e}^{\Lambda t}V^{*-1}. \tag{3.48}$$

For the eigenvalue of A with the maximum real part we write $\lambda_{max}(A) = \max_k\{\mathrm{Re}[\lambda_k(A)]\}$ and therefore

$$\begin{aligned}\|\mathrm{e}^{\tilde{A}_N^* t}\| &\leq \|V^*\mathrm{e}^{\Lambda t}V^{*-1}\| \\ &\leq \|V^*\|\|V^{*-1}\|\mathrm{e}^{\lambda_{max}(A)t} = k_{V^*}\mathrm{e}^{\lambda_{max}(A)t},\end{aligned}$$

where $k_{V^*} = \|V^*\|\|V^{*-1}$. Like in Remark 3.2, this bound does not include a general diagonal Jordan form representation and is only true for a diagonalizable matrix A. The same holds for

$$\|e^{\tilde{A}_N t}\| \leq \|V\|\|V^{-1}\|e^{\lambda_{max}(A)t} = k_V e^{\lambda_{max}(A)t}.$$

The trigger functions (3.43) enforces $||\varepsilon(t)|| \leq \sqrt{N}ce^{-\alpha\tau}$ and hence an upper bound for the analytical solution with $\|e^{-\bar{L}_n t}\| \leq 1$ is

$$\begin{aligned}
\|\dot{u}(t)\| &\leq \|e^{(\tilde{A}_N^* - \bar{L}_n)t}\|\|u(0)\| + \int_0^t \|e^{(\tilde{A}_N^* - \bar{L}_n)(t-\tau)}\|\|\tilde{B}_N^{-1}\|\|e^{\tilde{A}_N\tau}\|\|\bar{L}_n\|\varepsilon(\tau)\|d\tau \\
&\leq k_{V^*}e^{\lambda_{max}(A)t}\|u(0)\| + \int_0^t k_{V^*}e^{\lambda_{max}(A)(t-\tau)}\|\tilde{B}_N^{-1}\|k_V e^{\lambda_{max}(A)\tau}\|\bar{L}_n\|\sqrt{N}ce^{-\alpha\tau}d\tau \\
&= k_{V^*}e^{\lambda_{max}(A)t}\|u(0)\| + k_{V^*}k_V\|\bar{L}_n\|\|\tilde{B}_N^{-1}\|\sqrt{N}ce^{\lambda_{max}(A)t}\int_0^t e^{-\alpha\tau}d\tau \\
&= k_{V^*}e^{\lambda_{max}(A)t}\|u(0)\| + \frac{k_{V^*}k_V}{\alpha}\|\bar{L}_n\|\|\tilde{B}_N^{-1}\|\sqrt{N}ce^{\lambda_{max}(A)t}\left(1 - e^{-\alpha t}\right) \\
&\leq k_{V^*}\|u(0)\| + \frac{k_{V^*}k_V}{\alpha}\|\bar{L}_n\|\|\tilde{B}_N^{-1}\|\sqrt{N}c.
\end{aligned}$$

The derivative of the error between two consecutive is

$$\begin{aligned}
\dot{\varepsilon}(t) &= e^{-At}B\dot{u}_i(t) \\
&\leq e^{-\tilde{A}_N t}\tilde{B}_N(\tilde{A}_N^* - \bar{L}_n)u(t) - \bar{L}_n\varepsilon(t) \\
&\leq \|e^{-\tilde{A}_N t}\|\|\tilde{B}_N\|\|\tilde{A}_N^* - \bar{L}_n\|\|u(t)\| + \|\bar{L}_n\|\|\varepsilon(t)\| \\
&\leq k_V\|\tilde{B}_N\|\|\tilde{A}_N^* - \bar{L}_n\|\|u(t)\| + \|\bar{L}_n\|\sqrt{N}ce^{-\alpha t}.
\end{aligned}$$

Defining

$$\begin{aligned}
d_1 &= k_V\|\tilde{B}_N\|\|\tilde{A}_N^* - \bar{L}_n\|\left(k_{V^*}\|u(0)\| + \frac{k_{V^*}k_V}{\alpha}\|\bar{L}_n\|\|\tilde{B}_N^{-1}\|\sqrt{N}c\right) \\
d_2 &= \|\bar{L}_n\|\sqrt{N}c
\end{aligned}$$

we get

$$\|\dot{\varepsilon}_i(t)\| \leq d_1 + d_2 e^{-\alpha t} \leq d_1 + d_2 e^{-\alpha t^*}.$$

Now we can argue like in the previous Section 3.2.1. Therefore, a lower positive bound is given by

$$\left(e^{\alpha t^*}\frac{d_1}{c} + \frac{d_2}{c}\right)\tau = e^{-\alpha\tau}.$$

□

Example 3.2. Same example system as in the previous Example 3.1 but now with trigger function (3.43). The event-based synchronization of the oscillating systems is illustrated in Figure 3.15/3.16. The control inputs of each agent are piecewise constant functions and converge to zero (see Figure 3.17). In Figure 3.18 one can see that the quantity of trigger events are almost the same as in Example 3.1.

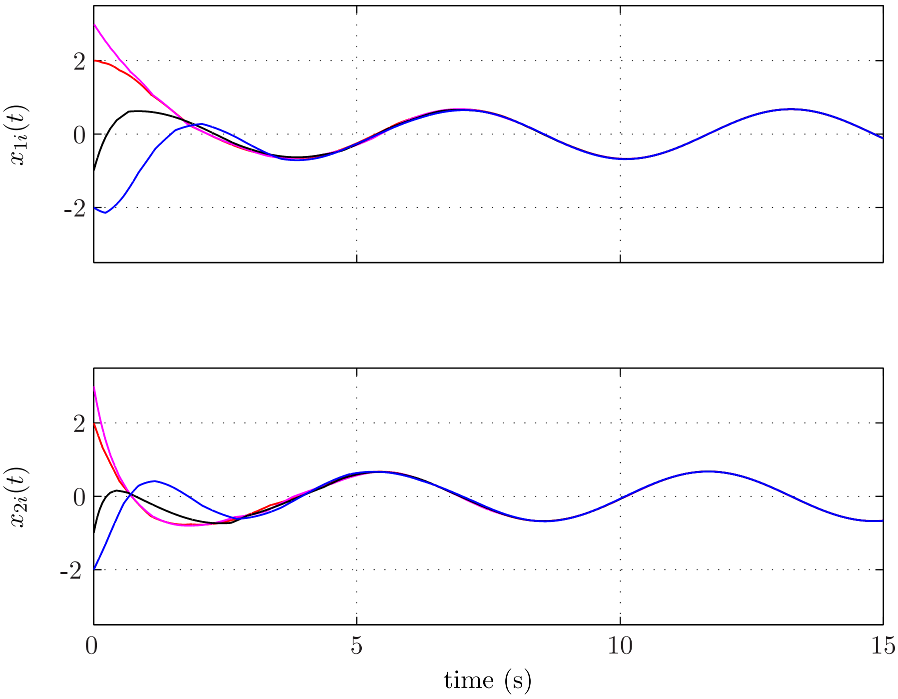

Figure 3.15: Synchronization with trigger function (3.43): System states $x_i(t)$

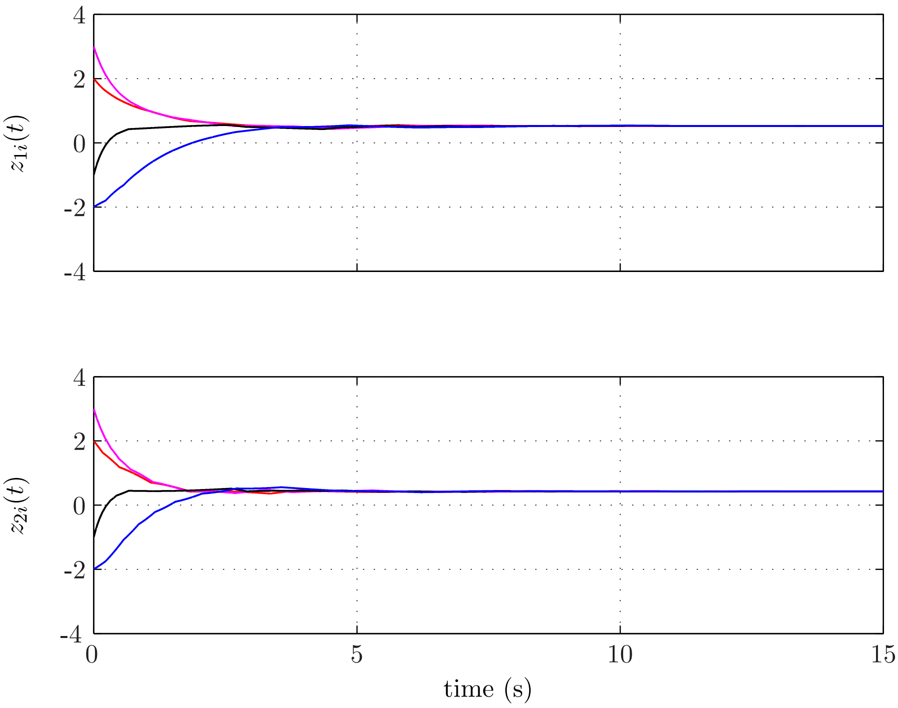

Figure 3.16: Synchronization with trigger function (3.43): Transformed system states $z_i(t)$

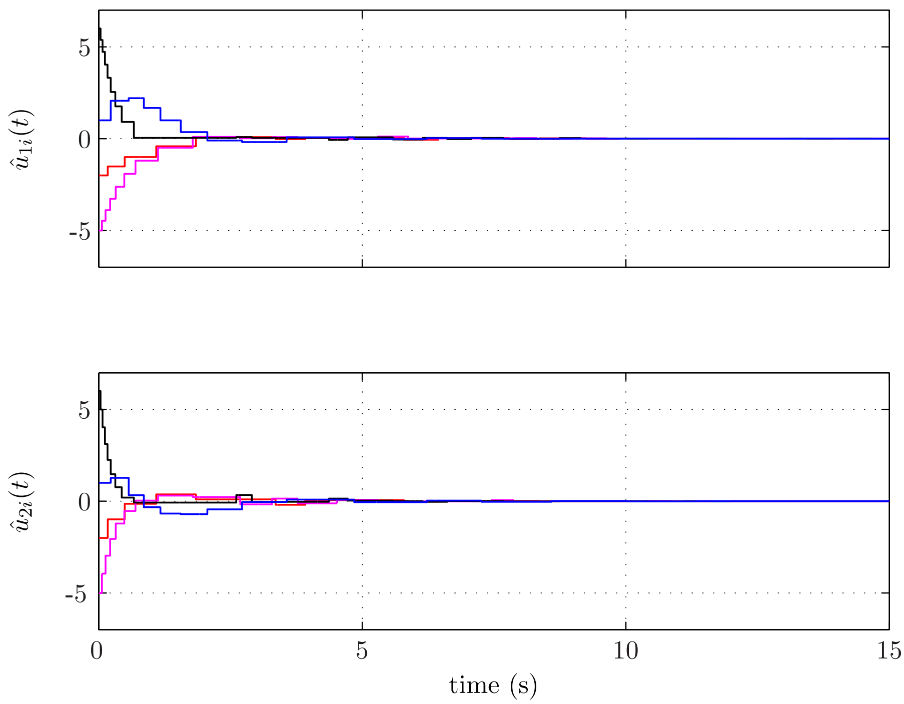

Figure 3.17: Synchronization with trigger function (3.43): Control inputs $u_i(t)$

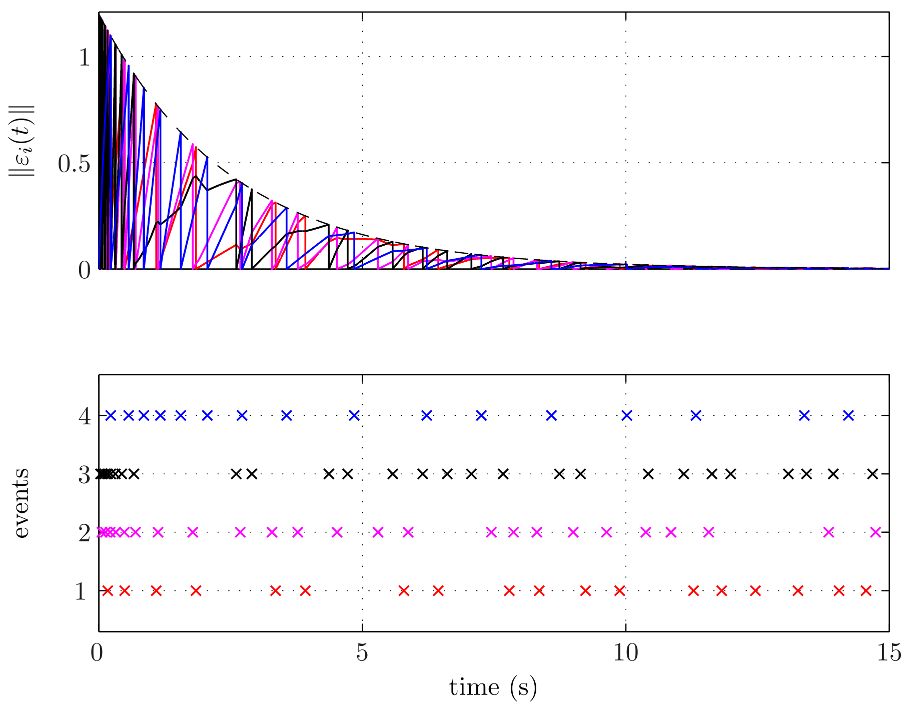

Figure 3.18: Synchronization with trigger function (3.43): Control measurement errors $\|\varepsilon_i(t)\|$

3.3 Discussion

In this chapter two different event-based strategies for the synchronization of identical systems (3.1) are presented. Both solve the problem statement in Section 2.4.1 but the setups of the event-trigger mechanism differ from each other (see Figure 3.1 and 3.9). The trigger functions of Setup A depend on the transfered system states $f_i\left(z_i(t), \hat{z}_i(t)\right)$ and the trigger functions $f_i\left(u_i(t), \hat{u}_i(t)\right)$ of Setup B on the control inputs.

Setup A in Section 3.1 synchronizes the agents in an event-based fashion, rendering both the control inputs and the system states piecewise constant. The neighboring agents do not require to exchange information continuously. The measurement broadcasts over the network are transmitted in an event-based manner, which reduces the traffic between each agents. Furthermore, we can use trigger functions of the form (3.20), which enable us more flexibility to adjust event-based synchronization. However, each agent i need to monitor the transformed system states $z_i(t)$. A permanent change of variables is necessary and thus we have to take more calculation into account. Moreover, we need a very exact model of the real system for a correctly working event-trigger mechanism.

Setup B renders only the control signals of agent i piecewise constant. Each agent receives the own states and the states of its neighbors continuously in order to update the control law. Therefore, the strategy requires a continuous communication between the neighboring systems, which is a serious limitation. The approach is also liable to measurement noise since small noise amplitudes could lead to trigger events for large times t.
Each agent monitors only its control inputs. In particular, agent i updates its own piecewise constant control signal at event times it decides based on its own local information (actual control input $u_i(t)$ and the latest trigger control input $\hat{u}_i(t)$). This is a big advantage if we have a big number of states or if we cannot measure all states. Furthermore, the simulation results show also that we need much less events to achieve synchronization compared to the first method. Setup B exhibits a much better event-triggering behavior in comparison to Setup A. Due to the proof in Theorem 3.5 we have to restrict the assumptions on system matrix A. With Theorem 3.6 we avoid this restrictions but require again a change of variables. Several numerical simulations have shown that event-based synchronization with trigger function (3.29) is still working for the case with $\mathrm{Re}[\lambda_k(A)] \leq 0$. Moreover, we could use without any problems trigger functions with an constant offset of the form

$$f_i(\varepsilon_i(t)) = ||e_i(t)|| - (c_1 + c_2 \mathrm{e}^{-\alpha t}).$$

However, a proof for this circumstances is outstanding. Therefore, for the upcoming approaches we focus only on the approaches of Theorem 3.5.

As summarized both approaches have their advantages and disadvantages. Depending on the given requirements one can chose between one of them. In the next chapter we transfer both event-based methods to the synchronization of linear identical systems with a dynamic controller.

4 Event-Based Synchronization of Linear Systems with Dynamic Controller

In the last chapter we presented new event-based approaches for the synchronization of linear identical systems with a static controller. The strict assumption of a square nonsingular matrix B can be avoided by introducing of a dynamic feedback controller. The two different setups of the previous chapter can be adapted for the event-based synchronization with the dynamic controller which is presented in Section 4.1. In Section 4.2 the dynamic feedback controller is extended to a dynamic output controller, which yields to the general event-based synchronization results for linear systems. In the last section we summarize and discuss the results.

4.1 Dynamic Feedback Controller

In the previous chapter we have the strict assumption of a square B-matrix. We can weaken the assumption of B to a stabilizability assumption on the pair (A, B) and introduce the dynamic feedback controller for synchronization presented in [17]. The goal of this section is to derive an event-based approach for the synchronization with the dynamic feedback controller.
Consider the dynamic feedback controller

$$\begin{aligned} \dot{\eta}_i &= (A + BK)\eta_i + \sum_{j=1}^{N} a_{ij}(\eta_j - \eta_i + x_i - x_j) \\ u_i &= K\eta_i, \end{aligned} \tag{4.1}$$

which leads with (3.1) to the closed-loop system

$$\dot{x} = \tilde{A}_N x + \tilde{B}_N \tilde{K}_N \eta \tag{4.2a}$$

$$\dot{\eta} = (\tilde{A}_N + \tilde{B}_N \tilde{K}_N)\eta + \bar{L}_n(x - \eta) \tag{4.2b}$$

where K is an arbitrary stabilizing feedback matrix.

Theorem 4.1. *[17] Consider the system (3.1). Assume all eigenvalues of A belong to the closed left-half complex plane, the communication graph G is connected, the corresponding Laplacian matrix L is piecewise continuous and bounded, and that the pair (A, B) is stabilizable. Let K be a stabilizing matrix such that $A+BK$ is Hurwitz. Then the solutions of (4.2) exponentially synchronize to a solution of the open loop system $\dot{x}_0 = Ax_0$.*

Proof. For the insight we summarize the proof of [17]. The change of coordinates $s_i = x_i - \eta_i$ leads (4.2) to

$$\dot{x} = (\tilde{A}_N + \tilde{B}_N\tilde{K}_N)x + \tilde{B}_N\tilde{K}_N s \tag{4.3a}$$

$$\dot{s} = \tilde{A}_N s - \bar{L}_n s. \tag{4.3b}$$

The two subsystem now are decoupled. For sub-system (4.3b) the assumptions of Theorem 3.1 are satisfied, thus its solutions exponentially synchronize to a solution of $\dot{s}_0 = As_0$. Therefore, the subsystem (4.2b) is an exponentially stable system driven by an input $\bar{L}_n s(t)$ that exponentially converges to zero. Consequently its solution $\eta(t)$ exponentially converges to zero, which implies that the solutions of (4.2a) exponentially synchronize to a solution of $\dot{x}_0 = Ax_0$.

For the new following event-based approaches, there is a need to introduce some new variables. We know that (4.3b) exponentially synchronizes to a solution of $\dot{s}_0 = As_0$. By defining

$$\xi_i = \mathrm{e}^{-At}s_i = \mathrm{e}^{-At}(x_i - \eta_i) \tag{4.4}$$

we get for its time derivative

$$\begin{aligned}
\dot{\xi}_i = \mathrm{e}^{-At}s_i = -\mathrm{e}^{-At}A + \mathrm{e}^{-At}\dot{s}_i &= -\mathrm{e}^{-At}A + \mathrm{e}^{-At}\left(A - \sum_{i=1}^{N} a_{ij}(s_j - s_i)\right) \\
&= -\mathrm{e}^{-At}\sum_{i=1}^{N} a_{ij}(s_j - s_i) \\
&= -\sum_{i=1}^{N} a_{ij}(\xi_j - \xi_i)
\end{aligned}$$

and in compact form

$$\dot{\xi}(t) = -\bar{L}_n\xi(t). \tag{4.5}$$

From Theorem 2.1 we know that the solutions $\xi_i(t)$ converge to an average value. Analog to the previous chapter we define the average value for $\xi(t)$ to

$$b(t) = \frac{1}{N}\sum_{i=1}^{N}\xi_i(t),$$

which is a constant value and can be calculated with

$$b = b(0) = \frac{1}{N}\sum_{i=1}^{N}\xi_i(0) = \frac{1}{N}\sum_{i=1}^{N}\mathrm{e}^{-A0}(x_i(0) - \eta_i(0)) = \frac{1}{N}\sum_{i=1}^{N}(x_i(0) - \eta_i(0)).$$

Hence, we decompose

$$\xi(t) = \mathbf{1}b + \delta_\xi(t), \tag{4.6}$$

where $\delta_\xi(t)$ is the disagreement vector with the condition $\mathbf{1}^T\delta_\xi(t) = 0$. The time derivative of the disagreement vector leads with (4.5) and (4.6) to

$$\dot{\delta}_\xi(t) = \dot{\xi}(t) = -\bar{L}_n\xi(t) = -\bar{L}_n(\mathbf{1}b + \delta_\xi(t)) = -\bar{L}_n\delta_\xi(t) \tag{4.7}$$

since $\mathbf{1}^T\bar{L}_n = 0$.

4.1.1 Trigger Functions Depending on System States

In the following we propose a new event-based approach for the synchronization of N identical linear systems with a dynamic feedback controller. If we can show that the $\xi_i(t)$ converge to a region around the average value b, then the sub-system (4.3b) exponentially synchronize which implies that the solutions of (4.2a) exponentially synchronize to a solution of $\dot{x}_0 = Ax_0$. The idea is similar to that in Section 3.1, where we have the case that the variable $z(t)$ converge to a common value. For agent i only the local variables $\xi_i(t)$ and the latest broadcasted values $\hat{\xi}_i(t)$ are available. Therefore, we propose the time-depended trigger functions

$$f(e_{\xi i}(t)) = \|e_{\xi i}(t)\| - \left(c_1 + c_2 \mathrm{e}^{-\alpha t}\right), \tag{4.8}$$

with the measurement error

$$e_{\xi i}(t) = \hat{\xi}_i(t) - \xi_i(t). \tag{4.9}$$

The transfered system state of agent i

$$\hat{\xi}_i(t) = \xi_i(t_i^i), \quad t \in [t_k^i, t_{k+1}^i[$$

are piecewise constant, and thus also the system states $\hat{x}_i(t) = x_i(t_i^i)$ and the controller states $\hat{\eta}_i(t) = \eta_i(t_i^i)$ for $t \in [t_k^i, t_{k+1}^i[$.

The implementation is similar to that of Setup A. The trigger mechanism of agent i receives the actual system states x_i and controller states η_i in order to perform the change of variable according to (4.4). If trigger condition (4.8) holds, agent i broadcasts its actual measurements ($\hat{x}_i$ and $\hat{\eta}_i$) over the network. The dynamical controller of agent i is updated if there is a new measurement update from agent i or its neighbors $j \in N$. The proposed trigger mechanism renders $\hat{x}_i$, $\hat{\eta}_i$ and thus according to (4.2b) also $\hat{\dot{\eta}}_i$ piecewise constant. Analog to Setup A, this implementation does not require continuous communication between the neighboring systems.
The following theorem can be seen as an extension of Theorem 3.4 to a dynamic feedback controller.

Theorem 4.2. *Consider N linear system (3.1) with the dynamic feedback control (4.1) and trigger functions of the form (4.8). Assume for A that all eigenvalues $Re[\lambda_k(A)] \leq 0$, $k = 1, \dots, n$, the pair (A, B) is stabilizable and $A + BK$ is Hurwitz. Let the communication graph G be undirected and connected, then for all initial conditions $x(0) \in \mathbb{R}^n$ and $t > 0$, it holds*

$$\begin{aligned}\|\delta_\xi(t)\| \leq & \|\bar{L}_n\|\sqrt{N}\frac{c_1}{\lambda_2(G)} + e^{-\alpha t}\|\bar{L}_n\|\sqrt{N}\frac{c_2}{\lambda_2(G) - \alpha} \\ & + e^{-\lambda_2(G)t}\left(\|\delta_\xi(0)\| - \|\bar{L}_n\|\sqrt{N}\left(\frac{c_1}{\lambda_2(G)} + \frac{c_2}{\lambda_2(G) - \alpha}\right)\right)\end{aligned}$$

Furthermore, the closed-loop system does not exhibit Zeno behavior.

Proof. In presence of event-triggering the transformed closed-loop system (4.5) changes to

$$\dot{\xi}(t) = -\bar{L}_n\hat{\xi}(t) = -\bar{L}_n\xi(t) - \bar{L}_n e_\xi(t). \tag{4.10}$$

With (4.7) the disagreement dynamics with event-triggering can be derived to

$$\begin{aligned}\dot{\delta}_\xi(t) &= -\bar{L}_n \hat{\xi}(t) \\ &= -\bar{L}_n(\xi(t) + e_{\xi i}(t)) \\ &= -\bar{L}_n(\mathbf{1}b + \delta_\xi(t) + e_{\xi i}(t)) \\ &= -\bar{L}_n \delta_\xi(t) - \bar{L}_n e_{\xi i}(t)\end{aligned}$$

The outgoing proof is exactly the same as the proof of Theorem 3.4 but in place for $\delta(t)$ we have here $\delta_\xi(t)$. □

Example 4. We extend the example system with the dynamic controller (4.1) and trigger function (4.8). We set the input matrix to $B = \begin{bmatrix} 0 & 1 \end{bmatrix}^T$ such that the pair (A, B) is stabilizable. For the stabilizing feedback matrix we choose $K = \begin{bmatrix} 0 & -1 \end{bmatrix}$ such that $A + BK$ is Hurwitz. The initial condition of the controller states are set to $\eta(0) = \begin{bmatrix} 0, \ldots, 0 \end{bmatrix}^T$. Figure 4.1 shows the event-based synchronization of the system states $x_i(t)$ with the dynamic feedback controller. The transfered states $\xi_i(t)$ converge in a piecewise constant manner to a common value (see Figure 4.2). Figure 4.3 illustrates the events generated by trigger function (see Figure 4.8). Compared to Example 3 the events are more dense for at the beginning. Again the density of the events increase a little bit for larger times t.

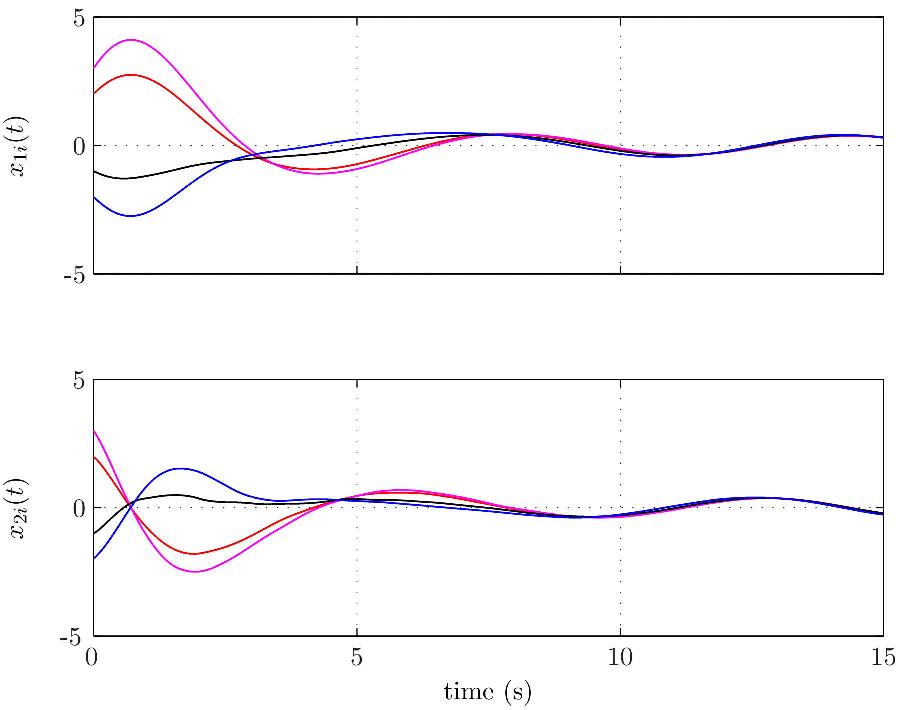

Figure 4.1: Synchronization with trigger function (4.8): System states $x_i(t)$

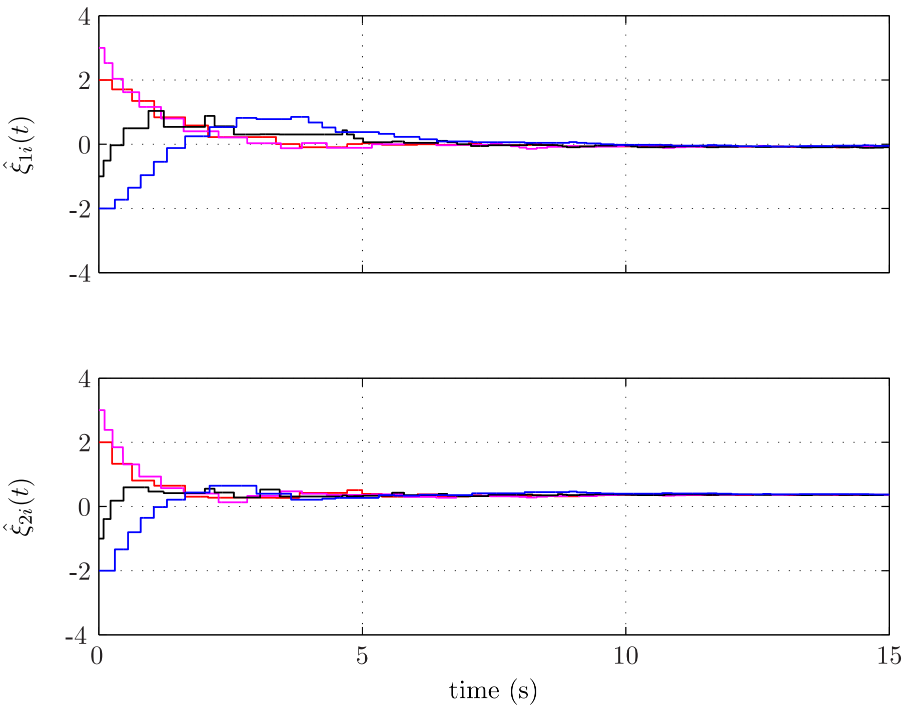

Figure 4.2: Synchronization with trigger function (4.8): Transfered states $\xi_i(t)$

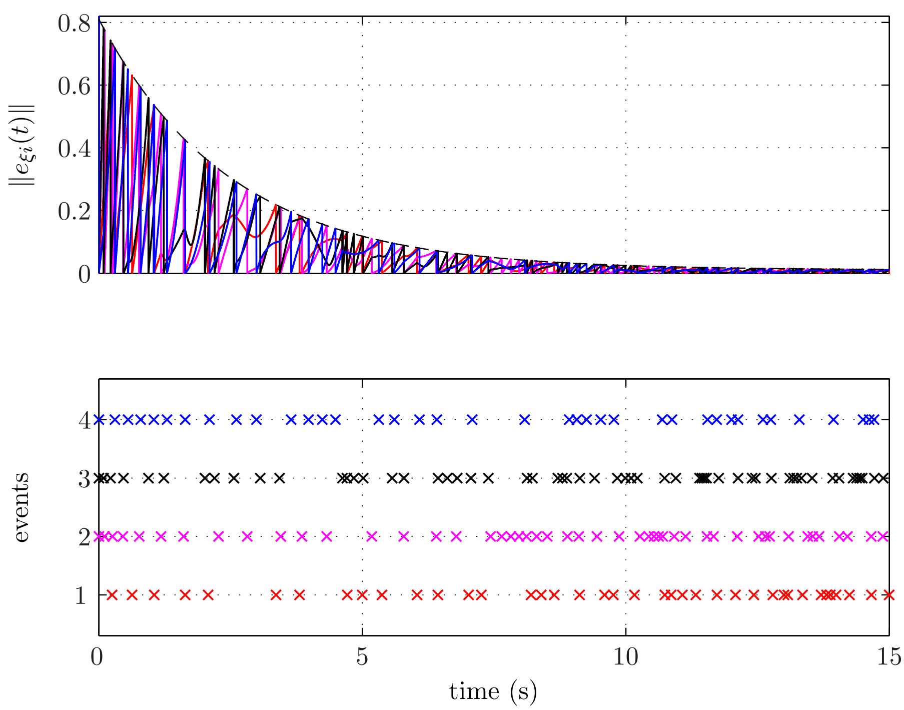

Figure 4.3: Synchronization with trigger function (4.8): Measurement errors $\|e_{\xi i}(t)\|$

4.1.2 Trigger Functions Depending on Controller States

In Section 3.2.1 we presented trigger functions which are only based on the control signals. In this section we adapt this trigger mechanism to the synchronization with dynamic feedback controller. The idea is again to show that $\xi(t)$ exponentially converge to a region around the average value but now with trigger functions depending on the controller states. Each agent requires knowledge only of the actual controller states $\eta_i(t)$ and the latest triggered controller states $\hat{\eta}_i(t)$ in order to verify the trigger condition. Therefore, we define

$$\epsilon_{\eta i}(t) = \hat{\eta}_i(t) - \eta_i(t) \tag{4.11}$$

and propose time-dependent trigger functions described by

$$f_i(\epsilon_{\eta i}(t)) = \|\epsilon_{\eta i}(t)\| - c\mathrm{e}^{-\alpha t}. \tag{4.12}$$

The controller states are held constant

$$\hat{\eta}_i(t) = \eta_i(t_i^i), \quad t \in [t_k^i, t_{k+1}^i[.$$

between two consecutive events. Remark that the trigger functions (4.12) have the same form as the trigger functions (3.29). The implementation is analogical to Setup B. The trigger mechanism is placed after the incoming controller states $\eta_i(t)$. Trigger condition (4.12) renders the controller states $\hat{\eta}_i$ and therefore according to (4.1) also the control inputs $\hat{u}_i(t)$ piecewise constant. This setup requires a continuous communication between the neighboring agents.

Theorem 4.3. *Consider N linear system (3.1) with the dynamic feedback control (4.1) and trigger functions of the form (4.12). Assume A is diagonalizable, all eigenvalues of A belong to the imaginary axis, the pair (A, B) is stabilizable and $A + BK$ is Hurwitz and diagonalizable. Let the communication graph G be undirected and connected, then for all initial conditions $x(0) \in \mathbb{R}^n$ and $t > 0$, it holds*

$$\|\delta_\xi(t)\| \leq e^{-\lambda_2 t}\|\delta_\xi(0)\| + k_V \frac{\|\bar{L}_n - \tilde{A}_N\|}{\alpha}\sqrt{N}c\left(1 - e^{-\alpha t}\right),$$

with a positive constant $k_V = \|V\|\|V^{-1}\|$, where V is the matrix of the eigenvectors of $\tilde{A}_N$. Furthermore, the closed-loop system does not exhibit Zeno behavior.

Proof. The event-triggered dynacmics of agent i are given by

$$\dot{x}_i = Ax_i + BK\hat{\eta}_i \tag{4.13a}$$

$$\dot{\eta}_i = (A + BK)\hat{\eta}_i + \sum_{i=1}^{N} a_{ij}(\hat{\eta}_j - \hat{\eta}_i + x_i - x_j). \tag{4.13b}$$

Thus, the derivative of s_i yields to

$$\begin{aligned}
\dot{s}_i &= \dot{x}_i - \dot{\eta}_i, \\
&= Ax_i + BK\hat{\eta}_i - \left((A+BK)\hat{\eta}_i + \sum_{i=1}^{N} a_{ij}(\hat{\eta}_j - \hat{\eta}_i + x_i - x_j) \right) \\
&= Ax_i - A\hat{\eta}_i - \sum_{i=1}^{N} a_{ij}(\hat{\eta}_j - \hat{\eta}_i + x_i - x_j) \\
&= Ax_i - A(\eta_i + \epsilon_{\eta i}) - \sum_{i=1}^{N} a_{ij}(\epsilon_{\eta j} + \eta_j - \epsilon_{\eta i} - \eta_i + x_i - x_j) \\
&= As_i - A\epsilon_{\eta i} - \sum_{i=1}^{N} a_{ij}(\epsilon_{\eta j} - \epsilon_{\eta i} + s_i - s_j).
\end{aligned}$$

With the change of variables $\xi_i = \mathrm{e}^{-At} s_i$ we get for its derivative

$$\begin{aligned}
\dot{\xi}_i &= -\mathrm{e}^{-At} As_i + \mathrm{e}^{-At}(As_i - A\epsilon_{\eta i} - \sum_{i=1}^{N} a_{ij}(\epsilon_{\eta j} - \epsilon_{\eta i} + s_i - s_j)) \\
&= \mathrm{e}^{-At} \sum_{i=1}^{N} a_{ij}(\epsilon_{\eta i} - \epsilon_{\eta j} + s_j - s_i) - \mathrm{e}^{-At} A\epsilon_{\eta i} \\
&= \sum_{i=1}^{N} a_{ij}(\xi_j - \xi_i) + \mathrm{e}^{-At} \sum_{i=1}^{N} a_{ij}(\epsilon_{\eta i} - \epsilon_{\eta j}) - \mathrm{e}^{-At} A\epsilon_{\eta i}
\end{aligned}$$

and in compact form

$$\begin{aligned}
\dot{\xi}(t) &= -\bar{L}_n \xi(t) + \mathrm{e}^{-\tilde{A}_N t} \bar{L}_n \epsilon_\eta(t) - \mathrm{e}^{-\tilde{A}_N t} \tilde{A}_N \epsilon_\eta(t) \\
&= -\bar{L}_n \xi(t) + \mathrm{e}^{-\tilde{A}_N t} (\bar{L}_n - \tilde{A}_N) \epsilon_\eta(t).
\end{aligned}$$

The disagreement dynamics can be derived to

$$\dot{\delta}_\xi(t) = -\bar{L}_n \delta_\xi(t) + \mathrm{e}^{-\tilde{A}_N t} (\bar{L}_n - \tilde{A}_N) \epsilon_\eta(t) \tag{4.14}$$

We obtain for the analytical solution of (4.14)

$$\delta_\xi(t) = \mathrm{e}^{-\bar{L}_n t} \delta_\xi(0) + \int_0^t \mathrm{e}^{-\bar{L}_n (t-\tau)} \mathrm{e}^{-\tilde{A}_N \tau} (\bar{L}_n - \tilde{A}) \epsilon_\eta(\tau) d\tau \tag{4.15}$$

By assumptions the system matrix A is stable and diagonalizable, thus $\|\mathrm{e}^{-\tilde{A}_N \tau}\| \leq k_V$ and with $\|\bar{L}_n\| \leq 1$ we bound as follows

$$\begin{aligned}
\|\delta_\xi(t)\| &\leq \|\mathrm{e}^{-\bar{L}_n t} \delta_\xi(0)\| + \| \int_0^t \mathrm{e}^{-\bar{L}_n (t-\tau)} \mathrm{e}^{-\tilde{A}_N \tau} (\bar{L}_n - \tilde{A}) \epsilon_\eta(\tau) d\tau \| \\
&\leq \|\mathrm{e}^{-\bar{L}_n t} \delta_\xi(0)\| + \int_0^t \|\mathrm{e}^{-\bar{L}_n (t-\tau)}\| \|\mathrm{e}^{-\tilde{A}_N \tau}\| \|(\bar{L}_n - \tilde{A})\| \|\epsilon_\eta(\tau)\| d\tau \\
&\leq \mathrm{e}^{-\lambda_2 t} \|\delta_\xi(0)\| + \int_0^t k_V \|\bar{L}_n - \tilde{A}_N\| \|\epsilon_\eta(\tau)\| d\tau.
\end{aligned}$$

The condition of trigger function (4.12) yields to

$$\|\delta_\xi(t)\| \leq \mathrm{e}^{-\lambda_2 t}\|\delta_\xi(0)\| + k_V\|\bar{L}_n - \tilde{A}_N\| \int_0^t \sqrt{N} c \mathrm{e}^{-\alpha\tau} d\tau$$

and the integration finally to

$$\|\delta_\xi(t)\| \leq \mathrm{e}^{-\lambda_2 t}\|\delta_\xi(0)\| + k_V \frac{\|\bar{L}_n - \tilde{A}_N\|}{\alpha} \sqrt{N} c \left(1 - \mathrm{e}^{-\alpha t}\right). \tag{4.16}$$

Next we have to show that there exists a positive lower bound on the inter-event times. We start with (4.13b)

$$\begin{aligned} \dot{\hat{\eta}}_i &= (A + BK)\hat{\eta}_i + \sum_{i=1}^{N} a_{ij}(\hat{\eta}_j - \hat{\eta}_i + x_i - x_j) \\ &= (A + BK)(\epsilon_{\eta i} + \eta_i) + \sum_{j=1}^{N} a_{ij}(\epsilon_{\eta j} + \eta_j - \epsilon_{\eta i} - \eta_i + x_i - x_j), \end{aligned}$$

which can be with $P = A + BK$ stacked to

$$\dot{\eta}(t) = (\tilde{P}_N - \bar{L}_n)\eta(t) + (\tilde{P}_N - \bar{L}_n)\epsilon_\eta(t) + \bar{L}_n x(t). \tag{4.17}$$

The analytical solution of (4.17) is

$$\eta(t) = \mathrm{e}^{(\tilde{P}_N - \tilde{L}_n)t}\eta(0) + \int_0^t \mathrm{e}^{(\tilde{P}_N - \bar{L}_n)(t-\tau)}(\tilde{P}_N - \bar{L}_n)\epsilon_\eta(\tau) d\tau + \int_0^t \mathrm{e}^{(\tilde{P}_N - \bar{L}_n)(t-\tau)} \bar{L}_n x(\tau) d\tau. \tag{4.18}$$

We know that P is Hurwitz and diagonalizable by assumption. For the eigenvalue of P with the maximum real part we write $\lambda_{max}(P) = \max_k\{\mathrm{Re}[\lambda_k(P)]\}$ and it follows

$$\begin{aligned} \mathrm{e}^{\tilde{P}_N t} &= U \mathrm{e}^{D_P t} U^{-1}, \\ &\leq \|U\|\|\mathrm{e}^{D_P t}\|\|U^{-1}\| \\ &\leq \|U\|\|U^{-1}\|\mathrm{e}^{\lambda_{max}(P)t}, \end{aligned} \tag{4.19}$$

where D_P is the diagonal matrix with the eigenvalues and U contains the eigenvectors of $\tilde{P}_N$. We know from the proof of Theorem 4.1 that the systems synchronize to a solution of the open loop system $\dot{x}_0 = Ax_0$. Since A is stable, $x(\tau)$ can be bounded with

$$x_{max} = \sup_{0 \leq \tau \leq t} \|x(\tau)\| \quad \forall\, \tau \geq 0. \tag{4.20}$$

Defining $k_U = \|U\|\|U^{-1}\|$ and with the bounds $\mathrm{e}^{-\bar{L}_n t} \leq 1$, (4.19) and (4.20) we bound (4.18) as

$$\begin{aligned} \|\eta(t)\| \leq & k_U \mathrm{e}^{\lambda_{max}(P)t}\|\eta(0)\| + \int_0^t k_U \mathrm{e}^{\lambda_{max}(P)(t-\tau)}\|\tilde{P}_N - \bar{L}_n\|\|\epsilon_\eta(\tau)\| d\tau \\ &+ \int_0^t k_U \mathrm{e}^{\lambda_{max}(P)(t-\tau)}\|\bar{L}_n\| x_{max} d\tau. \end{aligned}$$

The eigenvalues of P are all negative, thus $\lambda_{max}(P) = -|\lambda_{max}(P)|$ and the trigger function (4.12) enforces $\|\epsilon_\eta(\tau)\| \leq \sqrt{N} c \mathrm{e}^{-\alpha\tau}$. It follows

$$\begin{aligned}\|\eta(t)\| \leq & k_U \left(\mathrm{e}^{-|\lambda_{max}(P)|t} \|\eta(0)\| + \|\tilde{P}_N - \bar{L}_n\| \int_0^t \sqrt{N} c \mathrm{e}^{-|\lambda_{max}(P)|(t-\tau)-\alpha\tau} d\tau \right.\\ & \left. + \|\bar{L}_n\| x_{max} \int_0^t \mathrm{e}^{-|\lambda_{max}(P)|(t-\tau)} d\tau \right)\end{aligned}$$

and the integration yields to

$$\begin{aligned}\|\eta(t)\| \leq & k_U \left(\mathrm{e}^{-|\lambda_{max}(P)|t} \|\eta(0)\| + \frac{\|\tilde{P}_N - \bar{L}_n\|}{|\lambda_{max}(P)| - \alpha} \sqrt{N} c \left(\mathrm{e}^{-\alpha t} - \mathrm{e}^{-|\lambda_{max}(P)|t} \right) \right.\\ & \left. + \frac{\|\bar{L}_n\|}{|\lambda_{max}(P)|} x_{max} \left(1 - \mathrm{e}^{-|\lambda_{max}(P)|t} \right) \right).\end{aligned} \tag{4.21}$$

We obtain an upper bound for (4.21) for $t \geq 0$ with

$$\|\eta(t)\| \leq k_U \left(\|\eta(0)\| + \frac{\|\bar{L}_n\|}{|\lambda_{max}(P)|} x_{max} + \frac{\|\tilde{P}_N - \bar{L}_n\|}{|\lambda_{max}(P)| - \alpha} \sqrt{N} c \mathrm{e}^{-\alpha t} \right). \tag{4.22}$$

Between two consecutive trigger events we have

$$\epsilon_{\eta i}(t) = -\eta_i(t)$$

and we obtain with (4.17) the following bounds

$$\begin{aligned}\|\dot{\epsilon}_{\eta i}(t)\| &\leq \|\dot{\epsilon}_\eta(t)\| \leq \|\dot{\eta}(t)\| \\ &\leq \|\tilde{P}_N - \bar{L}_n\| \|\eta(t)\| + \|\tilde{P}_N - \bar{L}_n\| \|e_\xi(t)\| + \|\bar{L}_n\| x(t)\| \\ &\leq \|\tilde{P}_N - \bar{L}_n\| \|\eta(t)\| + \|\tilde{P}_N - \bar{L}_n\| \sqrt{N} c \mathrm{e}^{-\alpha t} + \|\bar{L}_n\| x_{max}.\end{aligned}$$

Defining

$$\begin{aligned}f_1 &= k_U \|\tilde{P}_N - \bar{L}_n\| \left(\|\eta(0)\| + \frac{\|\bar{L}_n\|}{|\lambda_{max}(P)|} x_{max} \right) + \|\bar{L}_n\| x_{max} \\ f_2 &= \|\tilde{P}_N - \bar{L}_n\| \sqrt{N} c \left(1 - \frac{1}{|\lambda_{max}(P)| - \alpha} \right)\end{aligned}$$

we arrive at

$$\|\epsilon_{\eta i}(t)\| \leq f_1 + f_2 \mathrm{e}^{-\alpha t} \leq f_1 + f_2 \mathrm{e}^{-\alpha t^*}$$

for all $t \geq t^*$. We have derived the same expression as in the proof in Section 3.2.1 but with other coefficients. Therefore, a lower positive bound on the inter-event times τ is given by

$$\left(\mathrm{e}^{\alpha t^*} \frac{f_1}{c} + \frac{f_2}{c} \right) \tau = \mathrm{e}^{-\alpha \tau}.$$

□

Example 5. We take the same system as in Example 4 but now with trigger functions (4.12). An synchronization of the system states is reached (Figure 4.4 and 4.5). The piecewise constant controller states are depicted in Figure 4.6. As expected the controller states converge to zero. The norm of measurement errors and the events of each agents are illustrated in Figure 4.7. As one can see, there are distinctly less events compared to Example 4.

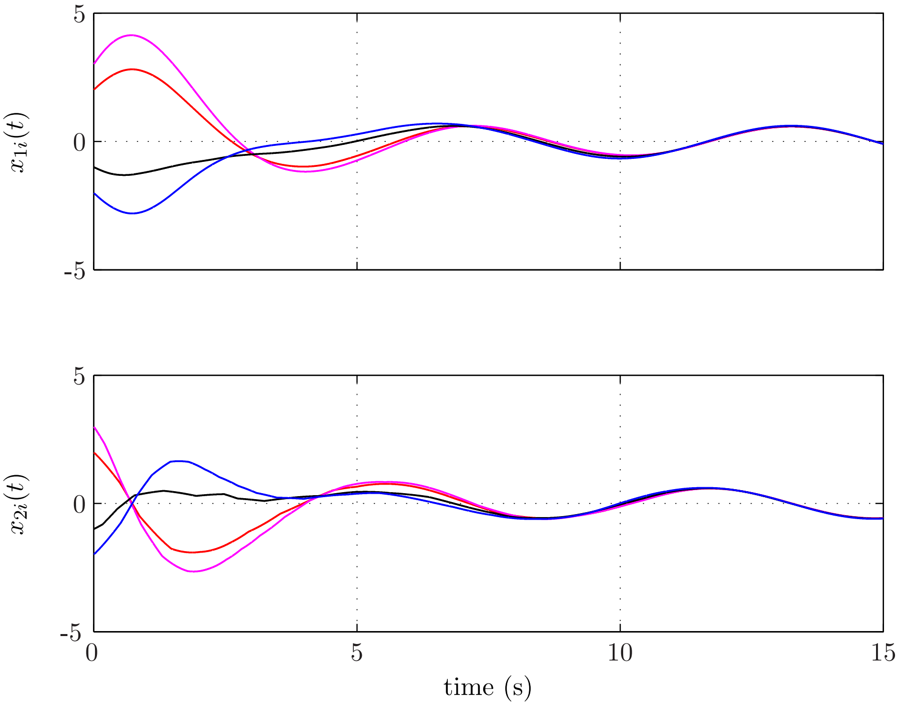

Figure 4.4: Synchronization with trigger function (4.12): System states $x_i(t)$

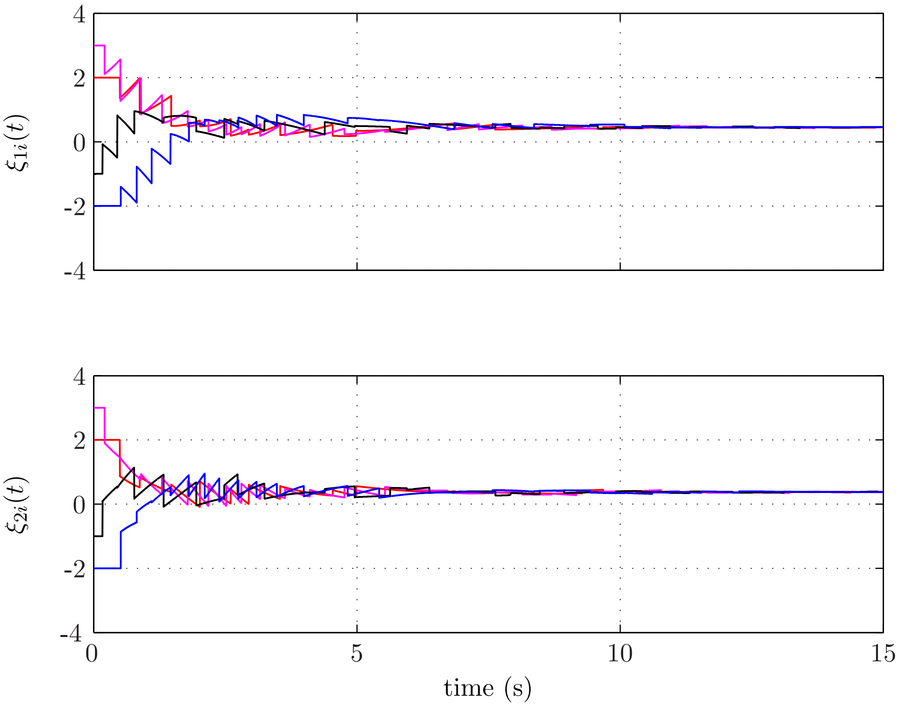

Figure 4.5: Synchronization with trigger function (4.12): Transfered states $\xi_i(t)$

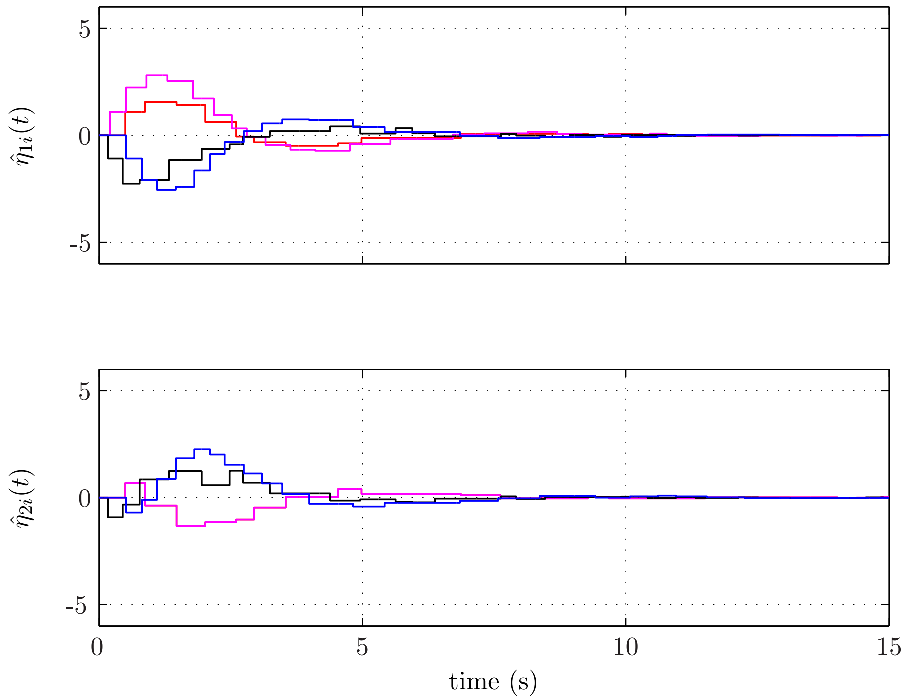

Figure 4.6: Synchronization with trigger function (4.12): Controller states $\hat{\eta}_i(t)$

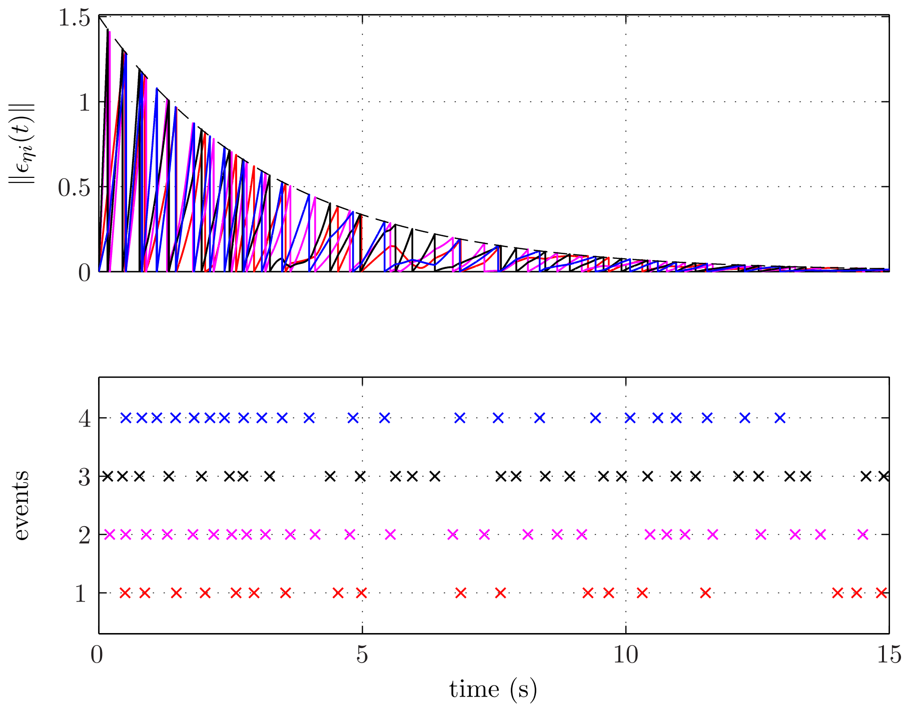

Figure 4.7: Synchronization with trigger function (4.12): Control measurement errors $\|\epsilon_{\eta i}(t)\|$

4.2 Dynamic Output Feedback Controller

By assuming that the pair (A, C) is detectable the dynamic feedback controller of Theorem 4.1 can be easily extended to an output feedback controller. We consider now N identical linear systems described by the model

$$\dot{x}_i = Ax_i + Bu_i, \tag{4.23a}$$
$$y_i = Cx_i \tag{4.23b}$$

for $i = 1, \dots, N$, with state vector $x_i \in \mathbb{R}^n$, control vector $u_i \in \mathbb{R}^m$ and output vector $y_i \in \mathbb{R}^p$. Let H be an observer matrix such that $A+HC$ is Hurwitz and we consider the output feedback controller

$$\dot{\eta}_i = (A + BK)\eta_i + \sum_{j=1}^{N} a_{ij}(\eta_j - \eta_i + \tilde{x}_i - \tilde{x}_j) \tag{4.24a}$$
$$\dot{\tilde{x}}_i = A\tilde{x}_i + Bu_i + H(\tilde{y}_i - y_i) \tag{4.24b}$$
$$u_i = K\eta_i \tag{4.24c}$$
$$\tilde{y}_i = C\tilde{x}_i. \tag{4.24d}$$

With the following theorem we arrive at a general synchronization result for linear systems.

Theorem 4.4. *[17] Consider the system (4.23). Assume all eigenvalues of A belong to the closed left-half complex plane, the communication graph G is connected, the corresponding Laplacian matrix L is piecewise continuous and bounded, the pair (A, B) is stabilizable and the pair (A, C) is detectable. Let K and H be any gain matrices such that $A + BK$ and $A+HC$ are Hurwitz. Then the solutions of (4.23) with dynamic controller (4.24) exponentially synchronize to a solution of the open loop system $\dot{x}_0 = Ax_0$.*

Proof. The proof is similar to the proof of Theorem 4.1 and is mainly based that the estimation error is decoupled from the consensus dynamics. With change of variables $s_i = \tilde{x}_i - \eta_i$ and $h_i = x_i - \tilde{x}_i$ we can rewrite the closed loop system as

$$\dot{x} = (\tilde{A}_N + \tilde{B}_N\tilde{K}_N)x + \tilde{B}_N\tilde{K}_N(h + s), \tag{4.25a}$$
$$\dot{s} = \tilde{A}_N s - \bar{L}_n s, \tag{4.25b}$$
$$\dot{h} = (\tilde{A}_N + \tilde{H}_N\tilde{C}_N)h. \tag{4.25c}$$

This system is the cascade of the closed-loop system analyzed in the proof of Theorem 4.1 with an exponentially stable estimation error dynamics, which proves the result.

The following approaches and proofs are similar to the case of event-based synchronization with the dynamic feedback controller in Section 4.1. We rewrite (4.25b) with the transformation

$$\xi_i' = \mathrm{e}^{-At}s_i = \mathrm{e}^{-At}(\tilde{x}_i - \eta_i) \tag{4.26}$$

to

$$\dot{\xi}'(t) = -\bar{L}_n\xi'(t). \tag{4.27}$$

Now, we only need to exploit the fact that the solutions of (4.27) according to Theorem 2.1 converge to an average value. Analog to the previous section we decompose

$$\xi'(t) = \mathbf{1}b' + \delta_{\xi'}(t) \tag{4.28}$$

with the disagreement vector $\delta_{\xi'}(t)$ and the average value b'. Therefore, we transfer the derived event-based approaches in Section 4.1 to the case for an output feedback controller.

4.2.1 Trigger Functions Depending on System States

We adapt Theorem 4.2 for an output feedback controller. Since we have exponentially stable estimation error dynamics, we can use trigger functions which are depending on the observer states $\tilde{x}_i$ instead of the real states x_i. The transfered states of agent i

$$\hat{\xi}'_i(t) = \xi'_i(t^i_i), \quad t \in [t^i_k, t^i_{k+1}[$$

are piecewise constant. Again, we propose time-depended trigger functions

$$f(e_{\xi' i}(t)) = \|e_{\xi' i}(t)\| - (c_1 + c_2 \mathrm{e}^{-\alpha t}), \tag{4.29}$$

with the measurement error

$$e_{\xi' i}(t) = \hat{\xi}'_i(t) - \xi'_i(t). \tag{4.30}$$

Theorem 4.5. *Consider N linear system (4.23) with the dynamic feedback control (4.24) and trigger functions of the form (4.29). Assume for A that all eigenvalues $\lambda_k(A) \leq 0$, $k = 1, \dots, n$, the pair (A, B) is stabilizable, the pair (A, C) is detectable, $A+BK$ and $A+HC$ are Hurwitz. Let the communication graph G be undirected and connected, then for all initial conditions $x(0) \in \mathbb{R}^n$ and $t > 0$, it holds*

$$\begin{aligned}\|\delta_{\xi'}\| \leq & \|\bar{L}_n\|\sqrt{N}\frac{c_1}{\lambda_2(G)} + e^{-\alpha t}\|\bar{L}_n\|\sqrt{N}\frac{c_2}{\lambda_2(G) - \alpha} \\ & + e^{-\lambda_2(G)t}\left(\|\delta_{\xi'}(0)\| - \|\bar{L}_n\|\sqrt{N}\left(\frac{c_1}{\lambda_2(G)} + \frac{c_2}{\lambda_2(G) - \alpha}\right)\right)\end{aligned}$$

Furthermore, the closed-loop system does not exhibit Zeno behavior.

Proof. Similar to the proof of Theorem the we rewrite (4.27) with (4.30) to

$$\dot{\xi}'(t) = -\bar{L}_n\hat{\xi}'(t) = -\bar{L}_n\xi'(t) - \bar{L}_n e_{\xi' i}(t). \tag{4.31}$$

Hence, the disagreement dynamics with event trigger are given by

$$\dot{\delta}_{\xi'}(t) = -\bar{L}_n\delta_{\xi'}(t) - \bar{L}_n e_{\xi i}(t). \tag{4.32}$$

For the remaining steps we use the same proof techniques as in Theorem 4.2 and derive the statement of Theorem 4.5. □

Example 6. We extend our system of Example 5 to an output (4.23b). Hence, we chose the output matrix $C = \begin{bmatrix} 1 & 0 \end{bmatrix}$ such that the pair (A, C) is detectable. The observer gain matrix is set to $H = \begin{bmatrix} -5 & -15 \end{bmatrix}^T$ such that $A + HC$ is Hurwitz and the observer dynamics are distinctly faster as the system dynamics. First, we consider the system without trigger mechanism. We need to check that the observer is correctly working. Therefore, we assume that the initial conditions $x(0)$ of the system are unknown for the observer. The initial conditions of the observer are arbitrarily chosen to $\tilde{x}(0) = \begin{bmatrix} 0, \ldots, 0 \end{bmatrix}^T$. For the case that the matrix H is correctly chosen, the observer states $\tilde{x}_i(t)$ have to converge to the system states $\tilde{x}_i(t)$. In Figure 4.8 one can see that the trajectories of the observed states $\tilde{x}_i(t)$ (dashed lines) converge to the true states $x_i(t)$ (solid lines). Next we add the trigger control described in Theorem 4.5. Figure 4.9 shows the event-based synchronization of the outputs $y_i(t)$ with trigger function (4.29). The transformed states converge to a common value in a piecewise constant manner, see Figure 4.10. The actual and observed system states are illustrated in Figure 4.10. Like with the system without trigger mechanism the observed states converge $\tilde{x}_i(t)$ (dashed) to the actual states $x_i(t)$ (solid). Compared to Example 4, the simulations shows that we have at the beginning much more trigger events (Figure 4.12).

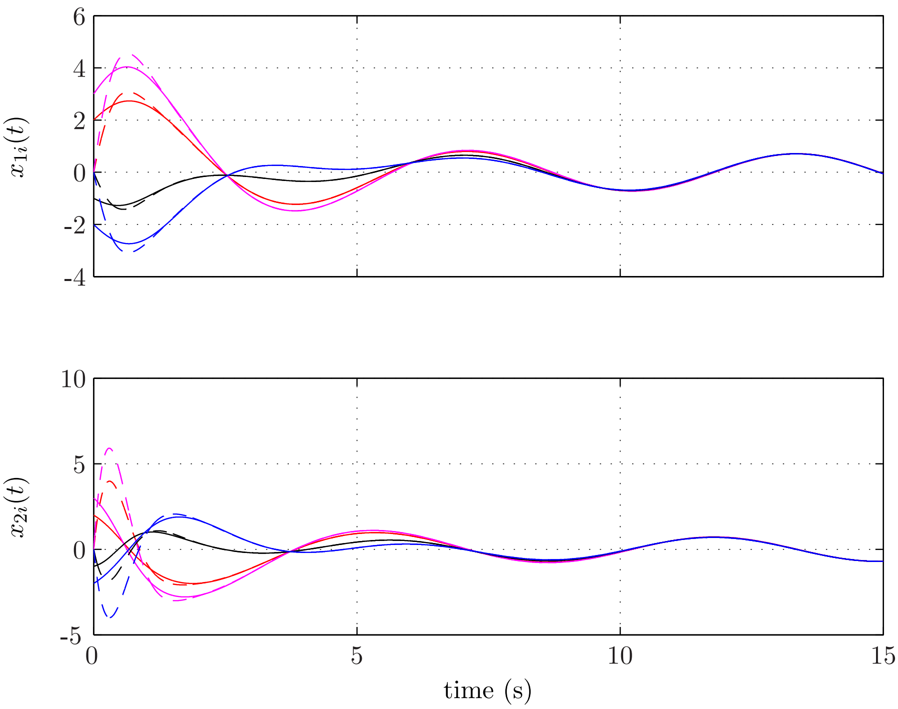

Figure 4.8: System states $x_i(t)$ (solid) and observed states $\tilde{x}_i(t)$ (dashed) of nominal system.

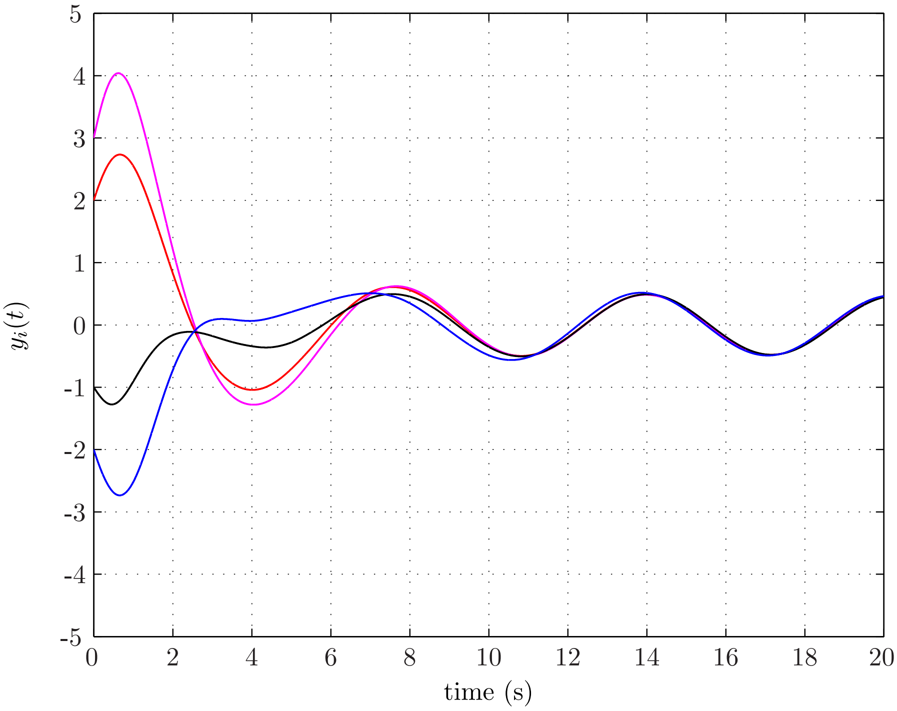

Figure 4.9: Synchronization with trigger function (4.29): Output $y_i(t)$

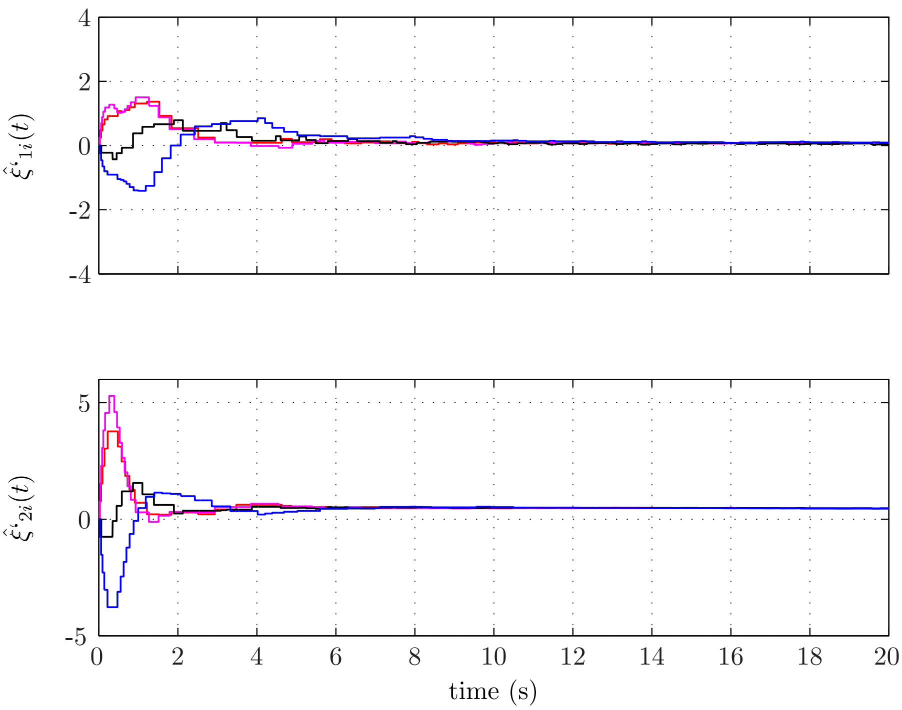

Figure 4.10: Synchronization with trigger function (4.29): Transformed system states $\hat{\xi}_i'(t)$

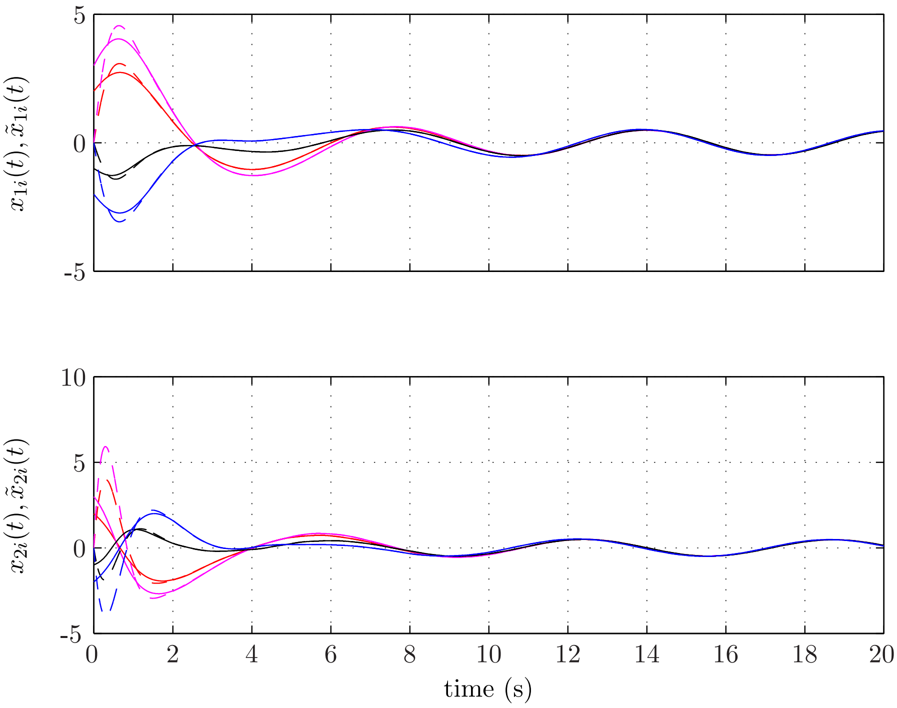

Figure 4.11: Synchronization with trigger function (4.29): System states $x_i(t)$ (solid) and observed states $\tilde{x}_i(t)$ (dashed)

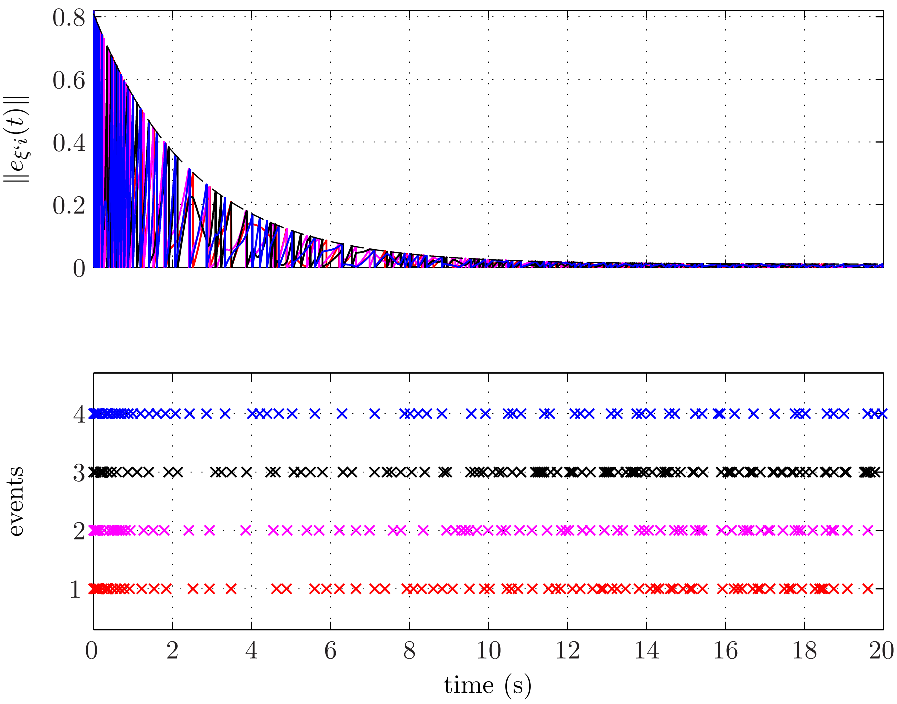

Figure 4.12: Synchronization with trigger function (4.29): Control measurement error $\|e_{\xi'i}(t)\|$

4.2.2 Trigger Functions Depending on Controller States

In this subsection we customize Theorem 4.3 to the case with an output dynamic controller. For that reason we define the measurement error

$$e_{\eta i}(t) = \hat{\eta}_i(t) - \eta_i(t) \tag{4.33}$$

and time-depended trigger functions

$$f_i(e_{\eta i}(t))) = \|e_{\eta i}(t)\| - c\mathrm{e}^{-\alpha t}. \tag{4.34}$$

Like in Section 4.1.2, the controller states are held constant

$$\hat{\eta}_i(t) = \eta_i(t_i^i), \quad t \in [t_k^i, t_{k+1}^i[.$$

between to consecutive events of agent i.

Theorem 4.6. *Consider N linear system (4.23) with the dynamic feedback control (4.24) and trigger functions of the form (4.29). Assume A is diagonalizable, all eigenvalues of A belong to the imaginary axis, the pair (A, B) is stabilizable, the pair (A, C) is detectable, $A + BK$ and $A + HC$ are Hurwitz, and $A + BK$ is diagonalizable. Let the communication graph G be undirected and connected, then for all initial conditions $x(0) \in \mathbb{R}^n$ and $t > 0$, it holds*

$$\|\delta_{\xi'}(t)\| \leq e^{-\lambda_2 t}\|\delta_{\xi'}(0)\| + k_V \frac{\|\bar{L}_n - \tilde{A}\|}{\alpha}\sqrt{N}c\left(1 - e^{-\alpha t}\right),$$

with a positive constant $k_V = \|V\|\|V^{-1}\|$, where V is the matrix of the eigenvectors of $\tilde{A}_N$. Furthermore, the closed-loop system does not exhibit Zeno behavior.

Proof. We can use the same proof technique as in Section 4.1.2, since (4.3b) and (4.25b) have the same form. We rewrite equation (4.25b) with event-triggering to

$$\dot{s}(t) == A(s(t) - e_\eta(t)) - \bar{L}_n(s(t) - e_\eta(t)). \tag{4.35}$$

With the transformation (4.26) we obtain

$$\dot{\xi}'(t) = -\bar{L}_n\xi'(t) + \mathrm{e}^{-\tilde{A}_N t}(\bar{L}_n - \tilde{A})e_\eta(t),$$

and therefore

$$\dot{\delta}_{\xi'}(t) = -\bar{L}_n\delta_{\xi'}(t) + \mathrm{e}^{-\tilde{A}_N t}(\bar{L}_n - \tilde{A})e_\eta(t)$$

Now we can proceed like in Section 4.1.2 from Equation (4.14) on, which proofs the results. □

Example 7. We consider the same example system as in Example 6 but now with trigger function (4.34). As one can see in Figure 4.13/4.14 the systems are synchronized. Each agent renders the transfered system states piecewise constant, which are converging to zero (see Figure 4.15). In Figure 4.16 the synchronized system states are depicted. Furthermore, one can see that the trajectories of the observed states $\tilde{x}_i(t)$ (dashed) converge to to them of the current states $x_i(t)$ (solid)(see Figure 4.16). Again, at the beginning the events are more dense (see Figure 4.17) compared to Example 5, but distinctly less compared to the previous Example 6.

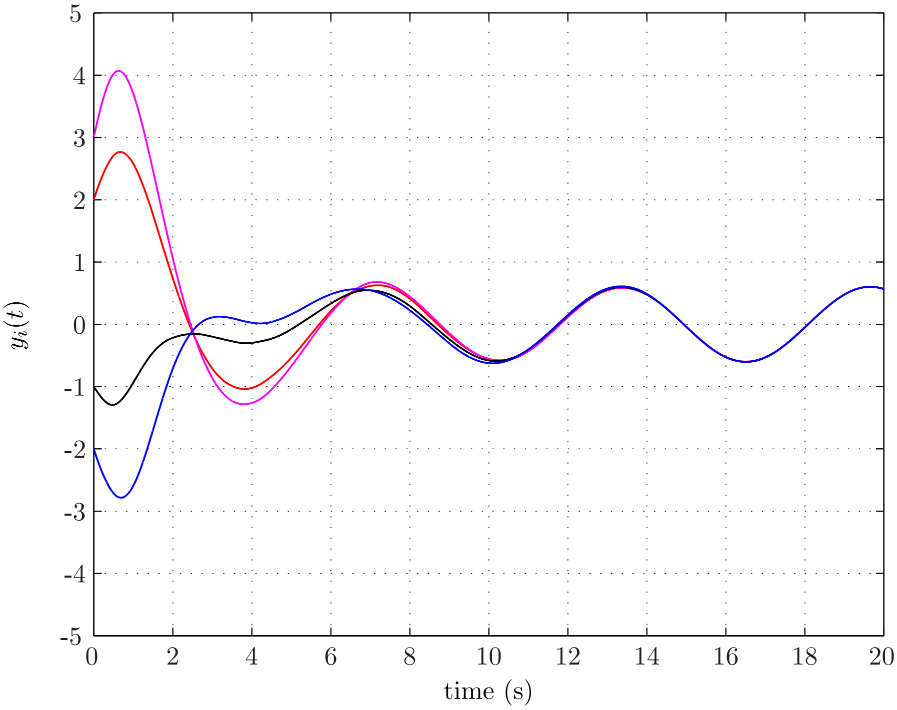

Figure 4.13: Synchronization with trigger function (4.34): Output $y_i(t)$

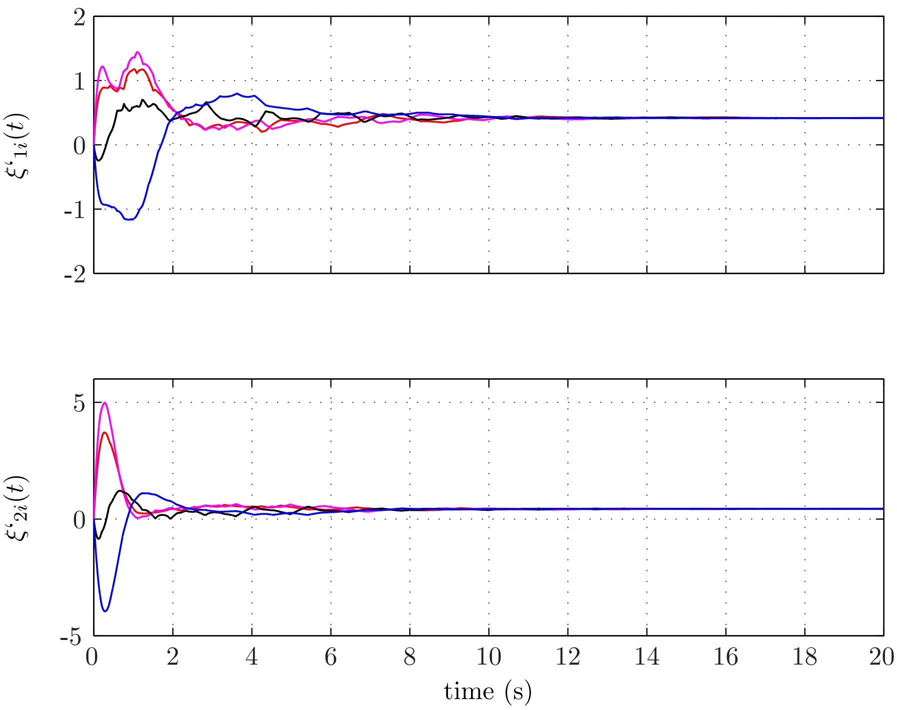

Figure 4.14: Synchronization with trigger function (4.34): Transformed system states $\hat{\xi}'_i(t)$

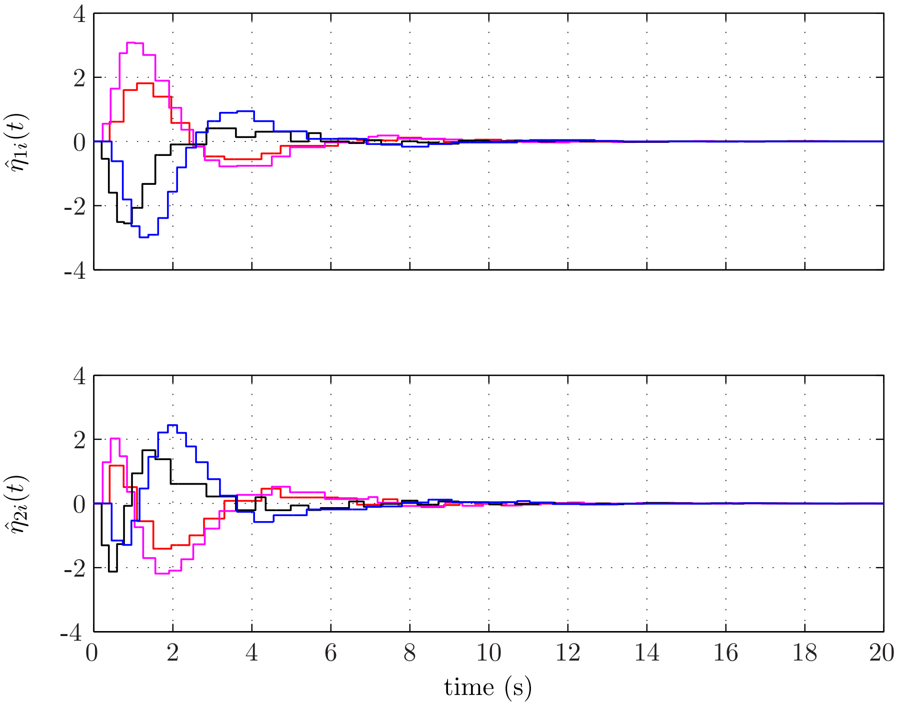

Figure 4.15: Synchronization with trigger function (4.34): Controller states $\eta_i(t)$

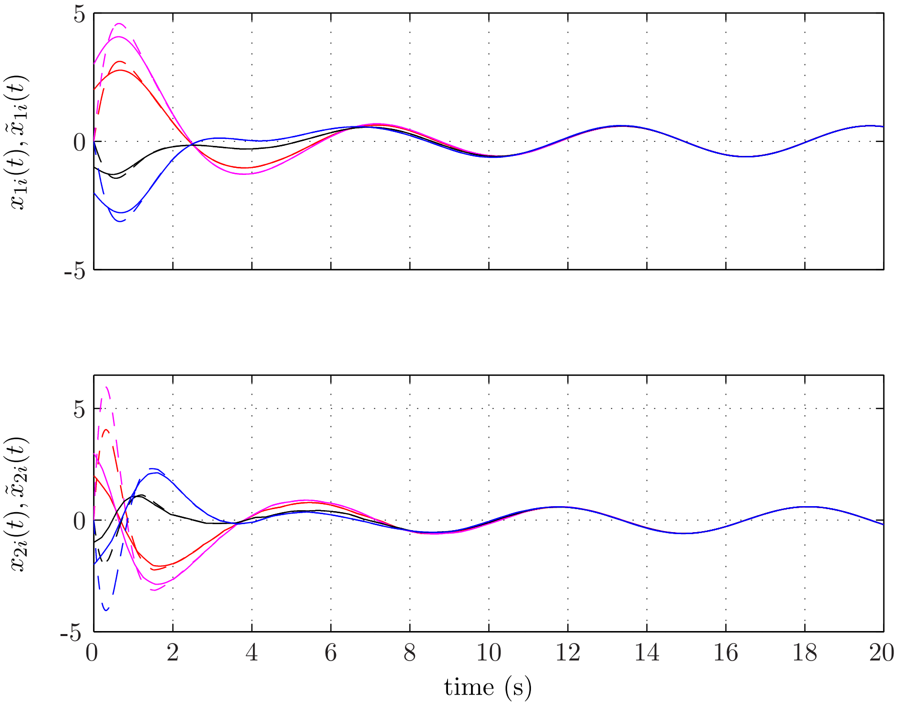

Figure 4.16: Synchronization with trigger function (4.34): System states $x_i(t)$ (solid) and observed states $\tilde{x}_i(t)$ (dashed)

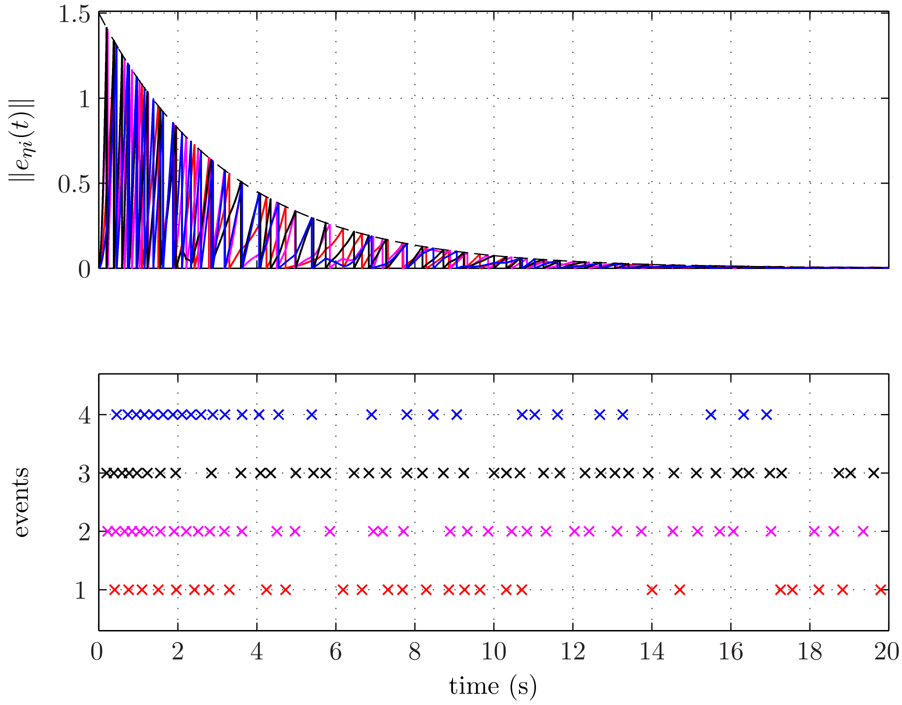

Figure 4.17: Synchronization with trigger function (4.34): Control measurement error $\|e_\eta(t)\|$

4.3 Discussion

In this chapter we avoid the strict assumption on B by introducing a dynamic controller. For the event-based synchronization of linear system with dynamic feedback controller we present two new approaches which are based on the two different setups in Chapter 3.
The first approach requires again a mostly exact model of the real system. Moreover, we have to track the system states $x_i(t)$ and the controller states $\eta_i(t)$ in order to perform the transformation. However, the communication between the agents happens in a piecewise constant manner. We have here the same advantages and disadvantages like for Setup A.
The second approach monitors only controller states $\eta_i(t)$ and thus renders the control signals piecewise constant. The event-based behavior is better compared to the first approach. The approach is similar to that of Setup B and has also the same advantages (or otherwise). Again, several simulations show that the trigger mechanism leads to a synchronization for the case with $\text{Re}[\lambda_k(A)] \leq 0$ and also with trigger functions with an additional constant offset.
In the last section we extended the two approaches to the event-based synchronization with the dynamic output controller. The proposed methods are the general results for the event-based synchronization of linear identical system. For the two approaches of the dynamic output controller the events are more dense for small t compared to the dynamic feedback controller. This is due to the fact that at the beginning the observed states $\tilde{x}_i(t)$ differ from the actual states $x_i(t)$. A bad configured observer leads to more events than we normally need. Therefore, we require a good working observer for our two proposed event-based strategies.

5 Event-based Synchronization of Kuramoto Oscillators

In this chapter we depart from the event-based synchronization of linear systems. Another active field of research is the synchronization of Kuramoto oscillators. We present a new method for the event-based synchronization of Kuramoto oscillators. The algebraic graph theory is used to encode the communication between the oscillators, which is a big advantage for the later considered analysis.

5.1 Synchronization of Kuramoto Oscillators

In this section we summarize the main results of [40]. This is the basis for our event-based approach in the next Section 5.2. The uniform Kuramoto model consists of N oscillators which are described by

$$\dot{\theta}_i = \omega_i + \frac{K}{N} \sum_{j=1}^{N} \sin(\theta_j - \theta_i), \quad i = 1, 2, \dots, N \tag{5.1}$$

where θ_i is the phase of oscillator i, ω_i is its natural frequency and $K > 0$ is the coupling gain. In this section we consider a finite (N) number of Kuramoto oscillator with an *all - to - all* topology, i.e. that all nodes are connected to all other nodes. Furthermore, we let the natural frequencies ω_i be from the set of reals and we do not claim any particular probability distribution on them. The problem is finding a coupling gain K so that the oscillators synchronize. The oscillators are said to be synchronized if

$$\dot{\theta}_i - \dot{\theta}_j \to 0 \text{ as } t \to \infty \; \forall i, j = 1, \dots, N$$

holds. The phase difference $\theta_i - \theta_j \;\; \forall i, j = 1, \dots, N$ become asymptotically constant.
Following [41], we use a graph theoretical formulation of Kuramato's model. The incidence matrix is $B_{ij} = 1$ if the edge j is incoming to vertex i, $B_{ij} = -1$ if edge j is outcoming from the vertex i, and 0 otherwise. The Laplacian of G is given by $L = BB^T$. The matrix $L_W = BWB^T$ is a weighted Laplacian with the weighting matrix $W = \text{diag}(W_i)$. The oscillator dynamics (5.1) can be equivalently rewritten in compact form as

$$\dot{\theta} = \omega - \frac{K}{N} B \sin(B^T \theta). \tag{5.2}$$

Moreover, we define the phase differences $\phi := B^T \theta$.
We assume all initial phase differences are contained in the compact set

$$D = \{\theta_i, \theta_j || \theta_i - \theta_j| \leq \frac{\pi}{2} - 2\epsilon \; \forall i, j = 1, \dots, N\}, \tag{5.3}$$

where $0 < \epsilon < \frac{\pi}{4}$. It is derived that if

$$K = K_{inv} > \frac{N|\omega_{max} - \omega_{min}|}{2\cos(2\epsilon)} \tag{5.4}$$

all phase differences $\theta_i - \theta_j \; \forall i = 1, \ldots, N$ are positively invariant with respect to the compact set D, i.e. $(\theta_i - \theta_j) \in D \; \forall t > 0$.

Theorem 5.1. *[40] Consider the system dynamics as described by (5.1). Let all initial phase differences be contained in the compact set D. Then there exists a coupling gain $K_{inv} > 0$ such that $(\theta_i - \theta_j) \in D \; \forall t > 0$. If the coupling gain is chosen such that $K = K_{inv}$, then all the oscillators synchronize i.e. $\dot{\theta}_i - \dot{\theta}_j \to 0$ as $t \to \infty \; \forall i, j = 1, \ldots, N$.*

The proof is based on Lyapunov analysis and uses also Lasalles' Invariance Principle [40]. The oscillators asymptotically converge to the mean natural frequency of all oscillators $\Omega = \frac{\sum_{i=1}^{N} \omega_i}{N}$. Furthermore, the time derivative of (5.2) can be written as

$$\ddot{\theta}(t) = -\frac{K}{N} B \mathrm{diag}(\cos(\phi)) B^T \dot{\theta}(t) \tag{5.5}$$

$$= -\frac{K}{N} L_K \dot{\theta}(t), \tag{5.6}$$

where $L_K = B\mathrm{diag}(\cos(\phi))B^T$. The weighted Laplacian is described as

$$l_{K,ii} = \sum_{k=1, k\neq i} \cos(\theta_k - \theta_i) \quad \forall i = 1, \ldots, N \tag{5.7}$$

$$l_{K,ij} = -\cos(\theta_i - \theta_j) \quad \forall i = 1, \ldots, N \; i \neq j \tag{5.8}$$

Since $\phi \in D$, the weighted Laplacian L_K is positive-semidefinite.

5.2 Event-based Approach

In this section we present a new method for the event-based synchronization of Kuramoto oscillators. The approach and proof technique is similar to them of the last chapters.
Agent i has only access on local information, i.e. the actual frequency $\dot{\theta}_i(t)$ and the latest triggered frequency $\hat{\dot{\theta}}_i(t)$. The frequency is held constant

$$\hat{\dot{\theta}}_i(t) = \dot{\theta}_i(t_k^i), \quad t \in [t_k^i, t_{k+1}^i[$$

between two consecutive events. In order to derive a decentralized event-based strategy, we define for each agent i the measurement error for frequencies

$$e_{\theta i}(t) = \hat{\dot{\theta}}_i(t) - \dot{\theta}_i(t). \tag{5.9}$$

We propose dynamic trigger functions of the form

$$f(\varepsilon_{\theta i}(t)) = \|e_{\theta i}(t)\| - (c_1 + c_2 \mathrm{e}^{-\alpha t}). \tag{5.10}$$

Since $\dot{\theta}(t)$ converge to the average frequency, we can decompose $\dot{\theta}(t)$ according to

$$\dot{\theta}(t) = \mathbf{1}\Omega + \delta_K(t), \tag{5.11}$$

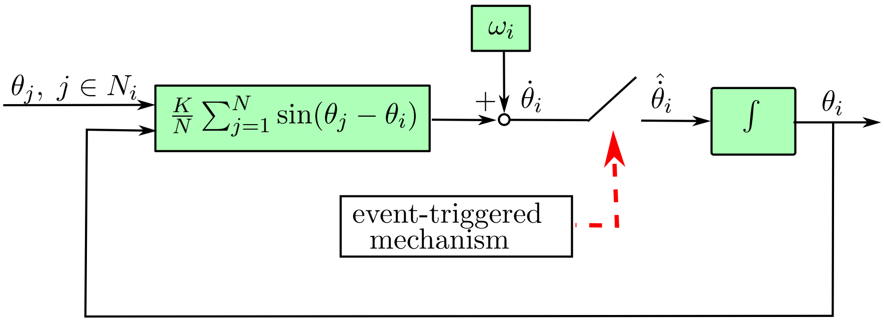

Figure 5.1: Event-triggered control schematic for trigger functions (5.10)

with the group disagreement vector $\delta_K(t)$, which satisfies $\mathbf{1}^T\delta_K(t) = 0$ and $L_K\dot{\theta}(t) = L_K\delta_K(t)$. For convenience we define $a = \frac{K}{N}$.
In Figure 5.1 the implementation of the event-triggered control is illustrated. The trigger mechanism is placed after the frequency θ_i and thus renders $\hat{\theta}_i$ constant piecewise. For this event-triggered synchronization of Kuramoto oscillators we require a continuous communication between the agents.

Theorem 5.2. *Consider the system dynamics as described by (5.1) and trigger functions of the form (5.10). Let all initial phase differences be contained in the compact set D and assume the coupling gain is chosen such that $K = K_{inv}$, then for $t > 0$ it holds*

$$\begin{aligned}\|\delta_K(t)\| \leq{}& a\|L_K\|\sqrt{N}\frac{c_1}{a\lambda_2} + e^{-\alpha t}a\|L_K\|\sqrt{N}\frac{c_2}{a\lambda_2 - \alpha} \\ &+ e^{-a\lambda_2 t}\left(\|\delta_K(0)\| - a\|L_K\|\sqrt{N}\left(\frac{c_1}{a\lambda_2} + \frac{c_2}{a\lambda_2 - \alpha}\right)\right).\end{aligned}$$

Furthermore, the closed-loop system does not exhibit Zeno behavior.

Proof. The time derivative of the disagreement vector $\delta_k(t)$ is given by

$$\dot{\delta}_K(t) = \ddot{\theta}(t) = -aL_K\dot{\theta}(t) \tag{5.12}$$

In presence of event-triggering we rewrite (5.12) to

$$\dot{\delta}_K(t) = -aL_K\hat{\dot{\theta}}(t) = -aL_K(\dot{\theta}(t) + e_\theta(t)) = -aL_K(\mathbf{1}\Omega(t) + \delta_K(t) + e_\theta),$$

and therefore

$$\dot{\delta}_K(t) = -aL_K\delta_K(t) - aL_Ke_\theta(t). \tag{5.13}$$

Now we can proceed like in the previous sections and bound the disagreement vector. The analytical solution of (5.13) is given by

$$\delta_K(t) = \mathrm{e}^{-aL_Kt}\|\delta_K(0)\| - a\int_0^t \mathrm{e}^{-aL_K(t-\tau)}L_Ke_\theta(\tau)d\tau \tag{5.14}$$

Remark 5.1. With the positive factor a one can still apply Lemma 3.2. We have

$$L_K = TD_{L_K}T^T = T\text{diag}(0, \lambda_2, \dots, \lambda_N)T^T,$$

where T is an orthogonal matrix with the eigenvectors of L_K as columns. With the factor a we get

$$aL_K = aTD_{L_K}T^T = T\,aD_{L_K}T^T = T\text{diag}(0, a\lambda_2, \dots, a\lambda_N)T^T.$$

For the exponential Laplacian we obtain

$$\begin{aligned}
\mathrm{e}^{-aL_K t} &= T\text{diag}(1, \mathrm{e}^{-a\lambda_2 t}, \dots, \mathrm{e}^{-a\lambda_N t})T^T \\
&= T\text{diag}(1, 0, \dots, 0)T^T + Ta\text{diag}(0, \mathrm{e}^{-a\lambda_2 t}, \dots, \mathrm{e}^{-a\lambda_N t})T^T \\
&= \frac{1}{N}\mathbf{1}\mathbf{1}^T + T\text{diag}(0, \mathrm{e}^{-a\lambda_2 t}, \dots, \mathrm{e}^{-a\lambda_N t})T^T
\end{aligned}$$

Next, with the zero average vector $v \in \mathbb{R}^N$ and condition $\|T\| = \|T^T\| \leq 1$ we get

$$\begin{aligned}
\|\mathrm{e}^{-aL_K t}v\| &\leq \|\frac{1}{N}\mathbf{1}\mathbf{1}^T v\| + \|T\text{diag}(0, \mathrm{e}^{-a\lambda_2 t}, \dots, \mathrm{e}^{-a\lambda_N t})T^T v\| \\
&= \|T\text{diag}(0, \mathrm{e}^{-a\lambda_2 t}, \dots, \mathrm{e}^{-a\lambda_N t})T^T v\| \\
&\leq \|T\|\|\text{diag}(0, \mathrm{e}^{-a\lambda_2 t}, \dots, \mathrm{e}^{-a\lambda_N t})\|\|T^T\|\|v\| \\
&\leq \|\text{diag}(0, \mathrm{e}^{-a\lambda_2 t}, \dots, \mathrm{e}^{-a\lambda_N t})\|\|v\|
\end{aligned}$$

and finally

$$\|\mathrm{e}^{-aL_K t}v\| \leq \mathrm{e}^{-a\lambda_2 t}\|v\|.$$

Since the vector $L_K e_\theta(\tau)$ has zero average, we can bound (5.14) as

$$\begin{aligned}
\|\delta_K(t)\| &\leq \|\mathrm{e}^{-aL_K t}\delta_K(0)\| + a\int_0^t \|\mathrm{e}^{-aL_K(t-\tau)}L_K e_\theta(\tau)\|d\tau \\
&\leq \mathrm{e}^{-a\lambda_2 t}\|\delta_K(0)\| + a\int_0^t \mathrm{e}^{-a\lambda_2(t-\tau)}\|L_K\|\|e_\theta(\tau)\|d\tau.
\end{aligned}$$

The trigger function (5.10) enforces $\|\varepsilon_{\theta i}(t)\| \leq \|\varepsilon_\theta(t)\| \leq \sqrt{N}(c_1 + c_2\mathrm{e}^{-\alpha t})$ and we derive

$$\|\delta_K(t)\| \leq \mathrm{e}^{-a\lambda_2 t}\|\delta_K(0)\| + a\int_0^t \mathrm{e}^{-a\lambda_2(t-\tau)}\|L_K\|\sqrt{N}(c_1 + c_2\mathrm{e}^{-\alpha\tau})d\tau.$$

After integrating and reordering we get

$$\begin{aligned}
\|\delta_K(t)\| \leq{}& a\|L_K\|\sqrt{N}\frac{c_1}{a\lambda_2} + \mathrm{e}^{-\alpha t}a\|L_K\|\sqrt{N}\frac{c_2}{a\lambda_2 - \alpha} \\
&+ \mathrm{e}^{-a\lambda_2 t}\left(\|\delta_K(0)\| - a\|L_K\|\sqrt{N}\left(\frac{c_1}{a\lambda_2} + \frac{c_2}{a\lambda_2 - \alpha}\right)\right).
\end{aligned} \tag{5.15}$$

The proof for a lower upper bound on the inter-event time is similar as for Section 3.1.2. By assuming the latest event trigger occurs at $t = t^* > 0$ it holds $\|\varepsilon_{\theta i}(t^*)\| = 0$. Between two consecutive trigger events it holds that $\dot{\varepsilon}_{\theta i}(t) = -\ddot{\theta}_i(t)$. We have

$$\|\dot{\varepsilon}_{\theta i}(t)\| \leq \|\dot{\varepsilon}_\theta(t)\| \leq \|\ddot{\theta}(t)\|$$

and with $\ddot{\theta}(t) = \dot{\delta}_K(t)$, (5.13) we obtain

$$\begin{aligned}\|\dot{\varepsilon}_{\theta i}(t)\| &\leq \|\dot{\delta}_K(t)\| \\ &\leq a\|L_K\|\|\delta_K(t)\| + a\|L_K\|\|e_\theta(t)\| \\ &\leq a\|L_K\|\|\delta_K(t)\| + a\|L_K\|\sqrt{N}(c_1 + c_2 \mathrm{e}^{-\alpha t}).\end{aligned}$$

We bound (5.15) with

$$\|\delta_K(t)\| \leq \|L_K\|\sqrt{N}\frac{c_1}{\lambda_2} + \mathrm{e}^{-\alpha t} a\|L_K\|\sqrt{N}\frac{c_2}{a\lambda_2 - \alpha} + \mathrm{e}^{-a\lambda_2 t}\|\delta_K(0)\|$$

By defining

$$\begin{aligned}k_4 &= a\|L_K\|\|\delta_K(0)\|\mathrm{e}^{-\alpha\lambda_2 t} \\ k_5 &= a\|L_K\|\sqrt{N}c_2\left(1 - \frac{a\|L_K\|}{a\lambda_2 - \alpha}\right) \\ k_6 &= a\|L_K\|\sqrt{N}c_1\left(1 - \frac{\|L_K\|}{\lambda_2}\right)\end{aligned}$$

we get

$$\|\dot{\varepsilon}_{\theta i}(t)\| \leq k_4 \mathrm{e}^{-a\lambda_2 t} + k_5 \mathrm{e}^{-\alpha t} + k_6.$$

Thus, a lower positive bound τ on the inter-execution time is given by

$$\tau = \frac{c_1}{k_4 + k_5 + k_6}.$$

□

Example 8. We consider $N = 3$ oscillators which are all-to-all connected. We set the natural frequencies to $\omega_1 = 10$, $\omega_2 = 30$, and $\omega_2 = 70$ (unit [rad/s]). The mean frequency of this group is $\Omega = 36.67$. We choose $\epsilon = 0.5$ and the desired compact set is

$$D = \{\theta_i, \theta_j \| \theta_i - \theta_j| \leq 0.5708\ \forall i, j = 1, \ldots, N\}.$$

The coupling gain is set to $K = K_{inv} = 167$ such that condition (5.4) is satisfied. For visualizing the event-based synchronization we calculate the oscillating motion

$$y_i(t) = \sin(\dot{\theta}_i t + \omega_i)$$

and without the natural frequencies

$$\bar{y}_i(t) = \sin(\dot{\theta}_i t).$$

In Figure 5.2 the piecewise constant frequencies and the phase differences are depicted. The phase differences are invariant with respect to the compact set D and become asymptotically constant, i.e. the oscillators are synchronized. Figure 5.3 shows the measurement errors and the events. For visualizing of the synchronization the oscillating motions $y_i(t)$ and $\bar{y}_i(t)$ are illustrated in Figure 5.4.

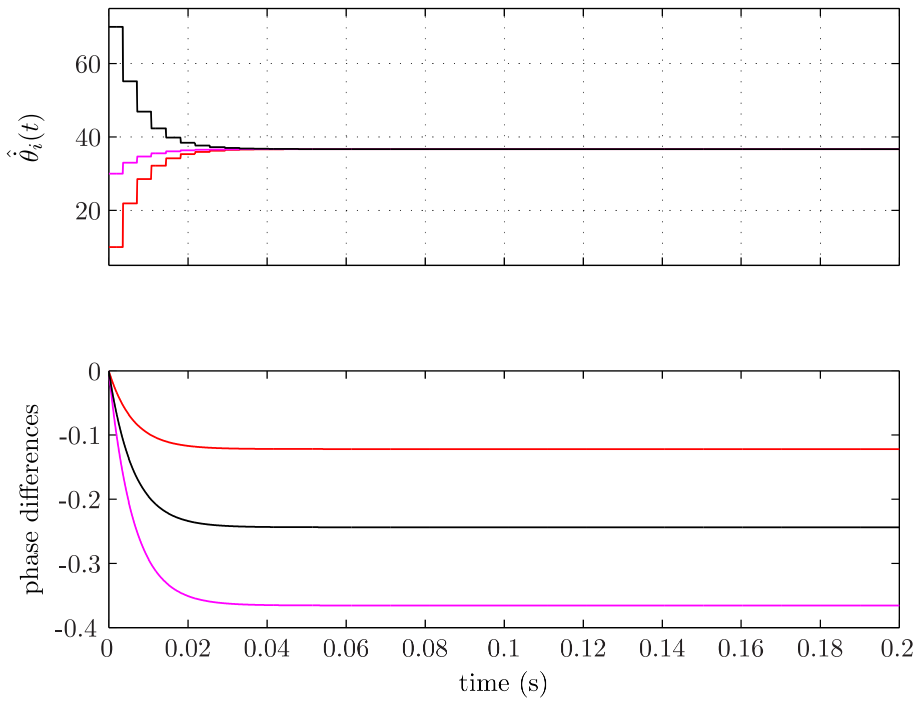

Figure 5.2: Synchronization with trigger function (5.10): $\hat{\dot{\theta}}_i(t)$ and phase differences

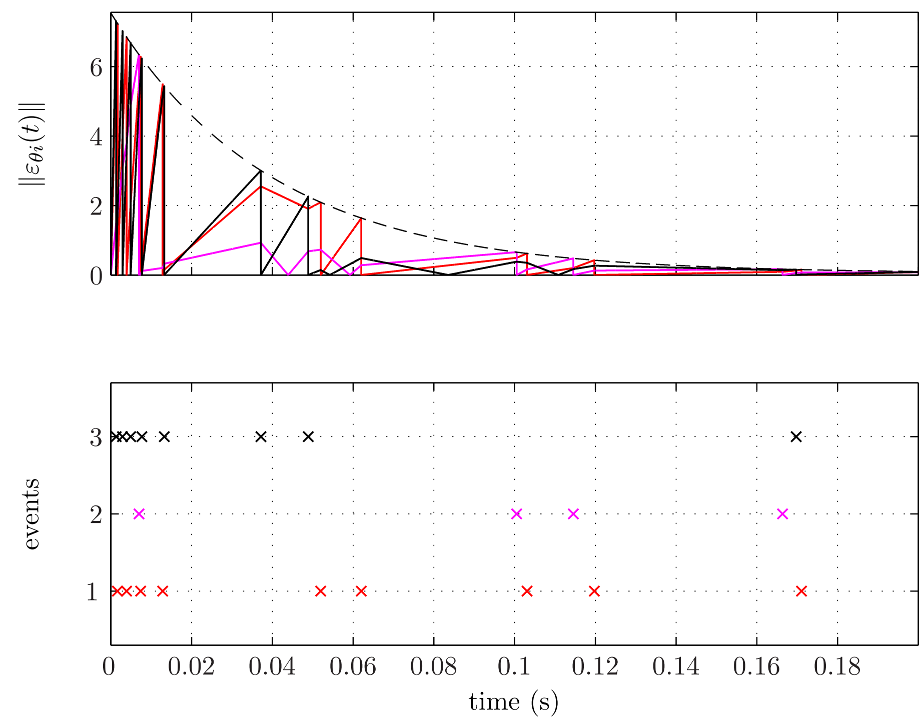

Figure 5.3: Synchronization with trigger function (5.10): Events

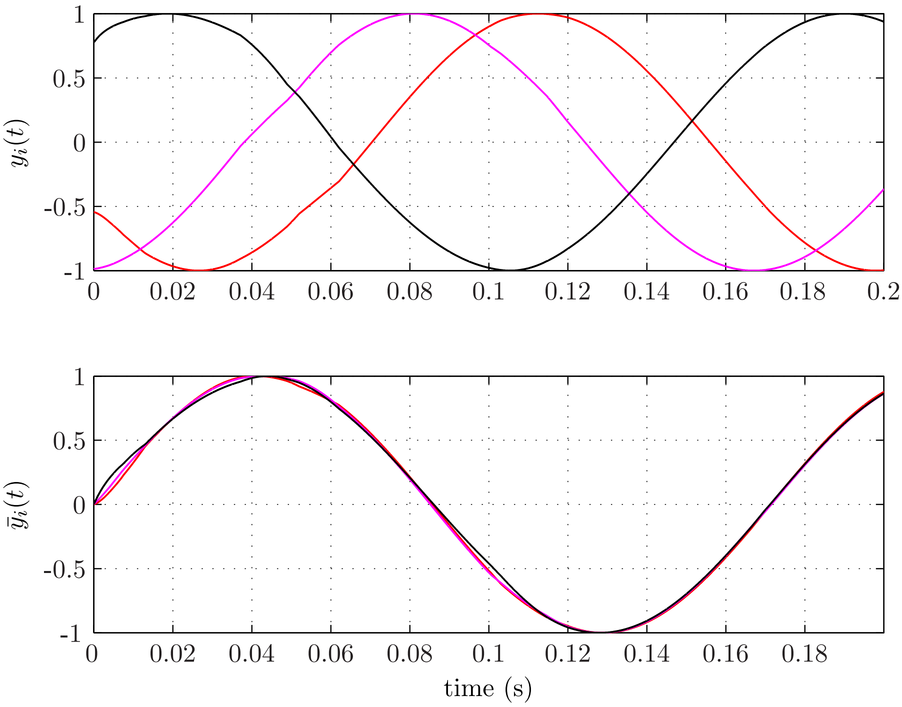

Figure 5.4: Synchronization with trigger function (5.10): Oscillating motion $y_i(t)$ and $\bar{y}_i(t)$

6 Conclusions and Future Work

This chapter presents some concluding remarks and makes some suggestions for the future work.

6.1 Conclusions

The contributions of this work were twofold. First, in the main part of this report we combine the fields decentralized event-based control and synchronization of linear identical systems. The starting point was the work of [55] and [17]. In Chapter 3 we derive first approaches for the event-based synchronization of linear systems with state feedback. We required that each agent had knowledge only of its own local information. The proof idea of the following theorems was to show that the transfered variables $z(t)$ converge to an adjustable region around the average value a, which implies according to Theorem 3.1 that the states $x(t)$ are synchronized. Theorem 3.3 exposed not to be suitable, since the density of events was very high for small times t. We avoid this problem with Theorem 3.4 by introducing dynamic trigger functions 3.4. The two theorems uses trigger function which are depended on the transfered system states $z_i(t)$. For the change of variables we require a mostly exact model A of the real system in order to perform a correctly working event-based mechanism. The implementation of this sets of trigger function yields to an event-based scheduling of the measurement broadcasts and the control inputs. We referred this implementation as Setup A.
The trigger functions of Theorem 3.5 and 3.6 are based on the control inputs $u_i(t)$. Theorem 3.5 outperformed the above-mentioned approaches, but we had to make stricter assumptions on the system matrix A. Theorem 3.6 avoided the stricter assumptions but we needed again a change of variables. Several numerical simulations had shown that event-based synchronization is still working for the case with usual assumptions on the system matrix A. The main limitations were here that we required a continuous connection between the neighboring agents, which was referred as Setup B. Both setups have their advantages and disadvantages.
In Chapter 4, the strict assumption of a square input matrix B can be weaken by introducing of a dynamic feedback controller. The two different event-based setups were transfered to this problem. Theorem 4.2 extends Theorem 3.4 to the case for a feedback controller. For the evaluation of the trigger conditions 4.8 we required to monitor the system states $x_i(t)$ and the controller states $\eta_i(t)$ in order to perform the change of variables. The implementation can be compared to that of Setup A, which renders the broadcasted measurement values $\hat{x}_i$ and $\hat{\eta}_i$ piecewise constant.
Furthermore, we adjusted Theorem 3.5 to Theorem 4.3 for the event-based synchronization with dynamic feedback controller. Analog to Setup B, we needed only to monitor the con-

troller states $\eta_i(t)$ for the trigger mechanism. Theorem 4.3 has a much better event-trigger performance compared to Theorem 4.2. Both approaches have the same advantages (or otherwise) like the previous corresponding setups.
After that, we extended the two approaches/setups to the event-based synchronization with dynamic output controller. The main difference is that we used instead of the actual state $x_i(t)$ the observed states $\tilde{x}_i(t)$. The simulation results showed that we require a good working observer for a correctly working event-based mechanism. We derived general results for an decentralized event-based control for synchronization of linear systems, which can be seen as a extension to general linear dynamical systems of the event-based control for the consensus problem of multi-agent systems with single integrators.
The second smaller contribution considered another field of synchronization, namely the event-based synchronization of Kuramoto oscillators. Kuramoto oscillators, synchronization and the consensus problem are closely related. Chapter 5 showed that is possible to derive an event-triggered approach for the synchronization of all-to-all coupled oscillators modeled by a uniform Kuramoto model. The proof technique is based on the ones of the previous chapters.

6.2 Future Work

The approaches corresponding to Setup A requires a change of variable. A question is how does the differences between the real system and the modeled effect the event-trigger mechanism and how to eliminate negative effects. Furthermore, the simulation results showed that for large time we have still trigger action. Further investigations of the exact reasons would be useful. The simulations of the approaches of Setup B showed that the event-based triggering is also working for the system matrix A with usual assumptions. A proof for this circumstances is outstanding. Besides, we require a continuous communication between the agents. It is desirable to derive an approach which renders also the broadcasted measurement piecewise constant.
The report aimed to derive novel event-based approaches for the synchronization of linear systems. It is interesting to compare the effectiveness of the event-based in comparison to time-scheduled implementation. In this thesis we considered only fixed communication topologies and required undirected connected graph. An extension to time switching communication topologies or directed graphs is desirable. Moreover, for real applications it is important to investigate the effects of time delays in networks. A further extend to the class of periodic linear systems [17] is possible.
The event-based synchronization of uniform Kuramoto oscillators shall serve as a first step for further investigations. An extension to the event-based synchronization of coupled oscillators described by a non-uniform Kuramoto model. As mentioned, the fields power network analysis, consensus protocol and non-uniform Kuramoto model are closely related. The main challenging goal and application is the event-based synchronization of power networks.

References

[1] L. Consolini, F. Morbidi, D. Prattichizzo, and M. Tosques, "Leaderfollower formation control of nonholonomic mobile robots with input constraints," *Automatica*, vol. 44, no. 5, pp. 1343–1349, 2008.

[2] S. G. Loizou and K. J. Kyriakopoulos, "Navigation of multiple kinematically constrained robots," *IEEE Transactions on Robotics*, vol. 24, no. 1, pp. 221–231, 2008.

[3] D. V. Dimarogonas and K. J. Kyriakopoulos, "A connection between formation infeasibility and velocity alignment in kinematic multi-agent systems," *Automatica*, vol. 44, no. 10, pp. 2648–2654, 2008.

[4] A. Arsie and E. Frazzoli, "Efficient routing of multiple vehicles with no communications," *2007 American Control Conference*, p. 32, 2006.

[5] R. Olfati-Saber and J. S. Shamma, "Consensus filters for sensor networks and distributed sensor fusion," *Proceedings of the 44th IEEE Conference on Decision and Control*, vol. 7, no. 0, pp. 6698–6703, 2005.

[6] A. Speranzon, C. Fischione, and K. H. Johansson, "Distributed and collaborative estimation over wireless sensor networks," *Proceedings of the 45th IEEE Conference on Decision and Control*, pp. 1025–1030, 2006.

[7] F. Xie and R. Fierro, "On motion coordination of multiple vehicles with nonholonomic constraints," *2007 American Control Conference*, no. 1, pp. 1888–1893, 2007.

[8] W. Ren and E. Atkins, "Distributed multi-vehicle coordinated control via local information exchange," *International Journal of Robust and Nonlinear Control*, vol. 17, no. November 2006, pp. 1002–1033, 2007.

[9] R. Olfati-Saber, J. A. Fax, and R. M. Murray, "Consensus and cooperation in networked multi-agent systems," *Proceedings of the IEEE*, vol. 95, no. 1, pp. 215–233, 2007.

[10] W. Ren, R. W. Beard, and E. M. Atkins, "Information consensus in multivehicle cooperative control: Collective group behavior through local interaction," *IEEE Control Systems Magazine*, vol. 27, pp. 71–82, 2007.

[11] F. Bullo, J. Cortes, and S. Martinez, *Distributed Control of Robotic Networks*, vol. 53. Princeton University Press, 2009.

[12] L. Moreau, "Stability of multiagent systems with time-dependent communication links," *Automatic Control, IEEE Transactions on*, vol. 50, no. 2, pp. 169–182, 2005.

[13] L. Moreau, "Stability of continuous-time distributed consensus algorithms," *43rd IEEE Conference on Decision and Control (2004)*, p. 21, 2004.

[14] V. D. Blondel, J. M. Hendrickx, A. Olshevsky, and J. N. Tsitsiklis, "Convergence in multiagent coordination, consensus, and flocking," *Proceedings of the 44th IEEE Conference on Decision and Control*, vol. 44, no. 3, pp. 2996–3000, 2005.

[15] A. Jadbabaie, J. Lin, and A. S. Morse, "Coordination of groups of mobile autonomous agents using nearest neighbor rules," *IEEE Transactions on Automatic Control*, vol. 48, no. 6, pp. 988–1001, 2003.

[16] R. Olfati-Saber and R. Murray, "Consensus problems in networks of agents with switching topology and time-delays," *Automatic Control, IEEE Transactions on*, vol. 49, no. 9, pp. 1520–1533, 2004.

[17] L. Scardovi and R. Sepulchre, "Synchronization in networks of identical linear systems," *Automatica*, vol. 45, no. 11, p. 19, 2008.

[18] J. K. Hale, "Diffusive coupling, dissipation, and synchronization," *Journal of Dynamics and Differential Equations*, vol. 9, no. 1, pp. 1–52, 1997.

[19] Q.-C. Pham and J.-J. Slotine, "Stable concurrent synchronization in dynamic system networks.," *Neural Networks*, vol. 20, no. 1, pp. 62–77, 2007.

[20] G.-b. Stan and R. Sepulchre, "Analysis of interconnected oscillators by dissipativity theory," *IEEE Transactions on Automatic Control*, vol. 52, no. 2, pp. 256–270, 2007.

[21] A. Y. U. Pogromsky, "Passivity based design of synchronizing systems," *International Journal Of Bifurcation And Chaos*, vol. 8, no. 2, pp. 295–319, 1998.

[22] L. Scardovi, A. Sarlette, and R. Sepulchre, "Synchronization and balancing on the n-torus," *Systems Control Letters*, vol. 56, no. 5, pp. 335–341, 2007.

[23] R. Sepulchre, D. A. Paley, and N. E. Leonard, "Stabilization of planar collective motion with limited communication," *IEEE Transactions on Automatic Control*, vol. 53, no. 3, pp. 706–719, 2008.

[24] L. Scardovi, N. E. Leonard, and R. Sepulchre, "Stabilization of collective motion in three dimensions: A consensus approach," *2007 46th IEEE Conference on Decision and Control*, no. 2, pp. 2931–2936, 2007.

[25] S. Nair and N. E. Leonard, "Stable synchronization of mechanical system networks," *SIAM Journal on Control and Optimization*, vol. 47, no. 2, p. 661, 2008.

[26] A. Sarlette, R. Sepulchre, and N. E. Leonard, "Autonomous rigid body attitude synchronization," *Automatica*, vol. 45, no. 2, pp. 572–577, 2009.

[27] Y. Kuramoto, *Chemical Oscillations, Waves, and Turbulence.* New York: Springer–Verlag, 1984.

[28] J. Buck, "Synchronous rhythmic flashing of fireflies. ii.," *The Quarterly review of biology*, vol. 63, no. 3, pp. 265–289, 1988.

[29] T. J. Walker, "Acoustic synchrony: two mechanisms in the snowy tree cricket.," *Science*, vol. 166, no. 3907, pp. 891–894, 1969.

[30] A. Arenas, A. Diaz-Guilera, J. Kurths, Y. Moreno, and C. Zhou, "Synchronization in complex networks," *Physics Reports*, vol. 469, no. 3, pp. 93–153, 2008.

[31] F. D. Smet and D. Aeyels, "Partial entrainment in the finite kuramoto model," *Physica D: Nonlinear Phenomena*, vol. 234, no. 2, pp. 81–89, 2007.

[32] J. L. Hemmen and W. F. Wreszinski, "Lyapunov function for the kuramoto model of nonlinearly coupled oscillators," *Journal of Statistical Physics*, vol. 72, no. 1-2, pp. 145–166, 1993.

[33] K. Wiesenfeld, P. Colet, and S. Strogatz, "Frequency locking in josephson arrays: Connection with the kuramoto model," *Physical Review E*, vol. 57, no. 2, pp. 1563–1569, 1998.

[34] R. Mirollo and S. Strogatz, "The spectrum of the locked state for the kuramoto model of coupled oscillators," *Physica D: Nonlinear Phenomena*, vol. 205, no. 1-4, pp. 249–266, 2005.

[35] E. Mallada, S. Member, A. Tang, and I. I. M. Odel, "Almost global synchronization of symmetric kuramoto coupled oscillators," *Control*, no. 2, pp. 1777–1782, 2005.

[36] D. Aeyels and J. A. Rogge, "Existence of partial entrainment and stability of phase locking behavior of coupled oscillators," *Progress of Theoretical Physics*, vol. 112, no. 6, pp. 921–942, 2004.

[37] S. Strogatz, "From kuramoto to crawford: exploring the onset of synchronization in populations of coupled oscillators," *Physica D: Nonlinear Phenomena*, vol. 143, no. 1-4, pp. 1–20, 2000.

[38] J. Acebron, L. Bonilla, C. Perez Vicente, F. Ritort, and R. Spigler, "The kuramoto model: A simple paradigm for synchronization phenomena," *Reviews of Modern Physics*, vol. 77, no. 1, pp. 137–185, 2005.

[39] Z. Lin, B. Francis, and M. Maggiore, "State agreement for continuous-time coupled nonlinear systems," *SIAM Journal on Control and Optimization*, vol. 46, no. 1, p. 288, 2007.

[40] N. Chopra and M. W. Spong, "On synchronization of kuramoto oscillators," *Proceedings of the 44th IEEE Conference on Decision and Control*, vol. 54, no. 2, pp. 3916–3922, 2005.

[41] A. Jadbabaie, N. Motee, and M. Barahona, "On the stability of the kuramoto model of coupled nonlinear oscillators," in *In Proceedings of the American Control Conference*, pp. 4296–4301, 2004.

[42] G. Filatrella, A. H. Nielsen, and N. F. Pedersen, "Analysis of a power grid using the kuramoto-like model," *European Physical Journal B*, vol. 61, no. 4, p. 24, 2007.

[43] H. A. Tanaka, A. J. Lichtenberg, and S. Oishi, "Self-synchronization of coupled oscillators with hysteretic responses," *Physica D*, vol. 100, no. 3-4, pp. 279–300, 1997.

[44] F. Dorfler and F. Bullo, "Synchronization and transient stability in power networks and non-uniform kuramoto oscillators," *Dynamical Systems*, pp. 1–26, 2009.

[45] D. Florian and F. Bullo, "Topological equivalence of a structure-preserving power network model and a non-uniform kuramoto model of coupled oscillators," *Dynamical Systems.*

[46] M. Miskowicz, "Send-on-delta concept: an event-based data reporting strategy," *Sensors*, vol. 6, no. 1, pp. 49–63, 2006.

[47] A. Karl J, "Event based control," *Control*, vol. 40, no. 6, pp. 127–147, 2002.

[48] K. Astrom and B. Bernhardsson, "Comparison of Riemann and Lebesgue sampling for first order stochastic systems," in *Decision and Control, 2002, Proceedings of the 41st IEEE Conference on*, vol. 2, pp. 2011–2016, IEEE, 2002.

[49] T. Henningsson, E. Johannesson, and A. Cervin, "Sporadic event-based control of first-order linear stochastic systems," *Automatica*, vol. 44, no. 11, pp. 2890–2895, 2008.

[50] M. Rabi, K. H. Johansson, and M. Johansson, "Optimal stopping for event-triggered sensing and actuation," *Electrical Engineering*, pp. 3607–3612, 2008.

[51] P. Tabuada, "Event-triggered real-time scheduling of stabilizing control tasks," *Automatic Control, IEEE Transactions on*, vol. 52, no. 9, pp. 1680–1685, 2007.

[52] D. V. Dimarogonas and K. H. Johansson, "Event-triggered cooperative control," *European Control Conference*, pp. 3015–3020, 2009.

[53] D. V. Dimarogonas and K. H. Johansson, "Event-triggered control for multi-agent systems," *System*, pp. 7131–7136, 2009.

[54] D. V. Dimarogonas and E. Frazzoli, "Distributed event-triggered control strategies for multi-agent systems," *2009 47th Annual Allerton Conference on Communication Control and Computing Allerton*, no. 0, pp. 906–910, 2009.

[55] G. Seyboth, D. Dimarogonas, and K. Johansson, "Control of multi-agent systems via event-based communication," in *World Congress*, vol. 18, pp. 10086–10091, 2011.

[56] J. Lygeros, K. H. Johansson, S. N. Simic, and S. S. Sastry, "Dynamical properties of hybrid automata," *IEEE Transactions on Automatic Control*, vol. 48, no. 1, pp. 2–17, 2003.

[57] K. H. Johansson, M. Egerstedt, J. Lygeros, and S. Sastry, "On the regularization of zeno hybrid automata," *Systems Control Letters*, vol. 38, no. 3, pp. 141–150, 1999.

[58] K. H. Johansson, J. Zhang, J. Lygeros, and S. Sastry, "Dynamical systems revisited: Hybrid systems with zeno executions," *Hybrid Systems Computation and Control*, vol. 1790, pp. 451–464, 2000.

[59] J. Zhang, K. H. Johansson, J. Lygeros, and S. Sastry, "Zeno hybrid systems," *International Journal of Robust and Nonlinear Control*, vol. 11, no. 5, pp. 435–451, 2001.

[60] C. D. Godsil and G. Royle, *Algebraic Graph Theory*. Springer, 2001.

[61] R. Merris, "Laplacian matrices of graphs: a survey," *Linear Algebra and its Applications*, vol. 197-198, pp. 143–176, 1994.

[62] C. Moler and C. Van Loan, "Nineteen dubious ways to compute the exponential of a matrix, twenty-five years later," *SIAM Review*, vol. 45, no. 1, p. 3, 2003.

[63] C. Van Loan, "The sensitivity of the matrix exponential," *SIAM Journal on Numerical Analysis*, vol. 14, no. 6, pp. 971–981, 1977.